The effect of lipid storage in regulating the immunological response of macrophages

Inaugural-Dissertation

to obtain the academic degree

Doctor rerum naturalium (Dr. rer. nat.)

submitted to the Department of Biology, Chemistry, Pharmacy of

Freie Universität Berlin

by

Sophiya Tabassum Tahir Siddiqui

From Mumbai, India

Berlin,

May, 2023

This work was conducted at the Department of Gastroenterology, Rheumatology and Infectious Diseases at Charité - Universitätsmedizin Berlin, Campus Benjamin Franklin under the supervision of Prof. Dr. Britta Siegmund between March 2019 and May 2023.

1st Reviewer: Prof. Dr. Britta Siegmund

2nd Reviewer: Prof. Dr. Sigmar Stricker

Date of defense: 01-09-2023

Declaration of Independence

Herewith I certify that I have prepared and written my thesis independently and that I have not used any sources and aids other than those indicated by me. Intellectual property of other authors has been marked accordingly. I also declare that I have not applied for an examination procedure at any other institution and that I have not submitted the dissertation in this or any other form to any other faculty as a dissertation.

_____ _____

(Place, Date) (Siddiqui, Sophiya Tabassum Tahir)

Table of Contents

Abstract

Macrophages originate from the myeloid lineage and maintain tissue homeostasis, and repair as well as regulate the physiological inflammatory responses associated with disease progression. Moreover, they are widely recognized for their adapt-able phenotypic changes in response to environmental as well as molecular cues which results in a broad phenotypic spectrum ranging from pro-inflammatory to immuno-suppressive subtypes. Metabolic, hypoxic, and cytokine imbalance within the tissue microenvironment in response to cancer and atherosclerosis progression, influences the phenotype of tissue-resident macrophages and infiltrating monocytes. Here, I generated and analyzed an *in vitro* model system to evaluate the effect of oleate-dependent polarization on macrophages. I identified that human monocyte-derived macrophages when polarized *in vitro* in the presence of oleate, result in a novel macrophage phenotype. This is due to lipid accumulation, which harbors an active immunosuppressive transcriptional phenotype based on the expression of the transcription factors sXBP-1 and GATA3 transcription factors albeit downregulates the immunosuppressive scavenger receptors CD200R1, CD163. These macrophages do not modulate T-cell proliferation capacity indicating an overall anergic immunosuppressive macrophage phenotype. These data emphasize the importance of increased lipid metabolism in macrophages and further identification of this phenotype in solid tumors and in atherosclerotic plaques. Herein I also reported that oleate-dependent murine bone marrow-derive macrophages polarize into immunosuppressive TAM phenotype independent of IL-4 signaling. Additionally, I also generated a novel genetic mouse model to evaluate the role of DGAT1 & 2 enzymes in regulating myeloid cell phenotype. Initial investigations based on oleate-dependent *in vitro* polarization of murine bone marrow-derived macrophages showed that the DGAT1 enzyme reduced lipid accumulation. Hence highlighting the importance of DGAT1 enzyme in regulating lipid droplet formation associated with macrophage phenotype.

Zusammenfassung

Makrophagen entstammen der myeloischen Linie und erhalten die Gewebehomöostase und -reparatur aufrecht und regulieren die physiologischen Entzündungsreaktionen, die mit dem Fortschreiten von Krankheiten einhergehen. Darüber hinaus sind sie weithin für ihre adaptiven phänotypischen Veränderungen als Reaktion auf umweltbedingte und molekulare Reize bekannt, die zu einem breiten phänotypischen Spektrum führen, das von entzündungsfördernden bis hin zu immunsuppressiven Subtypen reicht. Ein Ungleichgewicht von Stoffwechsel, Hypoxie und Zytokinen in der Mikroumgebung des Gewebes als Reaktion auf Krebs und Atherosklerose beeinflusst den Phänotyp der im Gewebe ansässigen Makrophagen und der infiltrierenden Monozyten. Hier habe ich ein *In-vitro*-Modellsystem entwickelt und analysiert, um die Auswirkungen der Oleat-abhängigen Polarisierung auf Makrophagen zu untersuchen. Ich konnte feststellen, dass aus menschlichen Monozyten abgeleitete Makrophagen, wenn sie *in vitro* in Gegenwart von Oleat polarisiert werden, einen neuartigen Makrophagen-Phänotyp entwickeln. Dies ist auf die Lipidakkumulation zurückzuführen, die einen aktiven immunsuppressiven Transkriptionsphänotyp hervorruft, der auf der Expression der Transkriptionsfaktoren sXBP-1 und GATA3 beruht, obwohl die immunsuppressiven Scavenger-Rezeptoren CD200R1 und CD163 herunterreguliert werden. Diese Makrophagen modulieren die T-Zell-Proliferationskapazität nicht, was auf einen insgesamt anergischen, immunsuppressiven Makrophagen-Phänotyp hinweist. Diese Daten unterstreichen die Bedeutung eines erhöhten Lipidstoffwechsels in Makrophagen und die weitere Identifizierung dieses Phänotyps in soliden Tumoren und in atherosklerotischen Plaques. Außerdem habe ich gezeigt, dass Makrophagen aus dem Knochenmark von Mäusen, die von Oleaten abhängig sind, unabhängig von IL-4-Signalen in den immunsuppressiven TAM-Phänotyp polarisieren. Darüber hinaus habe ich ein neues genetisches Mausmodell entwickelt, um die Rolle der Enzyme DGAT1 & 2 bei der Regulierung des Phänotyps myeloischer Zellen zu untersuchen. Erste Untersuchungen auf der Grundlage einer Oleat-abhängigen In-vitro-Polarisierung von Makrophagen aus dem Knochenmark der Maus zeigten, dass das Enzym DGAT1 die Lipidakkumulation reduziert. Dies verdeutlicht die Bedeutung des Enzyms DGAT1 bei der Regulierung der Bildung von Lipidtropfen im Zusammenhang mit dem Phänotyp von Makrophagen.

1 Introduction

1.1 Introduction to macrophages

1.1.1 Early recognition of macrophages:

Macrophages were first identified by Metchnikoff as motile cells that a capable of ingesting/phagocytosing and in turn maintaining organism's cellular integrity through a process called as 'physiological inflammation'. Metchnikoff, himself, later reframed this term into 'pathological inflammation', which is now broadly recognized as 'innate immunity'[1].

1.1.2 Ontogeny of macrophage

For decades, it was accepted that circulating monocyte arising from the progenitors of adult bone marrow (BM) were populating and maintaining the tissue resident macrophages. This constituted the basis of the Mononuclear Phagocyte System (MPS) concept developed by Van Furth and his colleagues[2, 3]. However, further developed MPS includes monocytes, macrophages, dendritic cells along with their respective BM progenitors[4]. Additionally, advances in the ontogenic classification of macrophages revealed the development and maintenance of tissue resident macrophage compartment from embryonic precursors developed in waves during embryo development and are independent of the adult BM progenitors[5]. The overall development of MPS occurs during various embryonic stages and after birth, the bone structures are formed and the bone marrow further accounts as the main site for haematopoiesis. At this stage of development, the MPS is defined to be fully established[6].

1.1.3 Macrophage phenotypic heterogeneity

Being of myelomonocytic origin, monocytes and macrophages are highly versatile in their response to environmental cues. They are well regarded for maintaining tissue homeostasis, repair, and development as well as to regulate inflammation derived physiological changes such as infection and cancer[7]. Based on different activation or phenotypic polarization stimuli such as cytokines, growth factors or other microbes or microbial products namely, interferon-γ (IFN-γ), granulocyte macrophage colony

stimulating factor (GM-CSF), macrophage colony stimulating factor (M-CSF) or lipopolysaccharide (LPS), respectively, macrophages differentiate into a broad spectrum of phenotypic subtypes. Other factors documented to influence macrophage phenotype include altered metabolic profile of the residing tissue as well as the macrophages[8]. Macrophages are broadly classified into M1 (classically activated) in response to LPS, Tumor necrosis factor- α (TNF-α) or IFN-γ stimulation or M2 (alternatively activated) in response to interleukins (IL) such as IL-4 and IL-13 mediated activation. Apart from these stimuli, GM-CSF and M-CSF are considered as important inducers of M1 or M2 phenotype, respectively.

The distinction of these phenotypes is based on surface marker expression profile, transcription factors as well as secreted cytokines and chemokines, as further outlined in the following paragraphs[9, 10]. The surface marker expression includes a number of plasma membrane receptors such as various types of scavenger receptors, leucine rich toll-like receptors (TLRs), C-type lectin receptors, GPI-anchored CD14 and opsonic receptors expressions. These receptors regulate an extensive range of macrophage functions including phagocytosis, adhesion, survival and differentiation as well as cytotoxic responses, in turn defining it's phenotypic state[11, 12].

1.1.4 Macrophage phenotype and surface receptors

Macrophage scavenger receptors have been identified for their role in maintaining homeostatic state as well as pathogenesis of various diseases such a type II diabetes, Alzheimer's disease and cancer. Macrophage scavenger receptor (MSR) are classified into classes A-J based of structural biology[13]. Class A SR includes receptors which are highly expressed on immunosuppressive tumor-associated macrophages (TAMs). Examples of class A SR are MSR-1 (CD204) and macrophage scavenger receptor with collagenous structure (MARCO). Both these receptors are associated with poor cancer prognosis[13, 14, 15]. Class B SR includes CD36, also known as fatty acid translocase (FAT), that plays a critical role in pathophysiology of atherosclerotic (AS) plaques where it is involved in uptake and storage of oxidized low density lipoproteins (ox-LDL), phospholipids in macrophages inducing the formation of plaque resident foam macrophages[16]. CD36 expressing macrophages are also identified in solid tumors with high fatty content and are associated with lipid accumulating TAMs[17, 18]. CD68 is a class D SR and is a highly glycosylated protein usually present

in the endosome or endolysosome and shuttles to the cell surface under activating conditions[19]. Class E SR such as lectin-like oxidized LDL receptor 1 (LOX-1) are receptors that are also involved in oxidized lipid uptake and macrophages expressing LOX-1 are associated to obesity, high fat containing solid tumor tissues such as breast cancer and prostate cancer as well as in dyslipidemia[20, 21]. Moreover, class I SR namely CD163, is expressed exclusively on immunosuppressive monocytes and macrophages as its expression is tightly regulated by inflammation mediators. Hence, only under highly anti-inflammatory activation conditions macrophages express CD163 receptor[13].

Other types of surface receptors include CD206, a mannose receptor, which is a C-type lectin receptor, expressed on macrophages and dendritic cells and plays a role in maintaining tissue homeostasis. Its expression increases in immunosuppressive macrophages that are infiltrating the tumor microenvironment (TME). Hence, it is also widely used as a prognostic marker for cancer progression[22, 23]. CD14, which is a glycosylphosphatidyl inositol (GPI) linked receptor, is widely expressed on antigen presenting cells and myeloid cells including B cells, neutrophils, promonocytes, myeloblasts, monocytes and macrophages[24]. Since, CD14 is a LPS binding protein, activation of monocytes and macrophages with LPS results in upregulation of CD14 expression. On the other hand, the expression of CD14 is reportedly downregulated during IFNγ or IL-4 mediated polarization into alternatively activated macrophages[25]. Another transmembrane glycoprotein receptor, CD200R1, associated with alternatively activated macrophages is associated with immunosuppressive macrophage phenotype and strongly inhibits polarization into classically activated macrophages. In addition to this, IFN-γ or LPS stimulated polarization into classically activated macrophages results in downregulation of CD200R1 expression[26].

Other relevant markers that are important for identifying macrophage phenotypes include intracellular chaperone proteins such as FABP4 and FABP5 (fatty acid binding protein). Proteins of the FABP family are interchangeably expressed across various tissue cell types. These intracellularly expressed proteins are known to reversibly bind to long chain saturated and unsaturated fatty acids and lipids[27]. FABP4 isoform, also known as aP2 has been identified in adipose tissue resident macrophages, which are responsible for initiating and promoting atherogenesis[28 29]. FABPs are lipid chaperones that mediate important metabolic changes in macrophages. Therefore,

regulating their immunological responses associated with high lipid accumulation in adipose tissue[27].

1.1.5 Macrophage phenotype and transcription factors

It is also known that dynamic changes in the activation status of transcription factors (TF) are associated with the macrophage phenotypic changes. Activation of these TFs is dictated by various environmental stimuli. IFN-γ and LPS stimulated macrophages reportedly activate transcriptional network including NFκB (nuclear factor κ B), ATF5 (activating transcription factor 5) and C/EBPδ (CCAAT-enhancer binding proteinδ) as well as IRF5 (interferon regulatory factor 5)[30, 31, 32]. Alternatively, IL-4, IL-13 or high lipid metabolism mediated activation of PPARγ (peroxisome proliferator-activated receptor γ), c-Myc, IRF4 (interferon regulatory factor 4) or GATA3 binding protein is associated to anti-inflammatory phenotype of macrophages[31, 33, 34, 35].

1.1.6 Macrophage phenotype and cytokine profile

Another factor associated with the macrophage phenotypic spectrum is its secretory cytokine profile. Classically activated or M1 macrophages are essential producers of IL-12, IL-6, IL-18, TNF-α and iNOS (nitric oxide synthase), which promotes T_H1-mediated inflammatory response whereas, M2 or anti-inflammatory macrophages are producers of IL-10, arginase-1 and low levels of IL-12 which are involved in resolving inflammation and wound healing[36]. Apart from these two extremes of macrophages, the cytokine secretion profile of macrophages is also reportedly different in TAMs infiltrating TME as well as atherosclerotic plaque resident foam cell macrophages. TAMs release high amounts of TGF-β (transforming growth factor-β), PGE2 (prostaglandin E_2), CCL2 (chemokine ligand 2), and CCL5 (chemokine ligand 5), which play a role in suppressing anti-tumor immune responses[36], whereas, atherosclerotic plaque resident foam macrophages secrete IL-6 and IL-1β demonstrating their role in mediating inflammation[37].

Based on varying expression profiles of the above-mentioned surface markers, activated transcription factors, and secretory cytokine profiles, macrophages are classified into a broad spectrum of functionally distinct phenotypes ranging from extreme

M1 or pro-inflammatory macrophages that sustain an inflammatory phenotype to extreme M2 or anti-inflammatory macrophages that promote resolution of inflammation as well as immunosuppression.

1.1.7 Macrophage phenotype and metabolic signature

Phenotypic heterogeneity of macrophages and accompanying activation statuses are also associated with dramatic cellular metabolic switching. Depending on the specific external stimuli and consequent internal transcriptional activation, macrophages can switch their metabolism from an aerobic oxidative phosphorylation to an anaerobic or aerobic glycolytic metabolism.

Macrophage metabolism was first studied in peritoneal macrophages in response to *Corynebacterium ovis* infection which resulted in glycolytic metabolic activation[38]. Newsholme *et al.* published a report in 1987 discussing the importance of glutamine, glucose, fatty acids, and pyruvate driven metabolism in mediating macrophage proliferation in areas of local infection or inflammation[39].

GLUT-1 (glucose transporter protein) overexpression in RAW264.7 macrophage cell line results in increased glucose uptake and metabolism which promotes a pro-inflammatory phenotype[40]. Hypoxia inducible factor-1α (HIF-1α), a basic helix-loop-helix transcription factor which is activated under hypoxic conditions, modulates the metabolic profile of immune cells. HIF-1α response elements (HRE) are reported on promoter regions of genes encoding enzymes aldolase-A, enolase-1, and lactate dehydrogenase 1 (LDH-1). Thus, activation of HIF-1α promotes glycolytic metabolism[41]. LPS mediated macrophage activation results in increased succinate production due to the overactive tricarboxylic acid (TCA) cycle. This increased succinate further activates HIF-1 α and also promotes IL-1β production to maintain the inflammatory signal transduction[42]. Overexpression of HIF-1α in myeloid compartment is associated with increased expression of glycolysis related proteins and increased inflammatory signaling[43]. HIF-1 α also regulates the activation of pyruvate dehydrogenase kinase 1 (PDK 1) in pro-inflammatory macrophages which further inhibits pyruvate dehydrogenase (PDH) activity and limits the entry of pyruvate into the Krebs cycle[44]. These independent reports confirm the crucial involvement of HIF-1α in aiding the M1 inflammatory macrophage responses.

Nrf2 transcriptional activation plays a role in pentose phosphate pathway (PPP) activation. LPS mediated stimulation of macrophages results in Nrf2 dependent pentose phosphate pathway (PPP) activation in pro-inflammatory macrophages. Yet, during hypercholesterolemia progression, Nrf2 activity is suppressed and results in lack of PPP driven metabolism[45].

PDK-1-dependent glycolytic metabolism is essential in M1 and in early M2 macrophage phenotype. PDK-1 knockdown results in decreased M1 activation even upon LPS stimulation. On the other hand, PDK-1 knockdown enhanced M2 activation and IL-4 receptor signaling, which is negatively regulated by PDK-1. The involvement of PDK-1 in maintaining M2 phenotype confirms the dependency of early M2 differentiation on glycolysis and consequent dispensability of fatty acid oxidation during early differentiation stages[46]. However, contrasting reports highlight the complete dependency on active OXPHOS and mitochondrial respiration and absence of glycolytic metabolism in M2 polarizing macrophages[47]. Additionally, several publications emphasize on the importance of fatty acid oxidation (FAO) and active glutamine dependent OXPHOS in IL-4 stimulated M2 polarizing macrophages[48, 49]. Overall, these contradictory studies, discussing varying metabolic pathways involved in M2 macrophages, point towards the metabolic flexibility of M2 polarized macrophages.

The tricarboxylic acid (TCA)/Kreb's cycle, is highly active in anti-inflammatory macrophages facilitating elevated production of adenosine triphosphate (ATP), which is required for synthesizing lectin or mannose surface receptors associated with immunosuppressive phenotype[50]. On the other hand, during pro-inflammatory macrophage polarization, the Kreb's cycle is interrupted at multiple points to supply by-products into generating inflammation-regulating proteins. For instance, citrate synthesized during the first step of TCA is exported into the cytosol by the enzyme, mitochondria citrate carrier (CIC). The subsequent increased accumulation of citrate within the cytosol is an important regulator for nitric oxide (NO), reactive oxygen species (ROS) and PGE2 production[51, 52]. The cytosolic citrate is also converted into itaconate by aconitate dehydrogenase 1 (ACOD1) enzyme[53]. Itaconate, itself, plays several important roles in classically activated macrophages. It inhibits succinate dehydrogenase enzyme activity and prevents the conversion of succinate into fumarate, thus interrupting Kreb's cycle. The accumulated succinate plays a role in increased HIF-1α activity and increased inflammatory cytokine and NO production[54].

On the contrary, anti-inflammatory effect of itaconate is also widely reported. Itaconate stabilizes Nrf2 transcription factor, resulting in downstream activation of genes associated with oxidative stress and anti-inflammatory response[55]. Nrf2 activation in response to itaconate accumulation also blocks the production of pro inflammatory cytokines IL-6 and IL-1β[56].

As mentioned above, M2 polarized macrophages display a rather flexible metabolic profile including FAO or glutamine-dependent OXPHOS or even glycolysis dependent metabolism during early activation stages. Several other reports discuss exclusive FAO and lipid metabolism in anti-inflammatory macrophages activated by IL-4 receptor signaling. LDL and VLDL (very low density lipoprotein) taken up *via* the CD36 receptor in IL-4 activated macrophages are broken down by the lipolytic enzyme lysosomal acid lipase (LAL) which results in increased oxidative respiration and is associated with the expression of M2-associated genes[57]. Other reports published demonstrated that IL-4 and IL-13 stimulated alternative activation of macrophages increased FAO as the main metabolic source in a PPARγ coactivator-1 β (PGC-1β) dependent manner[58]. The dependency of IL-4 stimulated macrophages on FAO is widely discussed. However, reports published show that FAO is dispensable in IL-4 stimulated human CD14 monocyte-derived macrophages with only moderate changes occurring in mitochondrial oxidation and unaltered expression of PGC-1β[59]. Divakaruni *et al.* further confirmed the contradicting metabolic phenotype of IL-4 activated macrophages in murine *in vivo* and *in vitro* based experiments confirming that fatty acid oxidation is dispensable to IL-4 macrophages and the phenotype is rather a result of altered intracellular coenzyme A (CoA) homeostasis[60]. Murine bone marrow-derived macrophages (BMDM) supplemented with oleate rich growth medium during polarization results in increased uptake and storage of fatty acids as lipid. This excessive lipid accumulation has been associated with CD206 expressing immunosuppressive macrophages and expressed other TAM related genes. Further, combined inhibition of DGAT1 and DGAT2 enzyme-mediated lipid droplet formation reversed this immunosuppressive phenotype. This study highlights the importance of FAO and lipid metabolism in immunosuppressive macrophage polarization[61, 62]. On the other hand, the importance of DGAT1 enzyme mediated triglyceride storage in lipid droplets in inflammatory macrophage[63]. High fat diet supplemented with oleic

acid results in increased CD206 expressing M2 macrophage infiltrating the mesenteric adipose tissue of wild type C57BL/6J mice and have anti-inflammatory phenotype[64].

According to the below cited studies, lipogenesis occurs in pro-inflammatory macrophages as well and is widely researched. SREBP-1a (sterol regulatory element binding protein-1a) mediates lipogenesis in macrophages and mice deficient in SREBP-1a are incapable of generating intracellular lipid stores and thus do not generate a pro inflammatory response to LPS stimulus[65]. Another study based on LPS stimulation of RAW 264.7 macrophage cell line, reportedly linked increased cholesterol ester (CE) accumulation and decreased FAO resulting in the formation of lipid accumulating macrophage subtype called foam cells[66, 67].

In conclusion, the above-mentioned information about macrophage phenotypic diversity in context to its metabolism and surface markers as summarized in **(Figure 1)** highlights the importance of further elaborating the research and further understanding the varying expression profiles in response to various distinct stimuli.

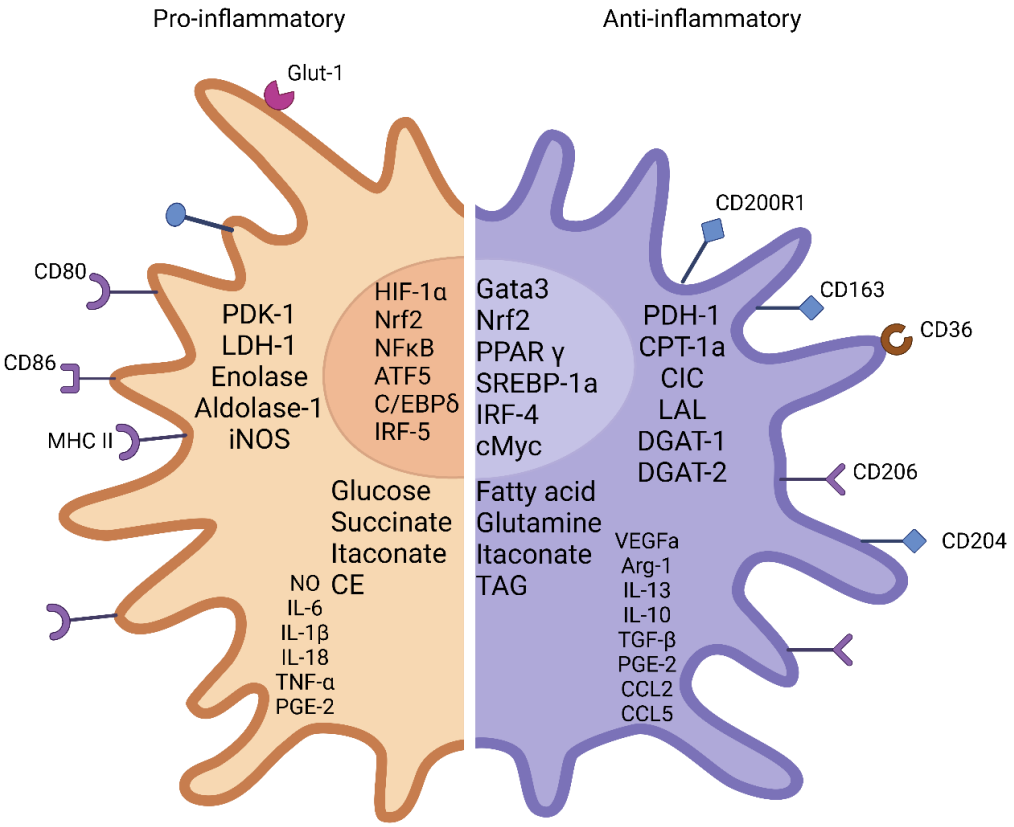

Figure 1 Metabolic, molecular and secretory cytokine signatures of macrophage activation status. *Pro-inflammatory stimuli induce transcriptional activation of HIF-1α, Nrf2, NF-κB, ATF5,C/EBPδ, and IRF-5 which are responsible for the expression of the metabolic enzymes PDK-1, aldolase-1, enolase-1, LDH-1, and iNOS as well as the surface marker expression of Glut-1, MHC-II, CD80 and CD86 and the secretion of NO, IL-6, IL-1β, IL-18, TNF-α, and PGE-2. Pro-inflammatory macrophages undergo metabolic switching towards the glycolytic, pentose phosphate pathway and interrupt the Kreb's cycle, therefore increasing the production of citrate, which is responsible for PGE2 synthesis and NADPH production. Citrate is also converted into itaconate, that stabilizes HIF-1α activity, Anti-inflammatory stimuli induces transcriptional activation of Gata3, Nrf2, PPARγ, SREBP-1a, IRF-4, and cMyc which are responsible for controlling characteristic expression of fatty acid oxidative and lipid metabolic enzymes including PDH-1, CPT-1a, LAL, and DGAT1 & 2. Anti-inflammatory macrophages are characterized by the expression of VEGFA, Arg-1 and surface marker expression of CD36, CD206, CD200R1, CD204, and CD163 as well as secretion of IL-13, IL-10, TGF-β, PGE2, CCL2 and CCL5. Abbreviations enlisted in section 6.1. Figure adapted from Sun et al.*[68].

1.2 Macrophage metabolic signature in altered state/diseases

Plasticity and phenotypic diversity are two main hallmarks of the myelomonocytic lineage. Although conventionally classified into M1- or M2- activated macrophages, which are the two extreme ends of a wide-ranging plethora of activation states, they can be further categorized into subtypes identified as M2-like, M2a, M2b, M2c, and M2d depending on the combination of stimuli, transcription factor activation, metabolic profile, and surface marker expression[69]. In addition, macrophages can be further classified into other subtypes depending on the associated diseases/tissue conditions. Following are examples of the same.

1.2.1 Cancer progression and tumor-associated macrophage phenotypes

Otto Warburg provided the first evidence of altered cancer cell metabolism. He identified that cancer cells utilize higher amounts of glucose and produce low amounts of ATP. In addition, they produce lactic acid anaerobically. The Warburg effect as described by Warburg himself defines this altered metabolic state of cancer cells [70]. The tumor microenvironment is a complex tissue comprising various other factors including immune cells, connective tissue, cytokines, chemokines, and metabolic by-products. Genetic, phenotypic and metabolic changes within the TME components contributes to cancer progression and have been outlined as hallmarks of cancer [71].

Macrophages and monocytes are one of the major immune infiltrates within the TME. Various reports discuss the importance of the altered lipid and fatty acid content of tumor site to influence TAM phenotype. Another myelomonocytic lineage cell type infiltrating tumors are myeloid derived suppressor cells (MDSCs).

Herein we discuss the well-characterized TAM **(Figure 2)** and MDSC **(Figure 3)** variants, which are reported in various types of cancers **(Table 1)**. Cancer patient derived data published over recent years shows that the clear segregation criteria of M1-M2 macrophages is not prominently observed in TAMs. The main subtypes of TAMs as defined across cancer types are defined below. Lipid-associated macrophages (LAMs) which were characterized by the expression of lipid metabolism associated genes including APOC1 (apoliporotein C1), APOE (apolipoprotein E), and LPL (lipoprotein lipase). These macrophage subtypes also expressed high levels of

TREM2, which is a lipid receptor protein and LGALS3 (galectin3 protein as the immune suppression mediator). However, these LGALS3 and FABP5 expressing LAMs or APOE and TREM2 expressing LAMs are also reported in glioblastoma and non-small cell lung carcinoma (NSCLC) patients, respectively[72, 73, 74]. Pro-tumoral MHC-low expressing TAMs, which expressed low levels of CD80 and CD86 and were characterized by upregulation of inflammatory chemokine related genes; IL-6, CXCL3, CXCL8, and IL-1β[74]. CD36 expressing macrophages, dependent on fatty acid metabolism and oxidative phosphorylation with inflammatory promoting pro tumoral LAMs, identified in human breast, colon and prostrate tumor tissues[75]. Additionally, tumor-derived lipid glucosylceramide (GC) utilizing lipid accumulating-TAMs (LA-TAMs) activated endoplasmic reticulum (ER) stress response upon storing lipid, resulting in splicing of XBP-1 transcription factor and downstream STAT6 activation. These GC dependent TAMs were also identified to be arginase-1 expressing immunosuppressive macrophages [76]. Monocyte-derived macrophages that are primed with IFN-γ and mature in CD40-CD40L dependent manner are categorized as IFN-γ TAMs. These TAMs express indolamine 2,3-oxygenase (IDO) enzyme and depend on tryptophan catabolism for energy production. Overall, the IFN-γ TAMs are PD-L1$^+$, IDO$^+$, TREM2$^+$ subsets that accumulate in human tumors and mediate immunosuppressive response[77]. As mentioned above, the tumor site is highly hypoxic and nutrient deprived, increasing angiogenesis within tumors is also an important hallmark of cancer [78]. Hypoxic environmental conditions induce the expression of HIF-1 α and HIF-2α in certain TAM subtypes characterized by their angiogenic activity. Hence referred to as angiogenic TAMs (angio-TAMs) and are identified in several types of cancers. They are characterized angiogenesis associated signature genes including *VEGFA, VCAN, SPP1*, *FCN1,* and *THBS1*[79, 80, 81]. Another TAM subtype identified in murine based breast cancer studies, FABP4$^+$ TAMs (FABP4$^+$CD11b$^+$F4/80$^+$ MHCII$^-$Ly6C$^-$) which promoted tumor growth and metastasis in an IL-6/STAT3 signaling dependent manner[82].

Table 1: Tumor-associated macrophages and myeloid derived suppressor cells

Nomenclature	Signature genes	Metabolic substrate	Reference
LAMs	CD36, FABP5, TREM2, APOC1, APOE, LGALS3, MAF	Lipids and fatty acid	72, 73, 74, 75
LA-TAMs	MHC Class II^{low}, XBP-1, LPCAT3, STAT6, Arg-1	Glucosylceramide (GC)	76
MHC Class II^{low} TAMs	MHC class II^{low}, CD80, CD86, CXCL3, CXCL5		74
IFNγ TAMs	IDO, PD-L1, IL-4I1	Tryptophan	77
Angio TAMs	HIF-1α, SLC2A1	Glucose	79, 80, 81
$FABP4^{+}$TAMs	FABP4, IL-6, NF-κB, STAT3	Lipids	82, 83
Oleate-dependent $CD206^{+}$ TAMs	CD206, DGAT1 & 2	Lipid droplet	84
PMN-MDSCs (murine)	$CD11b^{+}$,$Ly6C^{high}$, $Ly6G^{-}$, CD36	Lipids	85, 86, 87, 88, 89
PMN-MDSCs (human)	$CD14^{+}$ $CD11b^{+}$ HLA-DR $^{low/-}$ CD15, LOX-1	Lipids	90, 91
M-MDSCs (murine)	$CD11b^{+}Ly6C^{high}Ly6G^{-}$,SIRT-1	Glucose	87, 92, 93
M-MDSCs (human)	$CD14^{+}$ $CD11b^{+}$ HLA-DR $^{low/-}$ $CD15^{-}$, HIF-1α	Glucose	94, 95

Activated neutrophils and monocytes were identified with immunosuppressive capacity and were earlier classified as myeloid-derived suppressor cells (MDSCs). These cells are defined for their unique phenotype involved in regulating pathological conditions such as cancer, chronic inflammation, sepsis, and autoimmune diseases[87, 93].

Although MDSC nomenclature is debatable due to their overlapping phenotypes, there are two main classes of MDSCs defined depending on their source of origin, PMN-MDSCs /G-MDSC (polymorphonuclear or granulocytic MDSC) and M-MDSC (monocytic MDSC). An additional third small population of 'early MDSCs' which is recognized only in humans, is constituted by myeloid progenitors and myeloid precursors that exhibit an immunosuppressive characteristic as well[86]. Under normal physiological conditions, myeloid cells are activated in response to pathogens or tissue damage and are mobilized out of the bone marrow and spleen. However, under

pathological conditions such as cancer, autoimmune diseases or chronic inflammation, myeloid cells are activated in response to ER stress or altered and prolonged cytokine signaling mediated by IL-1β, IL-6, GM-CSF, and M-CSF. The expression of genes associated with ER stress response (XBP-1) and lipid metabolism receptor (LOX-1) are reportedly upregulated in PMN-MDSCs and immunosuppressive neutrophils isolated from the various types of human tumor tissues[90]. PMN-MDSCs rely on lipid metabolism and utilize polyunsaturated fatty acids (PUFA) metabolism[96]. Whereas hypoxia mediated upregulation of HIF-1α promotes glycolytic metabolism and stimulates differentiation of M-MDSCs[94]. M-MDSC and PMN-MDSC have overlapping gene signatures including CD84, STAT3, Arginase-1, S100A8/A9, and IL-1β which mediate the MDSC immunosuppressive activities[88, 95]. Other phenotypic traits of PMN-MDSCs include ROS production, peroxynitrite, and prostaglandin E2 (PGE2) synthesis which are distinct from M-MDSCs. M-MDSCs induce immune suppression via production of cytokines such as IL-10 and TGF-β, nitric oxide (NO) production, as well as expression of PD-L1 surface receptor[88].

Overall, various reports discuss the altered metabolism and transcription profile of neutrophils and monocytes which leads to increased proliferation of immature, immunosuppressive myeloid suppressors under pathological conditions. This provides further insights into understanding and targeting MDSC-driven immunosuppression.

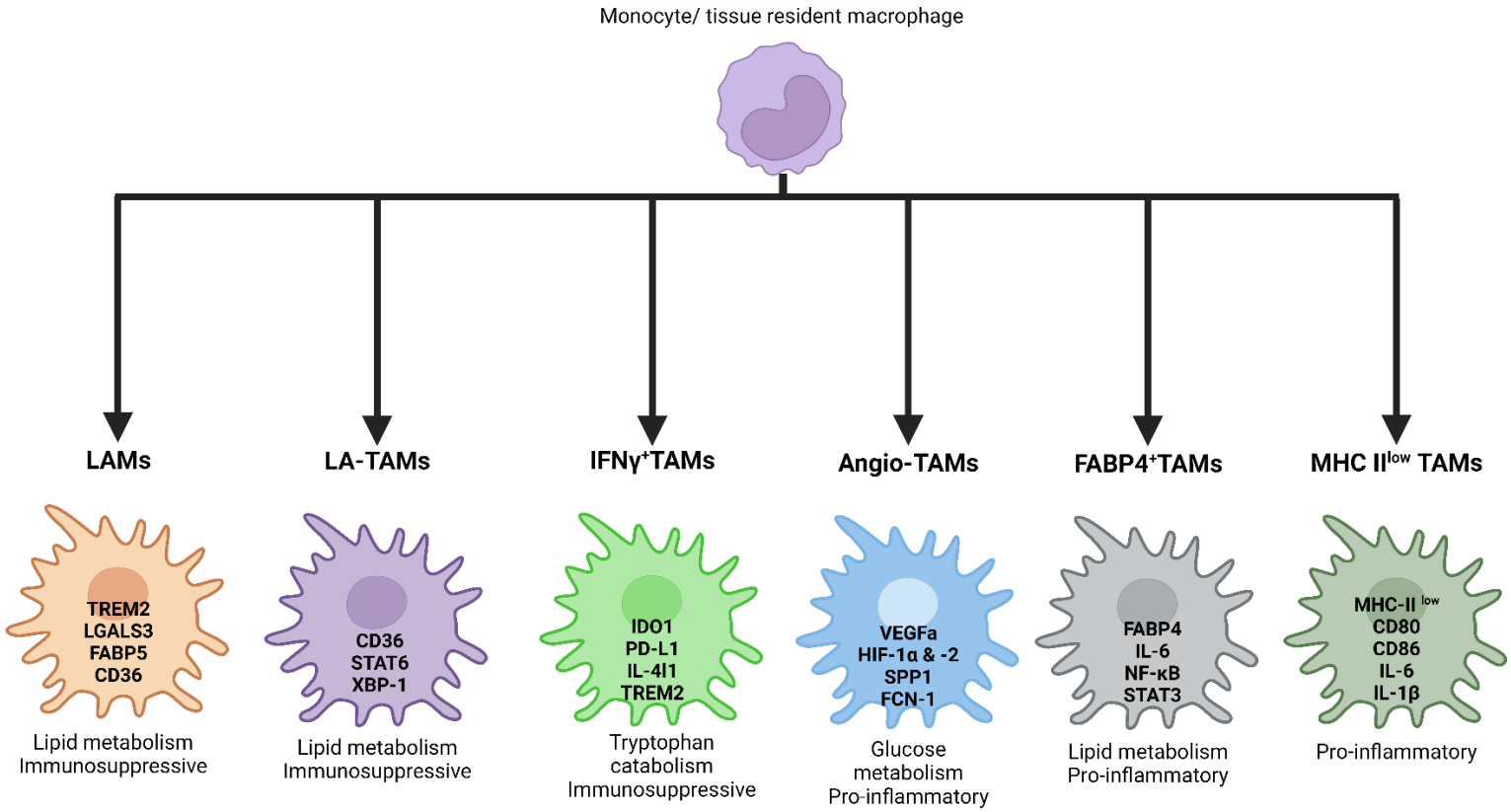

Figure 2: Tumor-associated macrophage subtypes. *Tumor microenvironment is enriched with altered metabolic by-products, cytokines, and chemokines that polarize macrophages into various immunosuppressive or pro-inflammatory subtypes with altered characteristic metabolic changes. Abbreviations enlisted in section 6.1.*

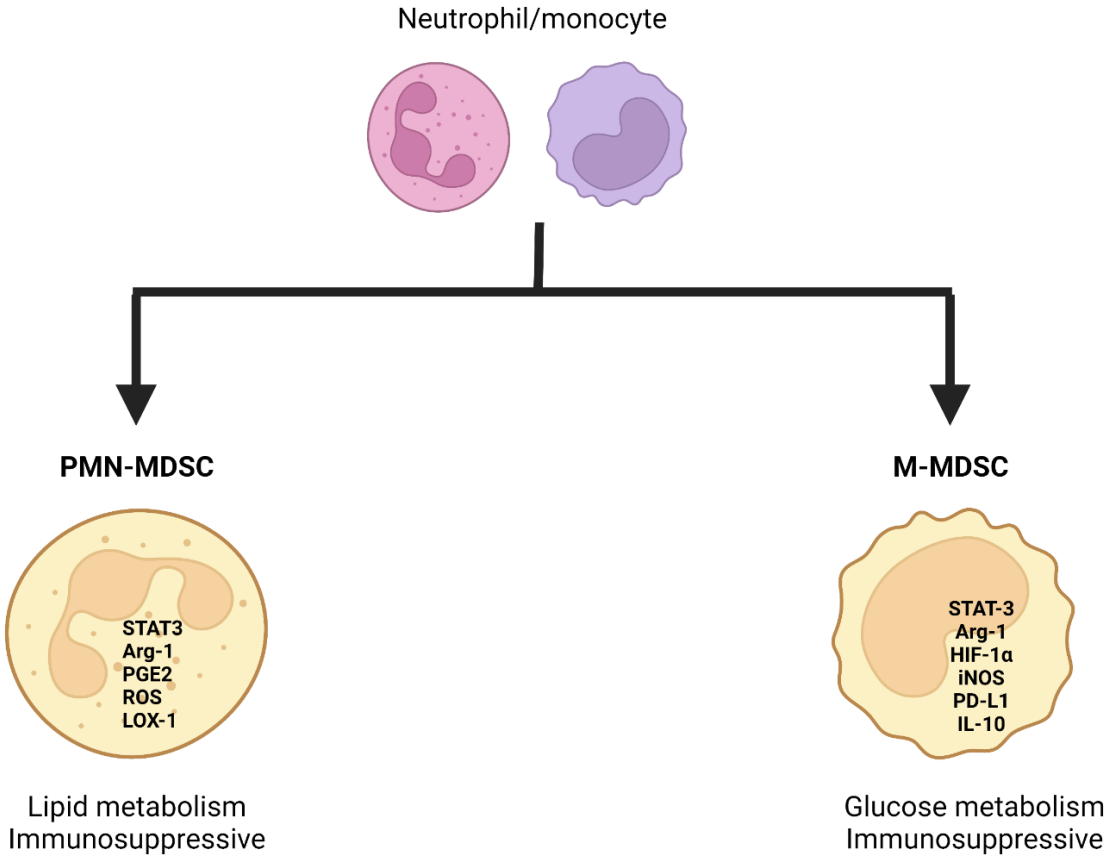

Figure 3: Tumor infiltrating MDSC subtypes. *Activation of immature neutrophils and monocytes infiltrating tumor site results in polarized immunosuppressive myeloid derived suppressor cells. Abbreviations enlisted in section 6.1.*

1.2.2 Obesity, atherosclerotic lesions and diabetes

Obesity is associated with various severe pathologies including type 2 diabetes, hypertension, cardiovascular diseases, arthritis, several types of cancer, and non-alcoholic liver diseases as well. TNF-α, IL-6, and iNOS producing macrophages have been identified as the most prominent immune cell population, which is also linked to obesity-induced insulin resistance. Adipose tissue resident macrophages (ATM) majorly express M2-like phenotype and are characterized by the expression of arginase-1 as well as high levels of anti-inflammatory cytokines such as IL-10. On the other hand, high fat diet and obesity-linked increased fatty content of AT induces switching of these M2-like macrophages into M1-like inflammatory macrophages[97]. Additional reports confirm diet-linked altered fatty acid accumulation in AT further results in changes in ATM lipid accumulation and its associated phenotype. ATM accumulating substantial amounts of triacylglycerols (TAGs), and CE identify as M1

macrophages where as glycerophospholipids, ether lipids and sphingolipid accumulating macrophages identify as M2 macrophages[98]. This provides a crucial link between understanding the role of specific types of lipids stored in macrophages and its control over the macrophage phenotype.

DGAT1 enzyme in conjugation with DGAT2 enzyme synthesizes TAGs and synthesis of TAGs in macrophages is linked M1 as well as M2 phenotype[67, 99]. Consistent with this information, Koliwad *et al*. investigated the relevance of DGAT1 enzyme activity in inflammatory macrophages. They concluded that ap2-driven knockout of DGAT1 enzyme in adipocytes and macrophages does not affect the lipid storing capacity of macrophages as macrophages are still synthesizing CE based lipids that are stored in lipid droplets and induce M1 phenotype[100].

The lipid rich core of atherosclerotic lesions harbors various subtypes of macrophages as well as smooth muscle cells[29, 101]. CD163 expressing, hemoglobin-haptoglobin utilizing macrophages have been defined as Mhem subtype. These macrophages are linked to hemorrhaging atherosclerotic plaques and secrete inflammation resolving IL-10 cytokine[102].

Atherosclerotic plaques are rich in oxidized phospholipids such as oxidized 1-palmitoyl-2-arachidonoyl-sn-3-glycero-phosphorylcholine (OxPAPC). OxPAPC plays a role in macrophage polarization into a unique phenotype known as Mox. OxPAPC uptake upregulates the expression of Nrf2 transcription factor, which results in switching of M1 as well as M2 macrophages into CCR2 expressing Mox macrophages[103, 104]. Furthermore, cytoplasmic FABP-dependent accumulation of acetylated low-density lipoprotein (Ac-LDLs) results in the formation of foamy macrophage phenotype. This macrophage subtype has been widely researched for the role of cholesterol ester dependent lipid droplet formation and inflammatory cytokine production in atherosclerotic plaques[105]. Similarly, other *in vitro* experiments performed with the THP-1 human monocyte cell line, describe FABP-dependent foam cell formation upon monocyte/macrophage differentiation in the presence of ox-LDL based CE, 7-ketocholesterol[106, 107, 108]. Lipid accumulating foam macrophages are also associated with insulin resistance development in obese patients. This highlights the importance of further evaluating the foam cell macrophages[109]. Gleissner *et al.* defined another subset of macrophages in atherosclerosis, polarizing in response to

CXCL4 signaling. When they polarized human monocyte-derived macrophages in the presence of CXCL4, they observed several differentially expressed genes between M-CSF and CXCL4 polarized macrophages. They also identified that despite its gene expression profile overlapping with M1 and M2 macrophages. Further transcriptome analysis identified CXCL4 polarized macrophages as novel macrophage phenotype defined as CXCL4-dependent M4 macrophages[110]. These overall macrophage subtypes associated with obesity-linked diseases are summarized in **Figure 4**.

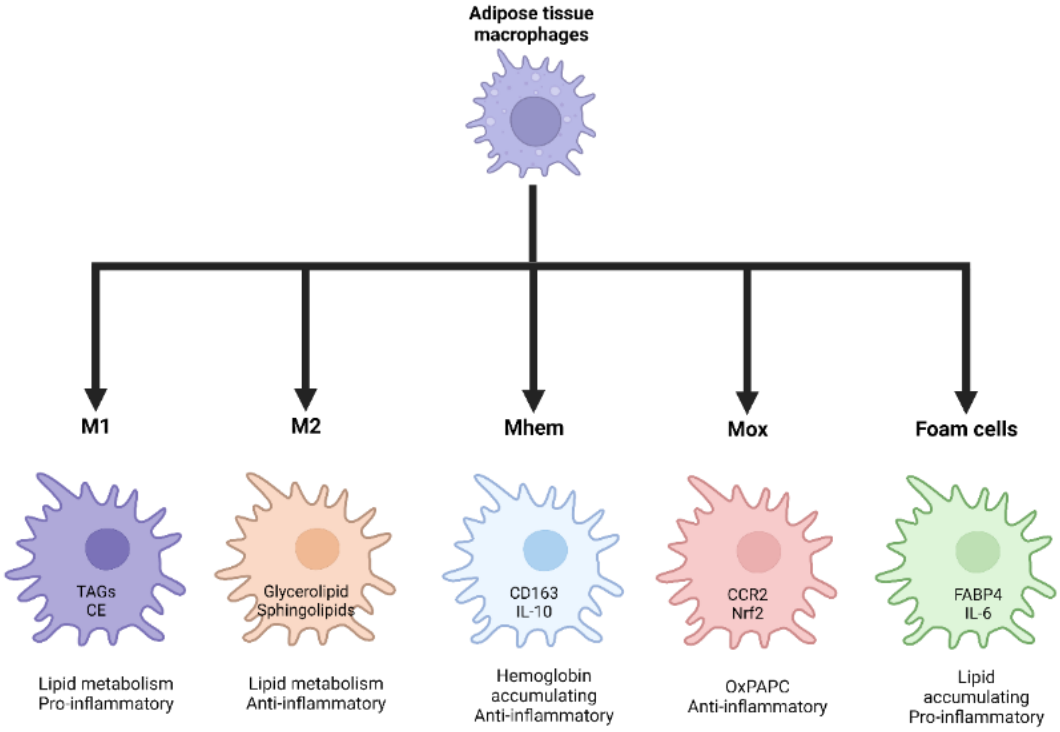

Figure 4: Macrophage phenotypic plasticity in atherosclerosis. *Adipose tissue resident macrophages are characteristically M2 subtype in lean individuals. Progression of obesity and atherosclerosis is associated with increased inflammation and altered metabolic content that modifies macrophage phenotype. This further aggravates inflammation and disease progression. Abbreviations enlisted in section 6.1.*

1.2.3 Macrophages as a link between atherosclerosis and cancer

CD36 expressing fatty acid accumulating macrophages have been reported in solid tumors as well as atherosclerosis[16, 18, 75] TREM2 expressing LAMs have been identified in primary colorectal cancer (CRC) and liver metastatic CRC as well as in adipose tissue of obese mice and humans[111]. MSR-1 expressing macrophages have

been well-defined in atherosclerosis and solid tumors[14]. Lipid accumulating macrophages as defined in the section 1.2.1 and 1.2.2 under distinct terminologies provide a further connecting link between TAMs and atherosclerotic plaque resident macrophages[18, 112].

In summary, the overall heterogeneous yet comparable phenotypes of macrophages within these two pathogenic conditions provide an understanding of the broad range of potential targets that can be identified and used as macrophage-based therapeutics for treating various inflammatory pathogenic conditions. Accumulating information about the influence of increased lipid accumulation in adipose tissue resident macrophages or in tumor infiltrating macrophages and consequently altered phenotype emphasizes the importance of further research on lipid metabolism in macrophages. As such, a better understanding of the lipid-based metabolic pathways could provide novel therapeutic targets in cancer and other inflammatory conditions.

1.3 Lipid droplet biology

Lipid droplets are distinct organelles responsible for storing neutral lipids in the form of sterol esters (SE) or triacylglycerols (TAGs), enveloped in a phospholipid monolayer. They are found in almost every eukaryotic cell type. Although initially identified as inert storage organelles, LDs are now considered to manipulate cellular signaling by regulating fatty acid storage. As mentioned in above sections, LD accumulation within immune cells, adipocytes, and, hepatocytes is linked to infectious or inflammatory and anti-inflammatory conditions[113, 114]. Excessive intracellular fatty acid accumulation triggers the formation of LDs in order to prevent increased lipotoxicity due to free fatty acid content within the cell[115]. Moreover, owing to the increased importance of LDs in mediating diseases such as obesity, atherosclerosis, etc. research on LD biology has accelerated dramatically.

1.3.1 Lipid droplet biogenesis

Lipid droplets are ubiquitous and dynamic energy-storing organelles. Apart from their involvement in lipid metabolism, LDs are also recognized widely for their involvement in ER stress management, autophagy, and pathogenic infections such as Mycobacterium tuberculosis, or LPS-induced septic shock[116, 117, 118].

LD formation begins when cellular uptake of fatty acid is higher than the utilization capacity. Under these conditions, LD formation occurs on the ER membrane and LDs can range in size from 100 nm to 100 µm. The lipids stored within LDs are of varying compositions ranging from SEs, TAGs, retinyl esters, waxes or ethers[99]. The process of LDs formation is not clearly understood. However, three main steps involved in LD synthesis are clearly defined. These steps are neutral lipid synthesis, neutral lipid accumulation and lens formations and lastly, droplet formation[99]. Enzymes involved in each step are enlisted in **Table 2.**

Fatty acids taken up via CD36 or cytosolic FABP4 and other surface scavenger receptors are first converted into fatty acyl CoA (an active form) by the enzyme fatty acyl CoA synthetase[28, 67, 119]. Enzymes including ACAT1 and 2 (acyl CoA:cholesterol transferase 1 & 2) and DGAT1 and-2 (diglycerol acyl transferase 1 & 2) catalyse the process of neutral lipid synthesis and are localized on the ER membrane[120]. ACAT1 & 2 utilize cholesterol and fatty acyl CoA to synthesize sterol esters while DGAT1 & 2 utilize 1, 2-diacylglycerol and fatty acyl CoA to synthesize triacylglycerols[121]. These enzymes catalyse the ester bond formation between the fatty acyl CoA and hydroxyl group of cholesterol or DAG[122]. Furthermore, two enzymes LDAF-1 (Lipid droplet assembly factor-1) and seipin together form a ≈600kDa oligomeric complex, which binds to TAGs, catalyses LD formation, and determines the site of LD formation on the ER membrane[123]. The next step in LD synthesis involves lens formation or blistering that occurs on the ER membrane. A number of enzymes catalyse these steps, for example, Fat storage inducing transmembrane protein (FIT1 & 2), which are present on the ER membrane and binds directly to the TAGs and SEs and mediates the critical step of separating the growing lipid droplets from the ER for establishing a separate organelle based storage[124]. The last step is defined as stabilization of mature LDs and is maintained by perilipin-3 & -4 enzymes [125].

Table 2: List of processes and enzymes involved in LD biogenesis

Process	Enzyme	Enzyme function	Enzymes/ Receptor location	Reference
Fatty acid uptake	CD36 FABP4 & FABP5	Scavenging and binding to free fatty acids, respectively	Cell surface & Cytoplasm	67, 119, 126
Synthesis of fatty acyl CoA	Fatty acyl CoA Synthetase	Thioester bond formation between fatty acid moiety and CoA	Cytosol	119
Synthesis of neutral lipids	ACAT1 & 2 DGAT1 & 2	Ester bond formation	ER membrane	122
ER membrane location determination	Seipin	Determines exact site to initiate TAG accumulation on ER membrane	ER membrane	123
ER membrane location determination	LDAF-1 Complex	Binds and accumulates TAGs within the lens and dissociates from seipin	ER membrane	123
Detaching LD from ER membrane	FIT1 & 2	Initiates lens formation/blistering at the ER membrane	ER membrane	124
Stabilization of free LDs	Perilipin-3 & -4	Recruited to the LD membrane to stabilize LDs	Cytosol	125

1.3.2 Lipid droplet formation, ER homeostasis, stress response, and autophagy

As described above, LDs are synthesized on the ER membranes which are important cellular organelles facilitating central cellular processes including calcium homeostasis, lipid metabolism, post translational modifications, and protein trafficking as well as protein synthesis. A number of physiological processes modulate ER homeostasis causing ER stress. These result in activation of intracellular signaling pathways referred to as unfolded protein response (UPR) which counteracts to maintain ER homeostasis and cell survival. Moreover, prolonged or excessive activation of UPR signaling leads to self-destruction and induction of apoptosis[127]. Three ER membrane-bound stress response proteins including inositol requiring enzyme-1 α (IRE-1α), ATF6α, and PERK regulate ER stress responses. Abundant mRNA levels of down-

stream targets of these proteins include XBP-1(spliced), AMP dependent transcription factor4 (ATF4), and 78 kDa glucose related protein (GRP78), respectively, can be used as markers for ER stress detection[127, 128, 129].

Free fatty acid accumulation and ER stress response is reported in various cell types. Cui *et al.* demonstrated that exposure of β cells to free fatty acids results in upregulation of ER stress markers including ATF6 and phosphorylated PERK and IRE-1α. This is also associated with ER stress signaling induced apoptosis[130]. Another report discussing the effect of saturated and unsaturated fatty acids in activating ER stress response in mammary epithelial cells (MEC) describes that saturated FFAs induce ER stress response in MEC and causes increased apoptosis compared to unsaturated FFAs[131]. An important effect of FFAs and active ER stress signaling is the downstream stimulation of genes associated to lipogenesis. ER stress related IRE-1α is a kinase that oligomerizes and autophosphorylates itself, activating its endoribonuclease activity. Activated IRE-1α further downstream excises a 26 nucleotide fragment from XBP-1 mRNA that gives rise to its functional form, spliced XBP-1 mRNA **(Figure 5)**[132]. The spliced XBP-1 (transcription factor) translocates into the nucleus and regulates expression of genes associated with lipogenesis including DGAT 2, acetyl CoA carboxylase (ACC) and stearyl CoA desaturase-1(SCD-1)[127, 133]. This response plays an important role in regulating FFA levels and storing them in the form of lipids. Further steps involved in LD biogenesis are described in section 1.3.1.

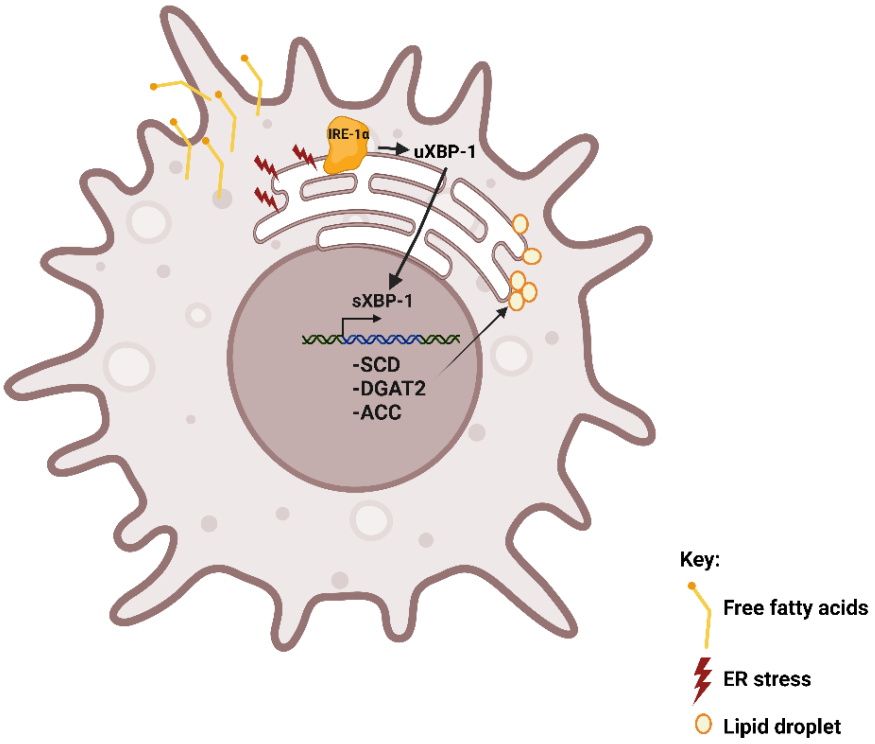

Figure 5: ER stress response pathway as seen in macrophages. *Free fatty acid uptake induces IRE-1α dependent ER stress response pathway, resulting in downstream XBP-1 splicing and translocation into the nucleus. sXBP-1 activates expression of genes associated with LD biogenesis.*

As discussed above, the ER stress response maintains ER homeostasis through UPR and prevents cell death. Another outcome in response to ER stress is autophagosome formation and subsequent cellular autophagy. Autophagy is a catabolic process associated with ‘’self-eating’’ under stressful cellular conditions. One such stressful trigger is nutrient deprivation, which instigates autophagy and involves lysosome-mediated degradation of macromolecular substances including complete organelles for the purpose of energy generation. There are three forms of autophagy, macroautophagy, microautophagy, chaperone mediated autophagy (CMA) which are differentially activated under varying cellular conditions[134]. During autophagy activation in starved cells, the cells can also utilize lipid stored in LD organelles for energy generation by a process known as lipolysis or lipophagy. Autophagy associated lipolysis can occur via any of the three autophagic pathways[135, 136]. Albeit excessive lipid accumulation also activates autophagy in order to protect the cell from lipotoxicity-induced stress. An example of this is reported in cells other than macrophages. Treatment of CAL27 and UM1 cell lines with oleic acid resulted in increased

LD formation. However, further lipid accumulation in turn activated the process of lipophagy to protect cells from lipotoxicity due to excessively accumulated lipids[137].

These reports emphasize on the fine connection between the processes of ER stress response, LD formation, autophagy, and lipotoxicity and a reasonable balance is required for maintaining the cell survival state and the corresponding phenotype.

1.3.3 Lipid droplet metabolism during myelopoiesis

Apart from playing a role in myeloid cell-mediated disease progression, lipid storage and metabolism play a role during myelopoiesis (the process of myeloid cell generation). Bone marrow cavity comprises of a large amount of fat cells that constitute 50 to 70% of the bone marrow volume of an adult human and called as bone marrow adipose tissue (BMAT). The BMAT is no longer defined as just space fillers but rather recognized to play a vital role in haematopoiesis[138]. BMAT is a major source of lipid and fatty acids within the bone cavity and influences the process of haematopoiesis[139]. The significant role of lipids as a fuel as well as a macromolecule source in both hematopoietic stem cell generation and asymmetric differentiation is widely documented[140]. Hematopoietic stem cell (HSC) gives rise to myeloid progenitors that differentiate into various subtypes of myeloid compartment including monocytes, granulocytes, macrophages, red blood cells, and megakaryocytes. The role of non-oxidative lipid metabolism during haematopoiesis & myelopoiesis is well established. It encompasses metabolic pathways for the production and degradation of sterols, phospholipids, sphingolipids and glycerolipids. Altered LDL uptake and increased cholesterol accumulation during myelopoiesis is reported in leukemic patients. Increased cholesterol levels as observed in cardiovascular diseases and atherosclerosis are linked to increased myelopoiesis[141]. LPL lipoprotein lipase (LPL) dependent release of free fatty acids is required for hematopoietic stem progenitor cell (HSPC) maintenance[142].

Altogether, these available reports discuss the importance of various enzymes involved in lipid metabolism in context to steady state myelopoiesis as well as during disease progression. Despite these available datasets regarding lipid metabolism in myelopoiesis, the role of lipid droplet synthesizing enzymes, namely, DGAT1 and DGAT 2 in this process are not yet researched.

2 Aims of the study

2.1 Aim 1: To investigate the role of oleate-mediated lipid droplet formation in human CD14$^+$ monocyte-derived macrophages

We recently reported in murine-based experiments that lipid droplet-mediated oleate storage plays an important role in CD206 expressing immunosuppressive M2- polarized TAM polarization. Moreover, pharmacological inhibition of DGAT1 & 2 dependent lipid droplets reverses the immunosuppressive M2 polarized TAMs as observed in a T cell proliferation dependent manner. Herein we investigated the role of oleate-dependent LD formation in human monocyte-derived macrophages (human MoDM) and the effect of DGAT1 & 2 inhibition.

Therefore, we aimed to study the effect of oleate supplementation during human CD14$^+$ monocyte-derived macrophage polarization as well as evaluate the effect of DGAT1 & 2 inhibitor treatment to curtail oleate driven effect.

2.2 Aim 2: Oleate-dependent polarization into CD206$^+$ tumor-associated macrophage phenotype is independent of IL-4 signaling

Available literature highlights the role of IL-4 signaling, fatty acid oxidation, and lipid metabolism in mediating CD206$^+$ immunosuppressive macrophages. However, the overall metabolic dependency on lipids as well as IL-4 signaling in immunosuppressive macrophages is controversial. Herein we investigate the role of lipid droplet formation and fatty acid oxidation as important drivers of macrophage phenotypic changes independent of IL-4 signaling.

Therefore, we hypothesized that oleate-dependent immunosuppressive phenotype is independent of IL-4 signaling and treatment with CPT-1a enzyme inhibitor, etomoxir reduces this CD206 expressing immunosuppressive phenotype.

2.3 Aim 3. To identify the role of the enzymes DGAT1 & 2 in regulating myeloid compartment and macrophage phenotype

We previously reported that DGAT1 & 2 play an essential role in regulating immunosuppressive macrophage phenotype and subsequent pharmacological combined inhibition of both enzymes reverses the immunosuppressive phenotype. Furthermore, recent research highlights the role of individual enzymes in modulating macrophage phenotype. Herein we generated myeloid compartment specific *Dgat1 & 2* knockout mice lines.

Therefore, the aim of this study was to generate novel genetic tool and perform basic assessment for evaluating role of the individual enzymes DGAT1 and DGAT2 in regulating myeloid cell phenotype.

3 Materials and Methods

3.1 Materials

3.1.1 List of instruments

Table 3 Instruments used in this study

Instrument	Company
Centrifuge 5810R	Eppendorf, Hamburg, Germany
CO2 cell culture incubator	Thermofisher Scientific, Waltham, MA, USA
HERAsafe Biological Safety Cabinets	Thermofisher Scientific
HLC Heating Thermomixer	DItabis, Phorzheim, Germany
Infinite® F50 plate reader	Tecan Group, Männedorf, Switzerland
T 3000 Thermocycler	Biometra, Göttingen, Germany
Waterbath 100	Pfm medical AG, Cologne, Germany
NovoSeq 6000	Illumina San Diego, CA
Tapestation D1000	Agilent, Santa Clara, CA
Primovert light microscope	Zeiss, Oberkochen, Germany
Agarose gel electrophoresis chambers	Peqlab, Erlangen, Germany
Seahorse XF 96 Extracellular flux Analyzer	Agilent, Santa Clara, CA
LAS Minifluorescence Image analyser	Fujifilm, Tokyo, Japan
StepOne Plus Real time PCR System	Agilent, Santa Clara, CA
Transilluminator	Peqlab
Quantstudio 5 Real time PCR systems	Thermofisher Scientific
Mini protean system for western blot	Biorad, Feldkirchen, Germany
FACS Canto II	BD, Franklin Lakes, NY, USA
FACS LSR II	BD, Franklin Lakes, NY, USA
Non-CO_2 incubator	Thermofisher Scientifc

3.1.2 List of antibodies

Table 4: Murine antigen specific antibodies used for flow cytometry

Target antigen	Clone	Fluorochrome	Catalog number	Company	Dilution
CD127	A7R24	APC	17-1271-82	eBioscience	1:100
Gr-1	RB6-8C5	APC	108408	Biolegend	1:500
MHC class II	M5 114.15.2	APC		Biolegend	1:1200
CD11b	M1/70	APC Cy7	101226	Biolegend	1:100
CD34	HM34	PE	128610	Biolegend	1:50
Ly6C	HK1.4	PE Dazzle	128044	Biolegend	1:300
Sca-1	D7	PE Cy7	108114	Biolegend	1:100
cKIT	2B8	BV 785	105841	Biolegend	1:200
FCRγ	90	BV 711	101337	Biolegend	1:200
Gr-1	RB6-8C5	BV 711	108443	Biolegend	1:500

Ly6G	1A8	Pacific blue	127612	Biolegend	1:200
F4/80	BM8	Alexa 700	123130	Biolegend	1:300
CD206	C068C2	Alexa Fluor 488	141709	Biolegend	1:50
Lineage cocktail	145-2C11; RB6-8C5; RA3-6B2; Ter-119; M1/70	FITC	133302	Biolegend	1:100
Zombie violet		Viability dye	423102	Biolegend	1:1000

FITC: Fluorescein isothiocyanate PE: Phycoerythrin APC: Allophycocyanin

BV: Brilliant violet

Table 5: Human antigen specific antibodies used for flow cytometry

Target antigen	Clone	Fluorochrome	Catalog number	Company	Dilution
CD14	63D3	APC	367118	Biolegend	1:50
CD4	GK1.5	APC	100412	Biolegend	1:1000
CD163	GHI/61	APC-Cy7	333621	Biolegend	1:200
CD204	REA460	PE	130-123-327	Miltenyi Biotech	1:100
CD200R1	OX-108	PE Cy7	329311	Biolegend	1:200
CD206	19.2	eFluor450	48-2069-41	eBioscience	1:50

Table 6: Human antigen specific antibodies used for western blot

Target antigen	Host	Catalog number	Company	Dilution
β-actin	Mouse/IgG1	AC5441	Sigma Aldrich	1:1000
LC-3B	Rabbit/IgG	PA1-46286	Invitrogen	1:1000

3.1.3 List of primers

Table 7: Primers for genotyping

Mouse strain	Primer target	Primer sequence (5' to 3')
DGAT1$^{fl/fl}$	DGAT1 Flox- forward	GGCTGTGCTCATGTATGTCC
DGAT1$^{fl/fl}$	DGAT1 Flox Reverse	CCCTGCAAGTTGCTGCTG
DGAT2$^{fl/fl}$	DGAT2 Flox- forward	TGCCAGTAGGTGCAAAGTAC
DGAT2$^{fl/fl}$	DGAT2 Flox Reverse	AGCCACTGAAGTCACTAAGG
LysMcre	LysMcre	CCC AGA AAT GCC AGA TTA CG
LysMcre	LysMcre	CTT GGG CTG CCA GAA TTT CTC
LysMcre	LysMcre	TTA CAG TCG GCC AGG CTG AC

Table 8: Primers for human specific real-time PCR and conventional PCR

All primers were purchased from TIBMOLBIO (Berlin, Germany)

Primer name	Sequence
Rpl13a forward	AAAGCCAAGATCCACTACCG
Rpl13a reverse	GGAATTAACAGTCTTTATTGGGCTC
FABP4 forward	ACTGGGCCAGGAATTTGACG
FABP4 reverse	CTCGTGGAAGTGACGCCTT
CPT1a forward	TCCAGTTGGCTTATCGTGGTG
CPT1a reverse	TCCAGAGTCCGATTGATTTTTGC
CD36 forward	GGCTGTGACCGGAACTGTG
CD36 reverse	AGGTCTCCAACTGGCATTAGAA
CCR2 forward	TGCAAAAAGCTGAAGTGCTTG
CCR2 reverse	CAGCAGAGTGAGCCCACAAT
MSR1 forward	CCAGGTCCAATAGGTCCTCC
MSR1 reverse	CTGGCCTTCCGGCATATCC
IL-6 forward	ACTCACCTCTTCAGAACGAATTG
IL-6 reverse	CCATCTTTGGAAGGTTCAGGTTG
Gata3 forward	GCCCCTCATTAAGCCCAAG
Gata3 reverse	TTGTGGTGGTCTGACAGTTCG
Mrc 1 forward	CTACAAGGGATCGGGTTTATGGA
Mrc 1 reverse	TTGGCATTGCCTAGTAGCGTA
XBP-1 forward	CTGAAGAGGAGGCGGAAGC
XBP 1 reverse	AATACCGCCAGAATCCATGG

3.1.4 Chemicals and media

Buffers used in flow cytometry

Magnetic–activated cell sorting (MACS) buffer (10X)

- 5 g Bovine serum albumin (BSA) (Fraction V) (Sigma-Aldrich, St. Louis, USA)
- 100 mL phosphate buffered saline (PBS) (1X), (Gibco, Darmstadt, Germany)

Erythrocyte lysis buffer (pH 7.3)

- 8.9 g NH_4Cl (Merck, Darmstadt, Germany)
- 1 g $KHCO_3$ (Merck)
- 0.038 g ethylenediaminetetraacetic acid (EDTA) (Sigma Aldrich)
- 1 L distilled water

Buffers used in western blot

Sodium dodecyl sulfate (SDS) running gel (8%, 10mL)

- 40% acrylamide mix (2 mL) (Biorad, Feldkirchen, Germany)
- 1.5 mM Tris base pH 8.8 (2.5 mL) (Carl Roth, Karlsruhe, Germany)
- 10% SDS (0.1 mL) (Carl Roth)
- 10% Ammonium persulfate (APS) (0.1 mL) (Sigma Aldrich)
- Tetramethlyethylenediamine (TEMED) (0.01 mL) (Biorad)
- Distilled water (5.3 mL)

Stacking gel (5%) (3 mL)

- 40% acrylamide mix (0.38 mL) (Biorad, Feldkirchen, Germany)
- 1.0 mM Tris base pH 6.8 (0.28 mL) (Carl Roth, Karlsruhe, Germany)
- 10% SDS (0.03 mL) (Carl Roth)
- 10% Ammonium persulfate (APS) (0.03 mL) (Sigma Aldrich)
- Tetramethlyethylenediamine (TEMED) (0.003 mL) (Biorad)

Protein lysis buffer

- Complete protease inhibitor cocktail (Merck)
- 1 mM NaF (Sigma Aldrich)
- 1 mM Na_3VO_4 (Merck)
- Radioimmunoprecipitation assay (RIPA) buffer (Sigma Aldrich)

Laemmli buffer 6X

- 60 mM Tris-HCL pH 6.8 (Carl Roth)
- 12% SDS (Carl Roth)
- 47% glycerol (Carl Roth)
- 0.06% bromophenol blue (Merck)
- 12.5% β-mercaptoethanol (Sigma Aldrich)

Electrophoresis buffer (10X)

- 144 g Glycine (Carl Roth)
- 30 g Tris base (Carl Roth)
- 10 g SDS (Carl Roth)
- 1 L distilled water

Transfer buffer (10X)

- 144 g Glycine (Carl Roth)
- 30.3 g Tris base (Carl Roth)
- 1L distilled water

Transfer buffer (1X)

- 100 mL Transfer buffer (10X)
- 200 mL 100% methanol (Merck)
- 700 mL distilled water

Tris-buffered Saline (TBS) pH 7.6 (10X)

- 24 g Tris base (Carl Roth)
- 88 g NaCl (Carl Roth)
- 1 L distilled water

Tris-buffered Saline-Tween20 (TBS-T) (1X)

- 100 mL TBS pH 7.6 (10X)
- 1 mL Tween (Carl Roth)
- 900 mL distilled water

Blocking buffer (5%)

- 2.5 g BSA (Fraction V) (Sigma Aldrich)
- 50 mL TBS-T (1X)

Cell culture and *in vitro* assay media

RPMI medium 1640 (1X) (Gibco, Darmstadt, Germany)

- 10% Fetal Bovine Serum (FBS) (Sigma Aldrich)
- 10% Penicillin-Streptomycin (Thermofischer Scientific)

DMEM medium (1X) (Gibco, Darmstadt, Germany)

- 10% Fetal Bovine Serum (FBS) (Sigma Aldrich)
- 10% Penicillin-Streptomycin (Thermofischer Scientific)

3.1.5 Mouse strains

Twelve to 20-week-old mice were used for the experiments. Wild type (WT) C57BL/6j were purchased from Charles River (Sulzburg, Germany). *Dgat1$^{fl/fl}$-LysMcre* and *Dgat2$^{fl/fl}$-LysMcre* mice were bred at the Charité animal facility under specific pathogen free (SPF) conditions. For subsequent analysis, mice were anaesthetized with isoflurane followed by cervical dislocation and organ harvest. All animal protocols were approved by the regional animal study committee of Berlin (LaGeSo, Berlin, Germany) and were accordingly conducted.

3.2 Methods

3.2.1 Genotyping

Genotyping of murine ear biopsies was done according to user manual of Nucleo Type Mouse PCR provided by the manufacturer (MACHEREY NAGEL, Düren, Germany). The ear biopsies were shortly digested in 100 µl of Lysis reagent M supplemented with 20 µg/ml proteinase K (Sigma-Aldrich) for 10 mins at room temperature by shaking at 800 rpm, followed by heat inactivation at 98 °C for 3mins at 300 rpm. The samples were directly used in the polymerase chain reaction (PCR) based genotyping. The primers were purchased from TibMolBiol and are listed in section 3.1.3, **Table 7**.

3.2.2 Fatty acid albumin conjugation

Sodium salt of oleate was solubilized in double distilled water in water bath at 37 °C. Fatty acid free bovine serum albumin (BSA) was dissolved in appropriate cell culture medium (DMEM for murine and RPMI for human cell culture) and was filter sterilized with 0.22 µM syringe filter prior to use. This was used for conjugation of Na-oleate at a molar ratio of 8:1 (Na-Oleate:BSA). The conjugated solution was freshly prepared prior to each experiment.

3.2.3 Inhibition of fatty acid oxidation and lipid droplet formation

Lipid droplets (LD) formation was inhibited using reagent-based inhibitors A922500 (Sigma Aldrich) and PF-06424439 (Sigma Aldrich) targeting DGAT1 & 2 enzymes

respectively (diacyl glycerol transferase 1 and 2). Various chemical inhibitor concentrations were tested by serial dilution to identify appropriate dilution for human monocyte-derived macrophage treatment.

3.2.4 Inhibition of foam cell formation

Lipid accumulation and foam cell formation was inhibited using reagent based chemical inhibitor SB203580 (Selleck chemicals). Appropriate 10 µM dilution was prepared as per company instructions. It was used to treat human monocyte-derived macrophages during seven days polarization process.

3.2.5 PBMC isolation from healthy donor blood sample or buffy coats

Healthy donor blood or buffy coat concentrates obtained from Deutsches Rote Kreuz (DRK) were used for PBMC isolation prior to $CD14^+$ monocyte sorting. Heparinized blood samples were diluted 1:1 using sterile 2% FCS-PBS. PBMCs were separated using sepmate tube-based layering of 15 mL ficoll followed by layering of 25 mL diluted healthy donor blood sample. The layered samples were centrifuged at room temperature for 10 min at 400 g. The upper layer from the sepmate tubes was collected in 50 mL falcon tubes and washed twice with 2 % FCS-PBS. The PBMC cell pellet was re-suspended in 1x MACS buffer and used for $CD14^+$ monocyte or $CD4^+$ T cell magnetic sorting. For isolation of PBMCs from buffy coats, samples were diluted 1:2 in sterile 1xPBS and ficoll based density gradient centrifugation was performed by carefully overlaying 25 mL of diluted buffy coat sample on 15mL ficoll in falcon tubes and centrifuged at 1200 g for 25 min at room temperature. The cloudy white layer of PBMCs is collected with a pasteur pipette and washed with 1x MACS buffer twice and re-suspended in 1x MACS buffer for further isolation.

3.2.6 In vitro polarization of human monocyte-derived macrophages and murine bone marrow-derived macrophages

$CD14^+$ monocytes isolated, sorted, and washed as mentioned in section 3.2.5, were seeded in 24-well tissue culture plates at a density of 3×10^5 cells/well/1.5 mL of complete RPMI media preparation as described in section 3.1.4. The culture medium was supplemented with GM-CSF or M-CSF and 0.2 mM oleate conjugated to BSA.

The cells were polarized for a period of 7 days. The media was replenished with freshly prepared oleate and GM-CSF/M-CSF after every 48 h.

Bone marrow-derived myeloid cells were obtained by flushing murine tibia and femur were flushed with sterile 1xPBS and erythrolysis was performed using erythrolysis buffer (preparation described in section 3.1.4). Afterwards, PBS washed cells were used for single cell suspension preparation in complete DMEM medium (preparation as mentioned in section 3.1.4). The culture medium was supplemented with 40 ng/mL of GM-CSF. The cells were plated in delta petri dishes for 24 h following which only non-adherent myeloid progenitors were collected and further cultured in 6-well plates at a cell density of 3 x 10^6 cells/1.5 mL. The polarization was carried out for 6 days, supplemented with 0.2 mM Oleate-BSA and 40 ng/ml of GM-CSF. The supplements and medium was renewed every 48 h.

3.2.7 Flow cytometric staining of polarized human and murine macrophages

The 7-days polarized macrophages were harvested on the last day of polarization by adding 5 mM EDTA containing 1xPBS into each well. The plate was incubated with EDTA-PBS for 10 min on ice, followed by addition of 1x PBS to neutralize the EDTA amounts and the cells were collected by carefully scraping off with 1 mL pipette tips. The cells were washed with 1x MACS buffer (preparation as mentioned in section 3.1.4).

The murine bone marrow-derived macrophages were collected in 1x PBS by carefully scrapping off with a 12 cm cell scraper from the 6-well plates.

When required the cells were stained with zombie violet in 1xPBS. Following which the cells were washed and re-suspended in 1x MACS buffer. The surface antibody staining was performed as per standard staining protocols for 15 mins on ice. The cells were washed and re-suspended in 200 µL MACS buffer for acquisition. For BODIPY based staining of LDs, the cells were labelled with 0.2 µg/mL of BODIPY® 493/503 in 1x PBS at 37 °C in CO_2 incubator for 30mins. Following the staining, cells are washed with 1x MACS buffer and further stained with surface markers as and when required.

3.2.8 T-cell suppression assay

CD4+ T cells isolated from human PBMCs or murine splenocytes with >98% purity were washed with 1x PBS to remove traces of proteins from medium or MACs buffer and were stained with 0.5 µM of carboxyfluorescein diacetate succinimidyl ester (CFSE) in 1x PBS for 10mins at 37°C in CO_2 incubator. After incubation, cells were washed twice with complete RPMI medium to stop the staining reaction and were re-suspended in10 mL RPMI complete medium. *In vitro* stimulation of the CFSE labelled CD^{4+} T cells was performed by pre-coating the 96-well plate with 5 µg/mL of anti-CD3 (clone 2C11) and anti-CD28 (clone37.51E1). 3 x 10^5 cells/100 µL were then seeded in each well of 96-well plate. The CD3-CD28 stimulated T cells were further cultured in the presence or absence of 7-day polarized macrophages for 72 h. Afterwards, the cells were collected and washed and analyzed for CFSE dilution based cellular proliferation by flow cytometry using FACS CANTO II device (BD Biosciences, Franklin Lakes, USA and data was analyzed using the Flowjo software (Flowjo LLC, Ashland, USA).

3.2.9 PCR-based ER stress analysis

RNA samples were prepared from polarized human monocyte-derived macrophages. Specifically polarized samples with high cellular viability as measured with Annexin V/PI staining (as described in section 3.2.10) were used for RNA preparation. Following which 500ng of each RNA sample was used for cDNA preparation. 1µl of the prepared cDNA was then amplified using Q5 high-fidelity DNA polymerase. The PCR reaction was run in a thermocycler for 35 cycles. The PCR product was run in 3% agarose gel with 2 µl of 5x Rotaq buffer using 100 bp DNA ladder. Polarized human MoDM were treated with 0.5 µM thapsigargin for 6 hours and was used as internal positive control for spliced XBP-1 expression.

3.2.10 Flow cytometry Annexin V PI based cytotoxicity assay

In vitro polarized human macrophages were harvested and stained with surface marker antibody cocktail, as mentioned in section 3.2.7. Following this, cells were washed twice with 1 x annexin V binding buffer (Thermofisher Scientific) and stained with annexin V diluted in the same buffer followed by incubation at room temperature

for 5mins. Cells were stained with propidium iodide (PI) and directly measured by flow cytometry.

3.2.11 RNA isolation

Monocytes derived macrophages were harvested following 7 days of polarization using 5 mM EDTA in 1x PBS. The cells were incubated with 5 mM EDTA in 1x PBS for 10 min followed by addition of 1 mL PBS to dilute the effect of EDTA. The collected cells were washed twice with 1x PBS and re-suspended in 500 µL of TRIzol and stored at -80°C. This was followed by RNA isolation by adding chloroform. The air dried pellet of RNA obtained from the isolation was assessed for quantity and quality either at the nanodrop or at the Tapestation.

3.2.12 Tape station based-RNA quality check

RNA concentration and quality prior to bulk RNA sequencing was checked by the Agilent 4200 TapeStation System (Agilent Technologies, Santa Clara, California, US) and the high sensitivity RNA ScreenTape Assay (Agilent Technologies). The RNA sample was mixed with 1 µL of RNA sample buffer (Agilent Technologies) and spun down briefly to collect sample at the bottom of the tube. Afterwards, the sample was vortexed for 1 minute at 2,000 rpm and then heated at 72°C for 3 minutes. Next, the sample was placed on ice for 2 minutes. After incubation, the sample was spun down again and loaded into the TapeStation instrument (Agilent Technologies) in order to assess RNA concentration and RNA integrity number (RIN).

3.2.13 Bulk sequencing

RNA samples were prepared from polarized human monocyte-derived macrophages. Specifically polarized samples with high cellular viability as measured with Annexin V/PI staining (as described in section 3.2.10) were used for RNA preparation. Following which the RNA samples with only high RIN value (≥ 8.0) measured at the Tapestation (as detailed in section 3.2.12) were sequenced by Novogene at the NovoSeq 6000 (Illumina, San Diego, CA). The reads were aligned to the GRCh38 reference genome with GENCODE v33 annotations. The analysis was performed by the company. The differential gene expression analysis was performed with DESeq2

v1.30.0 (Love, Huber and Anders, 2014). The volcano plots were visualized with the *EnhancedVolcano* package in R software (version 2.4.2).

3.2.14 Real time PCR

Total RNA was isolated using the Qiazol (Qiagen, Hilden, Germany) based phenol-chloroform method as mentioned in section 3.2.11. Following which, 1ng of the total RNA was used for cDNA preparation. The cDNA was reverse transcribed using high capacity cDNA reverse transcription kit (Life Technologies GmbH, Darmstadt, Germany). Quantitative PCR (qPCR) was performed using the SYBR green Universal Master Mix, and the StepOnePlus Realtime PCR System (all Applied Biosystems) or Quantstudio 5 real time PCR systems (Thermofisher scientific). Primer and probes were purchased from TibMolBiol (Berlin, Germany) and are mentioned in section 3.1.3.

3.2.15 Western blot analysis

For immunoblotting of LC3B, 1 x 10^6 polarized human macrophages were lysed using RIPA buffer including complete protease inhibitors (Roche). 30µg of the whole cell lysate was run on 12% SDS-PAGE gels. Separated proteins were transferred to PVDF membranes at 250mA for 1-2hours. Following this, the membranes were blocked with 5% non-fat milk Tris buffered saline with Tween20 (TBST) solution for 1 h and incubated overnight with 1:1000 diluted primary antibody at 4°C on a rotator. The primary antibody was prepared in 5% non-fat milk TBST solution. On the next day, the membrane is washed with 1x TBST solution and incubated for 1hour at room temperature with 1:5000 diluted HRP-linked secondary antibody (Dako, Denmark) prepared in 5% non-fat milk TBST solution. The detection of the protein was performed on chemi luminescent image analyzer LAS-4000 mini using the ECL reagent (western blot detection reagent) (GE Healthcare, Chicago,IL). The results were obtained by densitometric analysis using the ImageJ (1.48V software developed by National Institute of Health and Laboratory for Optical and Computational instrumentation).

3.2.16 Fatty acid oxidation and mitochondrial respiratory analysis

Real time cellular oxygen consumption rate (OCR) as an indicator of respiration was measured using Seahorse XFe96 Analyzer (Agilent). For OCR measurement, XF DMEM assay medium (Agilent) was supplemented with 1 mM sodium pyruvate (Sigma Aldrich), 2 mM Glutamine (Agilent) and 10 mM glucose (Carl Roth). Prior to using the assay medium, the pH was adjusted to 7.4. Bone marrow-derived polarized macrophages were washed and seeded in prepared XF DMEM assay medium (Agilent) at a density of 100,000 cells/well in seahorse 96 well TC coated cell culture microplate (Agilent). The seeded microplates were centrifuged at 400g for 2 min/4°C for assuring complete attachment to the base (unattached suspension culture may interfere with consistent readouts). The microplates were incubated for 2 hours in a cell culture CO_2 incubator prior to performing the assay to ensure complete macrophage attachment. The microplates were then transferred to a non-CO_2 incubator at 37 °C for 60 min. OCR was measured under basal conditions in response to ATP synthase and electron transport chain complexes inhibition using 2 µM oligomycin (Sigma Aldrich) 1 µM FCCP carbonyl cyanide 4-(trifluoromethoxy) phenylhydrazone and 0.5 µM rotenone and antimycin A. For fatty acid oxidation analysis, the OCR was measured in presence of 4 µM etomoxir based inhibition of CPT1α.

3.2.17 Statistics

Statistical differences were determined by using student's t-test. All statistical analysis were performed using Graphpad prism software Version 8 (Graphpad Software, La Jolla, CA).

4 Results

4.1 Aim 1: Investigating the role of oleate-mediated lipid droplet formation in human CD14$^+$ monocyte-derived macrophages

4.1.1 Oleate-dependent polarization of human CD14$^+$ monocyte-derived macrophages

The aim of this study was to analyze the effect of oleate-dependent polarization in human CD14$^+$ monocyte-derived macrophages (human MoDM) as well as to study the effect of pharmacological inhibition of the enzyme DGAT1 & 2. Towards this goal, human PBMCs were either obtained from buffy coats (centrifuged fraction of uncoagulated blood samples that contains white blood cells and platelets after density gradient centrifugation) or from fresh blood drawn from healthy donors. Isolated CD14$^+$ monocytes were then polarized *in vitro* in presence or absence of oleate and M-CSF as a growth factor for seven days. A schematic representation is shown in **Figure 6A**. We previously published that treatment of murine bone marrow-derived macrophages (BMDM) with oleate and a combined 5 µM dose of DGAT1 & 2 inhibitor (iDGAT), reversed the oleate driven immunosuppressive phenotype[84]. While replicating the protocol with the human MoDM, this treatment strategy resulted in high cellular apoptosis as measured with Annexin V/ PI based live dead staining **(Figure 6B)**. Therefore, lower doses of the drug for treatment of human MoDM were titrated and the cell viability was analyzed based on Annexin V/ PI based live dead staining using flow cytometry as shown in **Figure 6B**. Herein, a ten-fold lower dose i.e. 0.5 µM concentration of inhibitors for the enzymes DGAT1 & 2 (iDGAT) were identified for treating human samples. This selected concentration, resulted in comparatively low cellular apoptosis **(Figure 6C)** as well as successfully reduced lipid droplet formation as observed based on BODIPY staining **(Figure 6D)**.

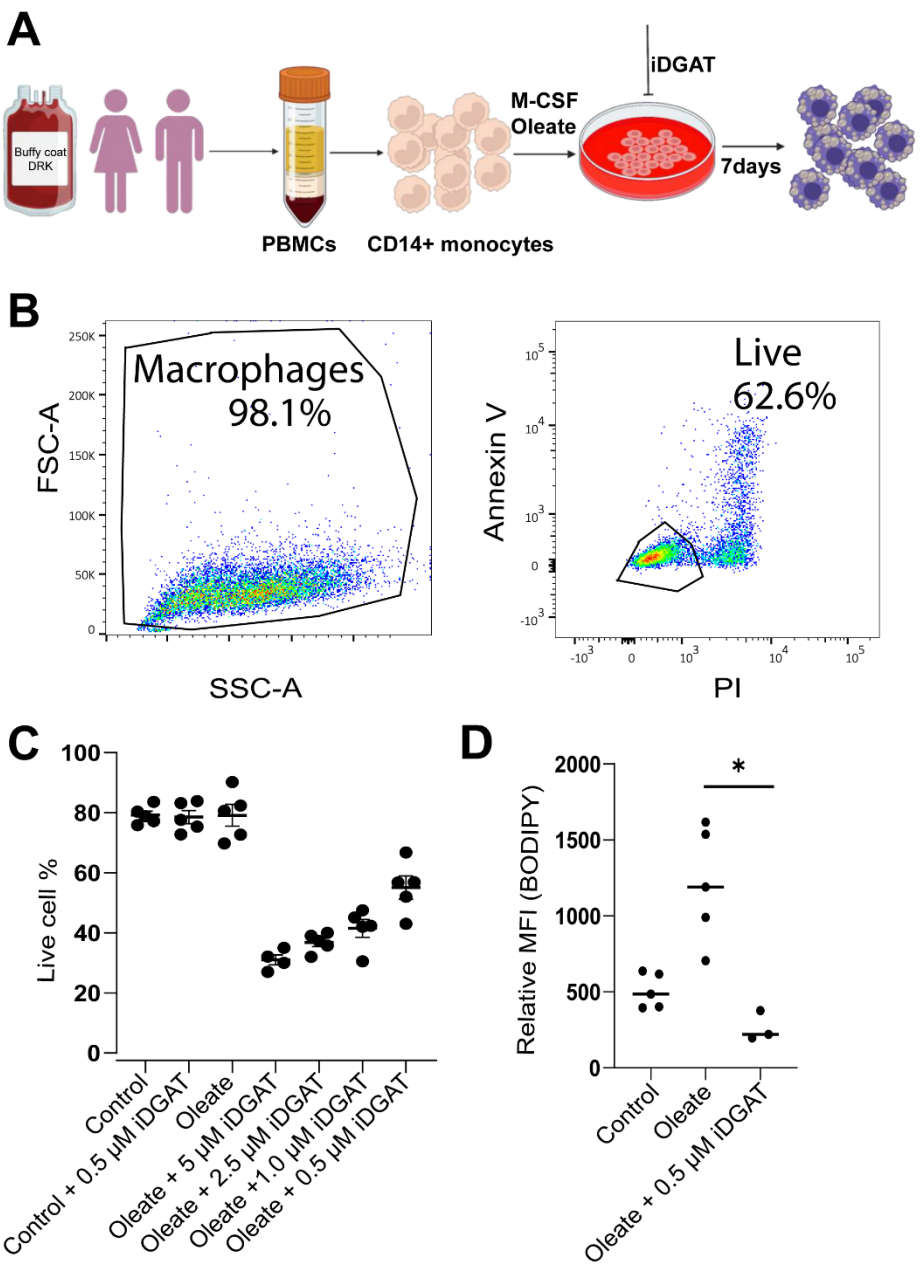

Figure 6: Oleate-dependent (0.2 mM) polarization of human CD14⁺ monocyte-derived macrophages and lipid droplet inhibition using pharmacological inhibitors for DGAT1 & 2 enzymes. *(**A**) Schematic representation of experimental setup. (**B**) Flow cytometry based Annexin V/PI gating strategy used for analyzing live/dead population (singlet gating not shown). (**C**) Live cell percentage in response to treatment with varying doses of combined DGAT1 & 2 inhibitor. (Shown as iDGAT in graph). (**D**) BODIPY based lipid droplet formation measured as relative MFI * P < 0.05. Error bars representative of standard error mean (SEM).*

4.1.2 *Immunosuppressive marker characterization of oleate-dependent human MoDM*

The next step of the study was to identify if oleate based lipid droplet (LD) accumulation manipulates the immunosuppressive phenotype of human MoDM as well as if treatment with iDGAT-mediated LD inhibition potentially reverses this phenotype. For this, we used the immunosuppressive marker CD206 as a phenotypic anchor to identify if supplementation of human monocytes with oleate results in immunosuppressive macrophages. Oleate-dependent polarization of human MoDM showed high expression of CD206. However, there was no significant increase in the expression compared to control group as polarization of MoDM with M-CSF itself increased the expression of CD206 in the control group **(Figure 7)**. Additionally, iDGAT treatment significantly downregulated the expression of CD206. However, since CD206 did not show significant upregulation in oleate-dependent MoDM, the next step was to select suitable markers that would show significant differences in oleate-dependent MoDM compared to control group and could be used to identify potential differences resulting from oleate treatment.

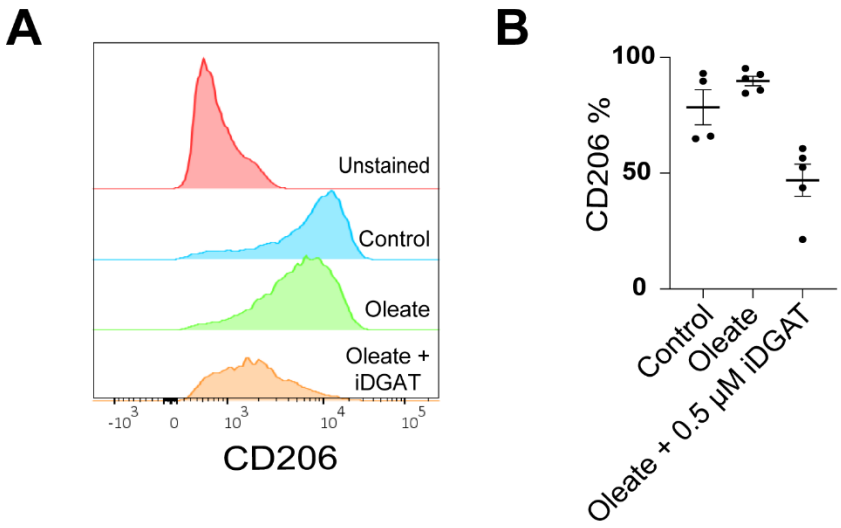

Figure 7: CD206 expression analysis in oleate-dependent human MoDM. *(**A**) Flow cytometry-based histograms depicting the relative expression of CD206 in control v/s treated samples. (**B**) The percentage of CD206⁺ macrophages in response to (0.2 mM) oleate or (0.2 mM) oleate + (0.5 µM) iDGAT in comparison to control.*

Available literature highlights that immunosuppressive markers CD163 and CD200R1 expression is upregulated in M-CSF as well as GM-CSF primed MoDM. Therefore, the polarization strategy using M-CSF or GM-CSF as growth factor was

applied, to compare if supplementation with oleate in the presence of either growth factor results in differential expression of these immunosuppressive markers. To this end, the expression of the following surface markers, CD163, CD200R1, CD14, and CD16 were tested in association to immunosuppressive macrophage phenotype. Flow cytometry-based analysis of relative mean fluorescence intensity (MFI), **Figure 8** indicated that expression of the markers was higher in M-CSF-dependent polarized MoDM in comparison to GM-CSF-polarized MoDM. This indicated that M-CSF growth factor is a better suited control for further evaluating the expression of the markers under investigation. Further analysis of the data revealed that oleate-dependent MoDM significantly downregulated the expression of immunosuppressive markers compared to the M-CSF control group. Additionally, the treatment with iDGAT inhibitor resulted in further downregulation of surface marker expression. The overall significant downregulation of the immunosuppressive markers in oleate-dependent M-CSF polarized MoDM indicated that oleate-dependent polarization resulted in significant phenotypic changes in human MoDM. To this end, the next step was to test functional changes in response to oleate treatment as well as to test lower doses of oleate to evaluate the reliability of this treatment strategy.

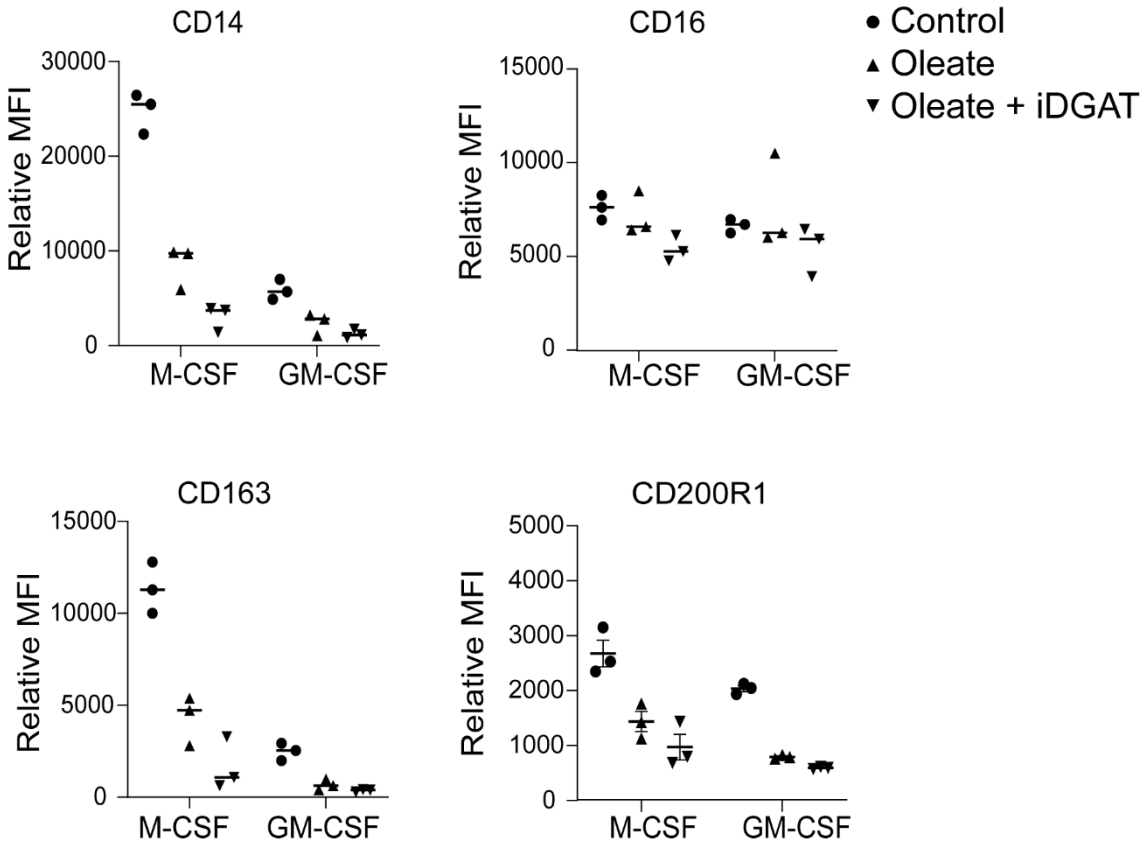

Figure 8: Human monocyte-derived macrophages polarized in the presence of 0.2 mM oleate and primed with M-CSF or GM-CSF. *Flow cytometry-based analysis of the relative MFI expression of surface markers. 0.5 µM dose of inhibitors of the enzymes DGAT1 & 2 defined as iDGAT.*

4.1.3 Functional characterization of oleate-dependent human MoDM

To test the immunosuppressive capacity of human MoDM, as a functional phenotype, T cell suppression assay was performed. The human monocyte-derived macrophages were co-cultured with $CD4^+$ T cells isolated from the same respective donor-derived $CD4^+$ T cells to avoid HLA cross reactivity. Prior to co-culture, the $CD4^+$ T cells were activated with CD3/CD28 stimulation and labelled with carboxyfluorescein diacetate succinimidyl ester (CFSE), which is used to detect the proliferative capacity of T cells based on flow cytometric analysis. The fluorescence of CFSE dye halves upon every cellular division **(Figure 9A)**. For this experiment, M-CSF- or GM-CSF-treated human MoDM were polarized in the presence of oleate for seven days with or without iDGAT inhibitor. Human MoDM polarized in the presence of M-CSF and oleate for seven days, when co-cultured with CFSE-labelled $CD4^+$ T cells for three days, resulted in a decreased proliferative index of the activated T cells. Further reduction was observed in T cells co-cultured with iDGAT-treated MoDM. However,

overall, no significant differences were observed in the proliferative index of the T cells **(Figure 9B)**. Further investigation of the proliferative index of CFSE-labelled $CD4^+$ T cells in co-culture with GM-CSF- and oleate-dependent human MoDM, **(Figure 9C)**, showed an insignificant reduced T-cell proliferative index. Furthermore, T cells co-cultured with iDGAT-treated human MoDM showed a tendency of increased proliferative capacity albeit no overall significant differences in proliferative capacity were observed. From these results we concluded, that oleate-dependent human MoDM polarized in presence of M-CSF or GM-CSF did not result in significant T-cell suppressive functional capacity.

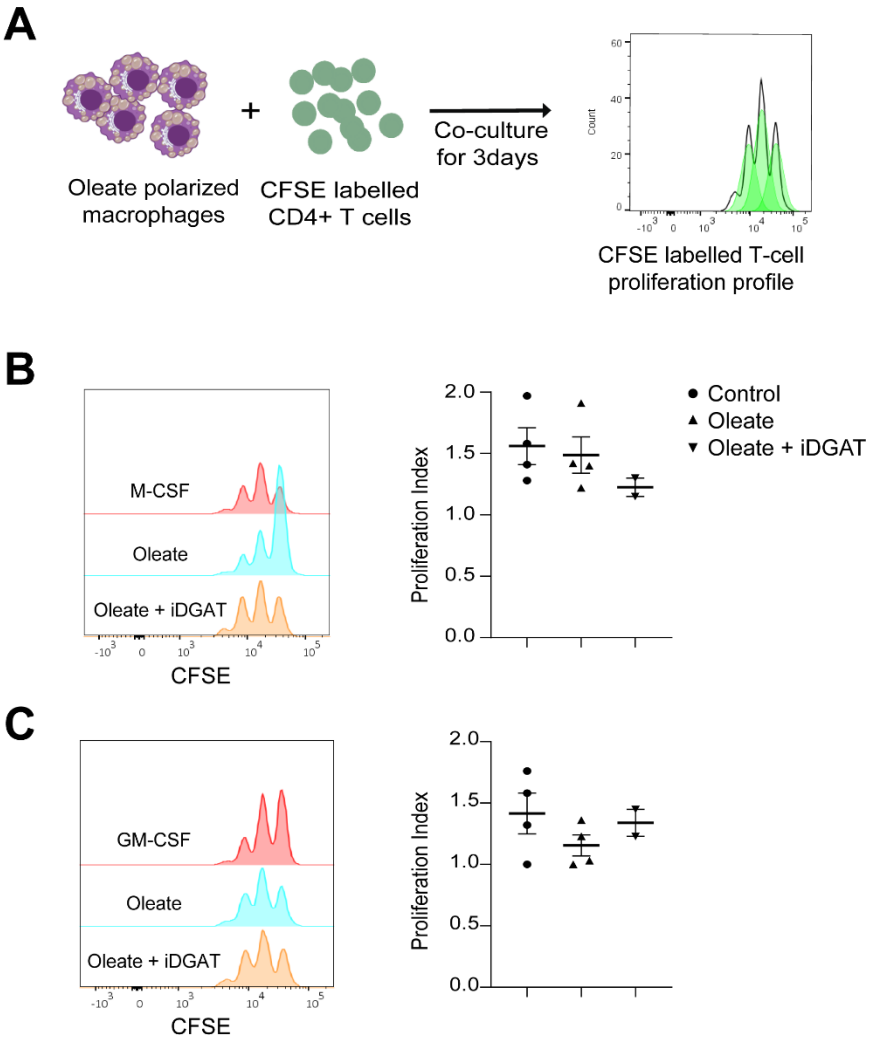

Figure 9: $CD4^+$ T-cell based analysis of immunosuppressive capacity of oleate-dependent human MoDM *(**A**) Schematic representation of the experimental set-up. (**B**) T-cell proliferative index in response to co-culture with M-CSF treated human $CD14^+$ monocyte-derived macrophages. (**C**) T-cell proliferative index in response to co-culture with GM-CSF treated human $CD14^+$ monocyte-derived macrophages. (0.2 mM oleate and 0.5 µM dose of inhibitors for enzymes DGAT1 & 2 were used).*

4.1.4 Human MoDM immunosuppressive marker expression in response to varying doses of oleate

As observed in the **Figure 8**, oleate-dependent human MoDM polarized in presence of M-CSF resulted in significant downregulation of various immunosuppressive markers. To determine dose-dependent expression changes, 0.2 mM, 0.1 mM, and 0.05 mM of oleate were tested. Increasing concentrations of oleate resulted in a significant downregulation of CD14, CD200R1 and CD163 in comparison to the control group **(Figure 10)**. Additionally, the presence of either 0.05 mM or 0.1 mM oleate did not result in significant downregulation of CD200R1 and CD163 compared to control group. Therefore, 0.2 mM oleate was decided as the final dose for further analysis. Additionally, iDGAT inhibitor treatment resulted in further downregulation of these surface markers with notably significant downregulation observed only in 0.2 mM oleate-dependent MoDM.

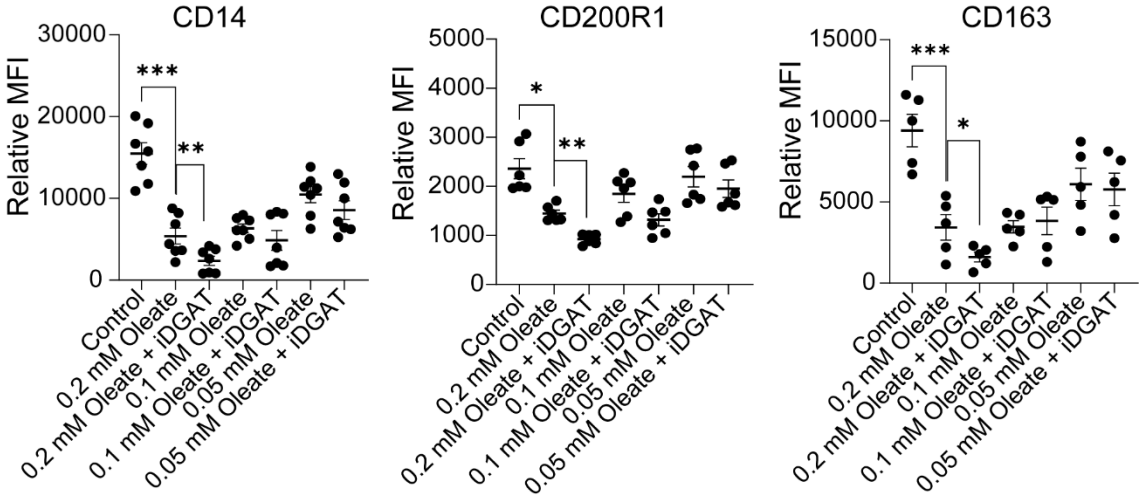

Figure 10: Dose-dependent effect of oleate on immunosuppression marker expression. *Flow cytometry-based analysis of the relative expression of surface markers in response to different doses of oleate ranging from 0.05 mM to 0.2 mM with or without 0.5 µM iDGAT inhibitor. *** P < 0.001 ** P < 0.01 * P < 0.05 ns P > 0.05. Error bars representative of standard error mean (SEM).*

4.1.5 ER stress response in oleate-dependent human MoDM

As observed in **Figure 10**, treatment with 0.5 µM dose of iDGAT inhibitor resulted in further downregulation of immunosuppressive markers as well as increased cellular apoptosis in some donor samples. DGAT1 & 2 enzymes are expressed on the ER membrane and subsequently synthesize lipid droplets on the ER membrane in order to regulate the levels of free fatty acids **(Figure 11A)**, (discussed in detail in **section**

1.3.1). Apoptosis in iDGAT treated samples and the available literature hints towards possible elevated ER stress response upon iDGAT treatment. Spliced version of XBP-1 mRNA is an indicator of ER stress activation. Under stead-state conditions, unspliced XBP-1 (uXBP-1) is expressed in the cells. Conversely, elevated cellular free fatty acid-mediated activation of unfolded protein response (UPR) signaling causes the cleavage of 26-bp intron in XBP-1 mRNA and subsequently generates spliced XBP-1 mRNA (sXBP-1). Both forms of XBP-1 can be detected by conventional PCR based XBP-1 expression analysis as indicators of ER stress. Herein, thapsigargin, which depletes calcium ion stores within the ER, is a known inducer of ER stress and was used as a positive control. As indicated in **Figure 11B**, treatment with 0.2 mM oleate instigated ER stress response and additional treatment with the iDGAT inhibitor resulted in prolonged ER stress response resulting in further elevated levels of spliced XBP-1 expression. Overall, the available literature and this experiment indicated that free fatty acids (oleate) treatment resulted in ER stress response activation indicated by expression of sXBP-1 which activated lipid droplet synthesizing enzymes. Furthermore, inhibition of LD synthesizing enzymes by using iDGAT, along with increased oleate supplementation resulted in prolonged ER stress response-associated apoptosis in iDGAT treated samples.

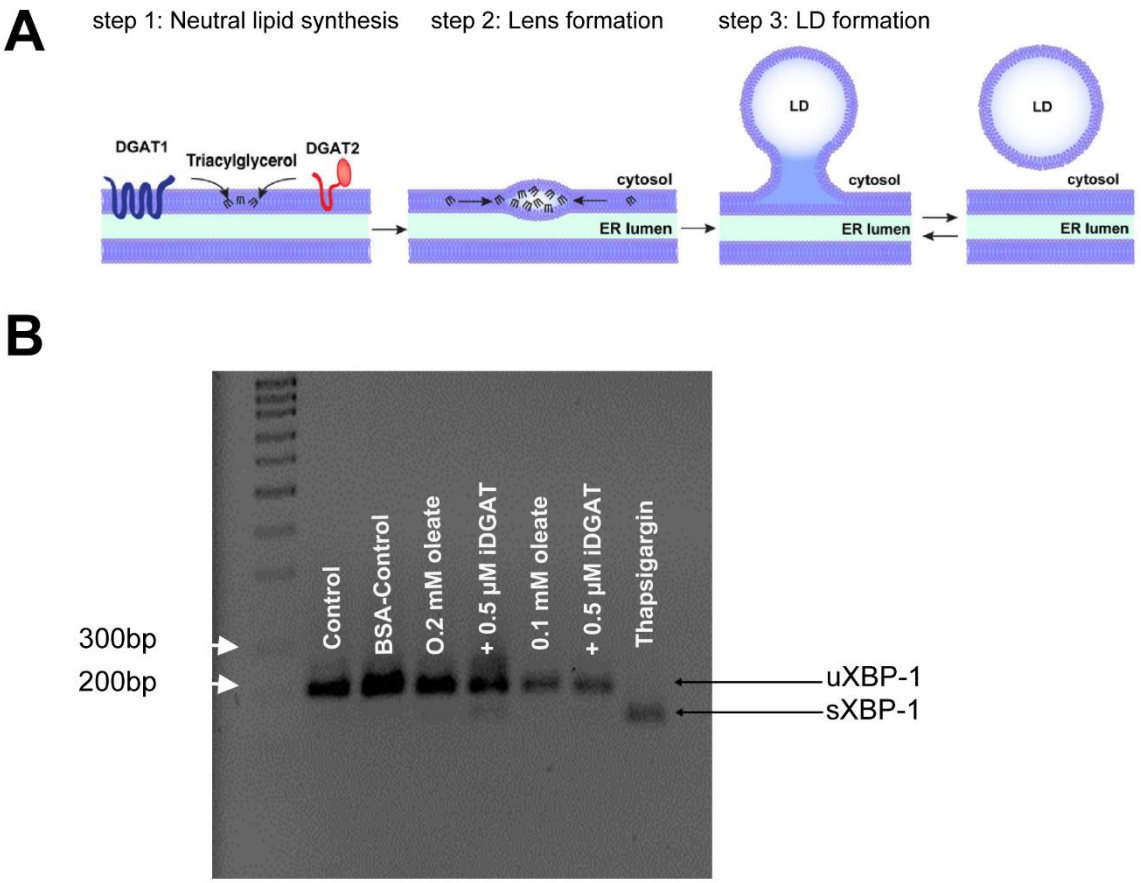

Figure 11: 0.2 mM oleate treatment leads to spliced XBP-1 expression which is further enhanced upon 0.5 µM iDGAT treatment. *(**A**) Schematic representation adapted from Wilfling et al. shows that DGAT1 and 2 enzymes are expressed on the ER membrane, which is the site of triacylglycerol accumulation and lipid droplet (LD) formation[99]. (**B**) Agarose gel electrophoresis image obtained from conventional PCR for XBP-1 gene expression in human macrophages after polarization. Thapsigargin treatment with 0.5 µM for 5h was used as positive control.*

4.1.6 Bulk RNA sequencing based gene expression analysis

To further evaluate the overall effect of oleate-dependent lipid accumulation in human MoDMs, we performed bulk RNA sequencing. Sample selection for sequencing was stringently regulated. Annexin V & Propidium iodide (PI) based live/dead staining was used as an indicator of live healthy cells. Only samples that did not show high cellular apoptosis upon treatment with oleate, **Figure 12B**, and with an RNA integrity (RIN) value above 9.0, **Figure 12D**, were selected for bulk RNA sequencing. Whereas polarized samples that showed increased apoptosis upon oleate treatment, **Figure 12A**, with a RIN value below 9.0, **Figure 12C**, were not selected for sequencing.

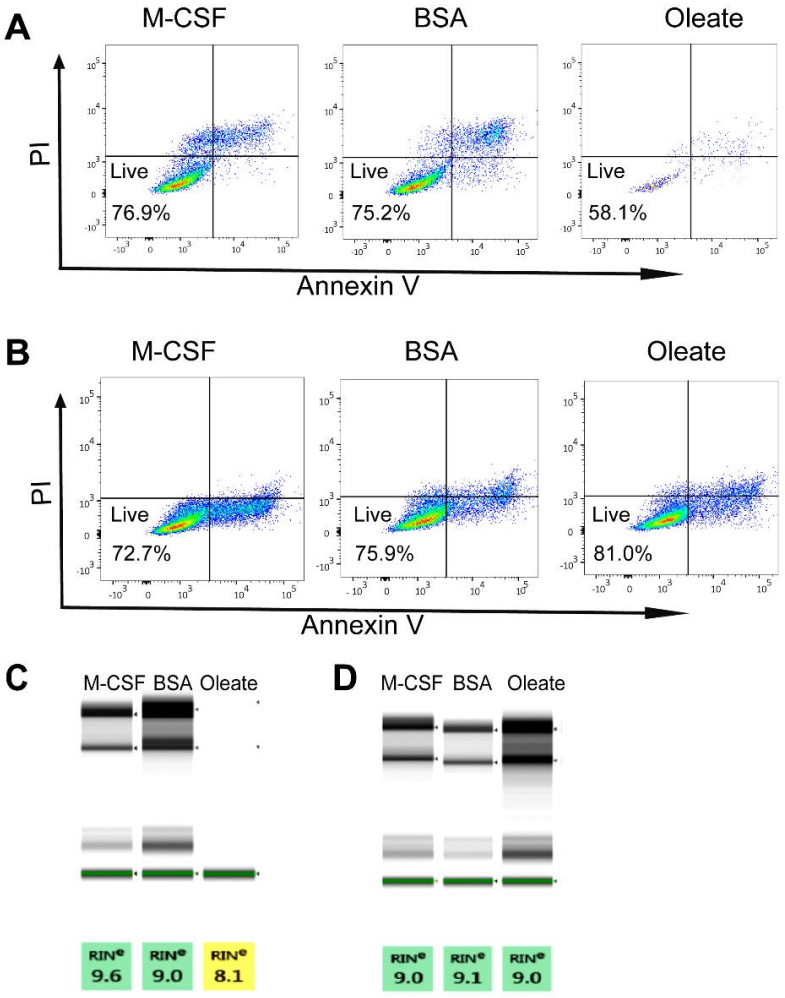

Figure 12: Sample selection and RNA preparation for RNA bulk sequencing. *(**A**) and (**B**) Flow cytometry-based live-dead analysis of polarized macrophages under the indicated conditions (**C**) and (**D**) Tape station-based RNA quality check. RIN: RNA integrity number.*

After stringent quality control for the samples, RNA from three polarized MoDM donor samples were sent for bulk RNA sequencing. The treatment conditions for each donor sample are defined below in **Table 9**. The bulk RNA sequencing principle component analysis (PCA), and heatmap generation was carried out by Novogene bioinformatics Technology Co, Ltd, Europe. As observed in **Figure 13A**, the principle component analysis indicated high intra-individual variability. The buffy coat samples were obtained from anonymous donors, whose age and gender were not matched. This could be a possible contributing factor for the increased variability in response to oleate treatment. However, on further analysis of the data **(Figure 13B**) the heatmap analysis depicted a clear difference in gene expression profile between control groups and oleate-dependent human MoDM. This indicated that even though we observed high intra-individual variability between the sample groups, the samples

did show a differential gene expression profile. Next, R script-based evaluation of top differentially expressed genes **(Figure 13C)** indicated that due to high variability among the sample groups, just a small number of differentially expressed genes was statistically significant. Among them, only two upregulated genes that are associated with metabolic and functional phenotype of macrophages, specifically, FABP4 and GATA3 were identified. Apart from these genes, the dataset was screened and other relevant metabolic (CD36 and CPT-1a) and functional (Msr-1, MRC-1, CCR7, and IL-6) genes in association with the macrophage phenotype were identified and further qPCR-based confirmation experiments were performed.

Table 9: List of treatment conditions for each donor sample (x3).

Condition 1	Condition 2	Condition 3
M-CSF	M-CSF + BSA	M-CSF + BSA + 0.2 mM Oleate

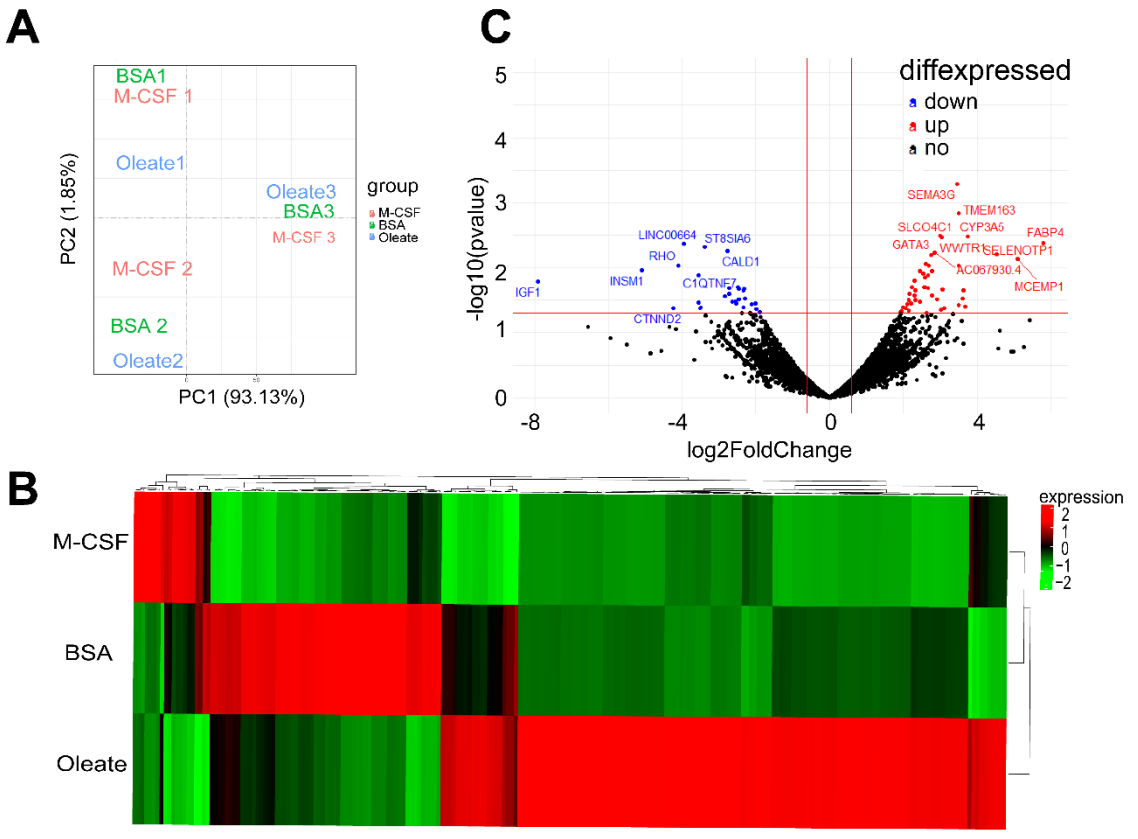

Figure 13: Differential gene expression analysis of human MoDM under indicated treatment conditions. *(**A**) Principle component analysis (PCA) depicting variability across individual donor samples. (**B**) Heatmap analysis reflecting differential gene expression in 0.2 mM oleate-dependent human MoDM compared to control groups (data as analyzed by Novogene, Europe). (**C**) Volcano plot based differential gene expression analysis, data analyzed using Enhancedvolcano package.*

4.1.7 Real-time PCR-based confirmation of differential gene expression

As observed from **Figure 13A**, the selection of anonymous donor samples resulted in high intra-individual variability while performing RNA sequencing. Therefore, to avoid intra-individual variability, while performing the qPCR-based confirmation experiments, $CD14^+$ monocyte samples were collected from three age and gender matched healthy donors. Following this, the macrophage polarization and subsequent RNA preparation and qPCR experiments were performed together for all the samples in order to avoid discrepancies possibly resulting from technical variability. As seen in **Figure 14A & B**, oleate-dependent human MoDM group, showed a significantly higher expression of CPT-1a in comparison to control group however, FABP4 and CD36 genes only revealed a tendency towards higher expression. On the other hand, the expression profile of functional genes, GATA 3 and Msr-1 showed a similar tendency towards higher expression but no significant difference. While the other functional genes under investigation MRC1, CCR2, and IL6 did not show any change in expression compared to the control group. These results prompted us to increase the sample number and verify if this would increase the differences. Therefore, qPCR with an increased number mixed donor samples sourced from buffy coats as well as healthy age & gender matched donors was performed. As shown in **Figure 14C & D**, increased sample size resulted in improved statistical power. Oleate-dependent MoDM showed a significantly higher expression of all the metabolic genes including FABP4, CD36 and CPT1a. Additionally, observed from **Figure 14D**, oleate-dependent MoDM showed significantly higher expression of GATA3, whereas the expression of other functional genes MSR1, MRCA1, CCR7 and IL6 did not show any changes in comparison to control.

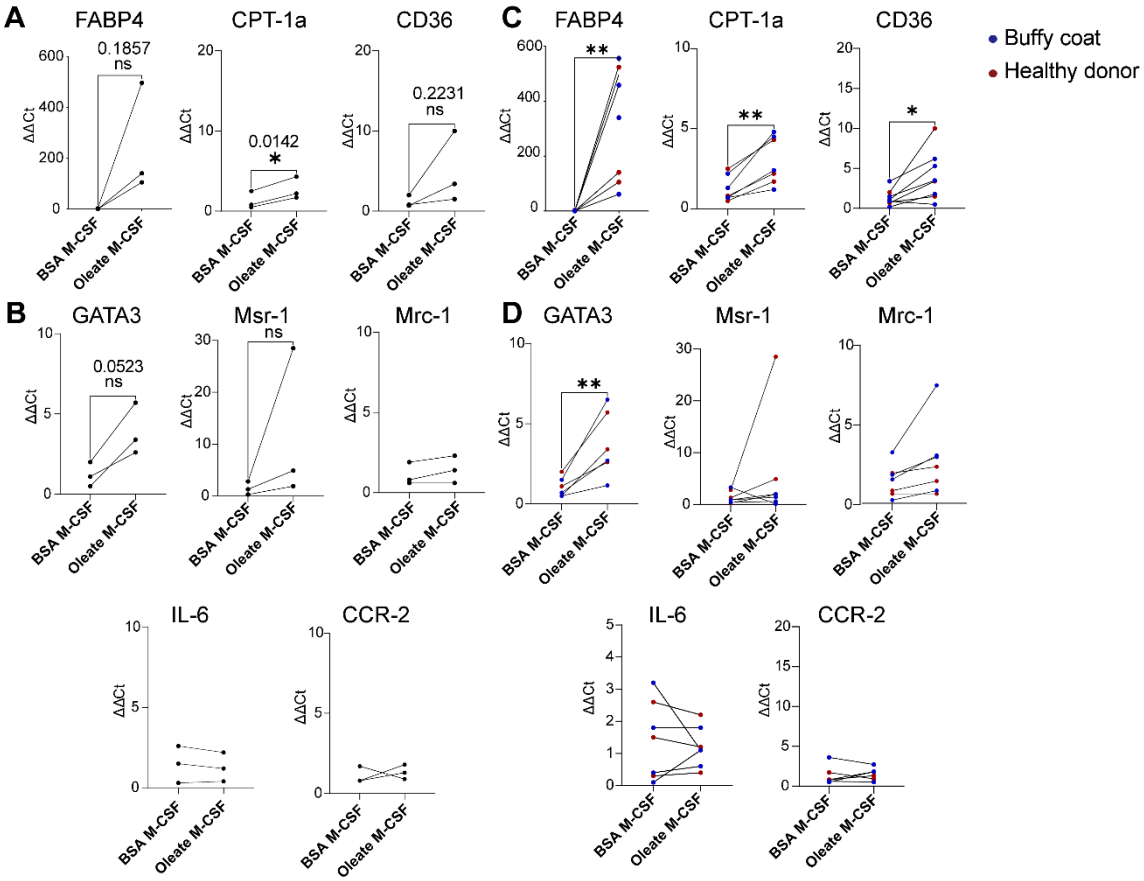

Figure 14: qPCR-based gene expression analysis of differentially expressed genes. *(**A**) Expression analysis of genes associated with metabolic phenotype in age matched healthy donors. (**B**) Expression analysis of genes associated with functional phenotype in age matched healthy donors. (**C**) Expression analysis of genes associated with metabolic phenotype in mixed donor population. (**D**) Expression analysis of genes associated with functional phenotype in mixed donor population. ** P < 0.01 * P < 0.05 ns P > 0.05. Error bars representative of standard error mean (SEM).*

4.1.8 Inhibition of p38 kinase reverses the lipid accumulating human MoDM phenotype

As concluded from the experiments so far, oleate-dependent human MoDM accumulate lipid droplets and upregulate metabolic markers including CD36 and FABP4. Available literature associates the expression of these fatty acid transporter proteins with a phenotype known as lipid accumulating foam cells. The next step was to verify the overall phenotypic similarity to foam cells. For this, the experimental setup was chosen from available literature **(Figure 15A)**. It is reported that increased accumulation of oxidized LDL/cholesterol in the THP-1 cell line results in foam cell formation and this phenotype can be reversed using a p38 inhibitor (SB203580) which increases lipophagy denoted by LC-3B expression, resulting in decreased lipid accumulation and reversed foam cell phenotype[107, 108]. Therefore, oleate-dependent human MoDM were treated with the p38 inhibitor, SB203580. Light microscopy images **(Figure 15B)** indicated already that the characteristic round lipid-laden phenotype resulting from oleate treatment was altered upon p38i treatment, towards a more elongated macrophage phenotype. This indicates a possible phenotypic modification occurring upon p38i treatment. Further western blot-based analysis of LC-3B expression ratio indicated that treatment of oleate-dependent MoDM with the p38 inhibitor resulted in increased LC-3BII/LC-3BI ratio (**Figure 15C & D)**. Thus, pointing towards an increased autophagic response in oleate-dependent MoDM.

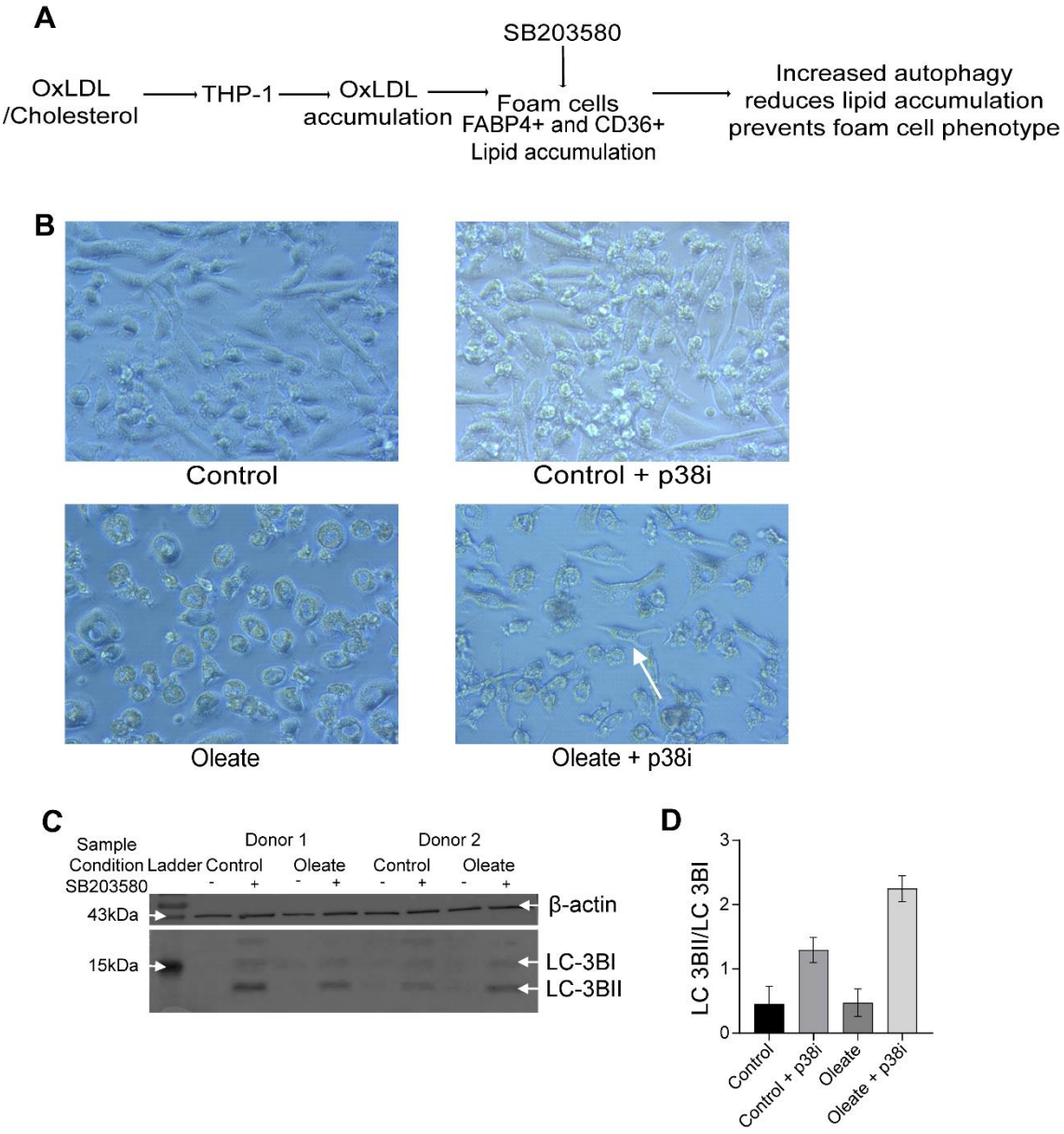

Figure 15: SB203508 treatment resulted in increased lipophagy in oleate treated human MoDM. *(**A**) Schematic representation of SB203508 treatment strategy adapted from Mei et al. and Zhao et al.[107, 108](**B**) Light microscopy images depicting phenotypic changes upon 10 µM SB203508 treatment of 0.2 mM oleate-dependent MoDM (**C**) & (**D**) Western blot based analysis of LC-3BII/ LC-3BI ratio*

As observed in Figure 15, treatment of oleate-dependent human MoDM with a p38 inhibitor resulted in increased autophagy, indicating increased utilization of stored lipids via a process known as lipophagy (discussed in detail in 1.3.2). Therefore, the next step was to assess the reduction in lipid droplets, using BODIPY staining. **Fig-**

ure 16A demonstrates reduced lipid droplet accumulation in oleate-dependent human MoDM upon treatment with p38 inhibitor. Available literature associates the reduced lipid accumulation and increased lipophagy with further related decreased expression of fatty acid transporter proteins CD36. Therefore, qPCR-based expression analysis was performed to evaluate the same p38 inhibitor-treated oleate-dependent MoDM. **Figure 16B** presents significant reduction in CD36 expression and a tendency towards lowered FABP4 expression upon p38 inhibitor treatment. Overall, p38 inhibitor treatment decreased the expression of CD36 and FABP4 and reduced lipid accumulation in macrophages. However, this reduced lipid accumulation, did not result in altered expression of immunosuppressive markers including CD163 and CD200R1 whereas, the expression of CD206 was further downregulated **(Figure 16C)**. Overall, these data indicate that oleate-dependent lipid accumulation in human MoDM functions via p38 pathway and subsequently results in a FABP4 and CD36 expressing foam cell phenotype. However, the downregulation of immunosuppressive surface markers in response to lipid accumulation is possibly regulated by other pathways that require further evaluation.

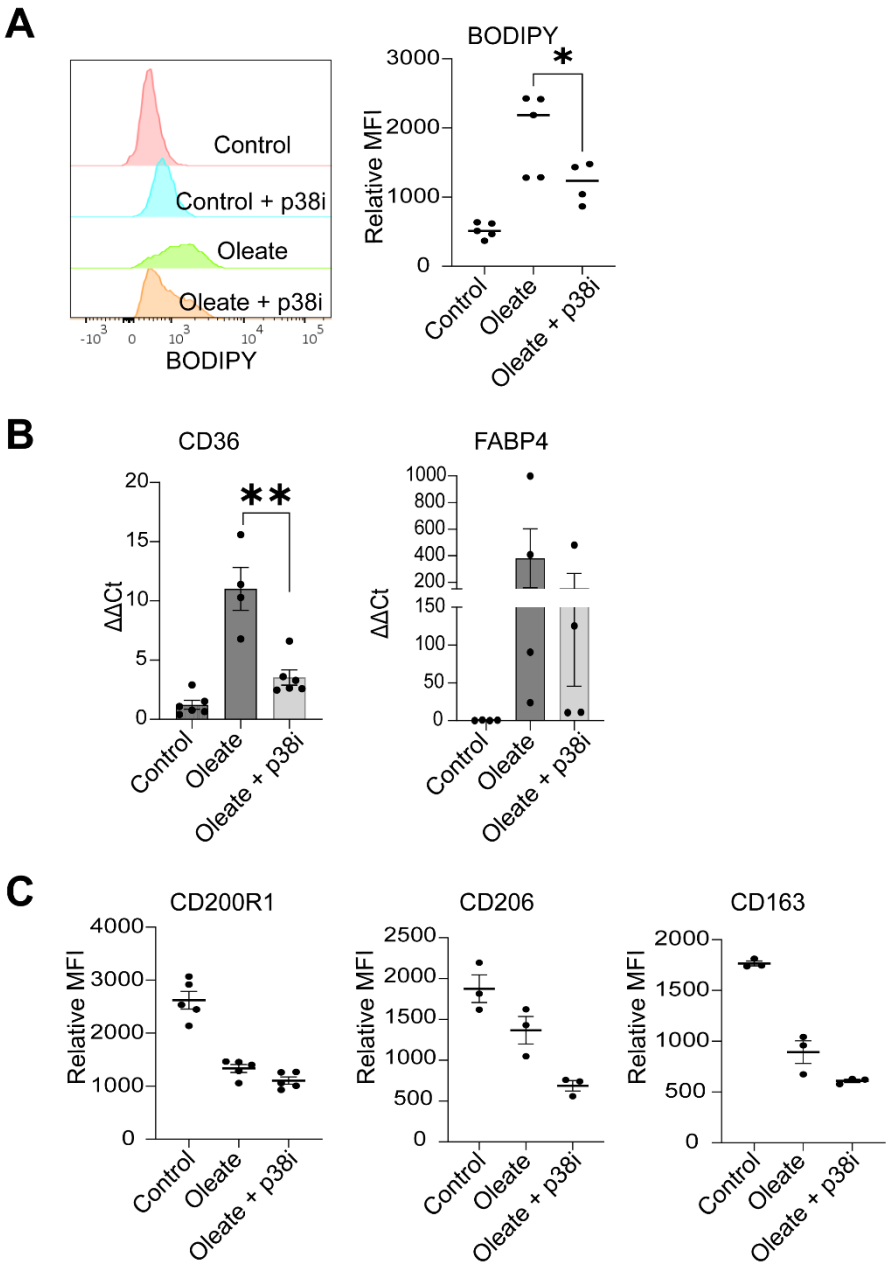

Figure 16: SB203508 treatment results in decreased lipid droplet (LD) formation in oleate-dependent human MoDM. (***A***) *Flow cytometric analysis of LD accumulation using BODIPY staining.* (***B***) *qPCR-based CD36 and FABP4 expression analysis.* (***C***) *Flow cytometry-based surface marker expression analysis. Shown as scatter plots generated using graphpad prism. Ten µM SB203508 (p38i) was used for performing experiments.*

4.2 Aim 2: Oleate-dependent polarization into CD206$^+$ tumor-associated macrophage phenotype is independent of IL-4 signaling

4.2.1 Oleate-dependent murine tumor-associated macrophage polarization is independent of IL-4 signaling

In our previous work, we demonstrated that oleate-dependent polarization of bone marrow-derived myeloid cells results in immunosuppressive CD206$^+$ tumor-associated macrophage (TAM) phenotype[61]. The next step was to further rule out the possible influence of IL-4 secreted by the bone marrow resident immune cell on the *in vitro* oleate-dependent polarization of immunosuppressive macrophages. For this, an *in vitro* oleate-dependent polarization of bone marrow-derived macrophages in presence of IL-4 blockers was performed **(Figure 17A)**. To do so, bone marrow cells from healthy wild type C57BL/6J mice were polarized *in vitro* over seven days in the presence of GM-CSF growth factor and supplemented with 0.2 mM oleate. During polarization, neutralizing anti-IL-4 antibody was added to the culture medium. After seven days, the cells were analyzed by flow cytometry. The gating strategy is demonstrated in **Figure 17B**. Polarization of bone marrow-derived myeloid cells in the presence of 0.2 mM oleate and anti-IL-4 antibodies did not reveal any significant reduction in CD206$^+$ TAMs as compared to 0.2 mM oleate treatment alone **(Figure 17C)**. Next, following the same workflow, the macrophages were polarized in the presence of different oleate concentrations to verify reliability of the dose used. As observed in **Figure 17D**, there was a substantial increase in the frequency of CD206$^+$ TAMs from the lowest dose of oleate (0.05 mM) to 0.2 mM oleate. Therefore, confirming that 0.2 mM oleate was an ideal dose for our experimental set-up and resulted in optimal upregulation of the TAM phenotypic marker under investigation.

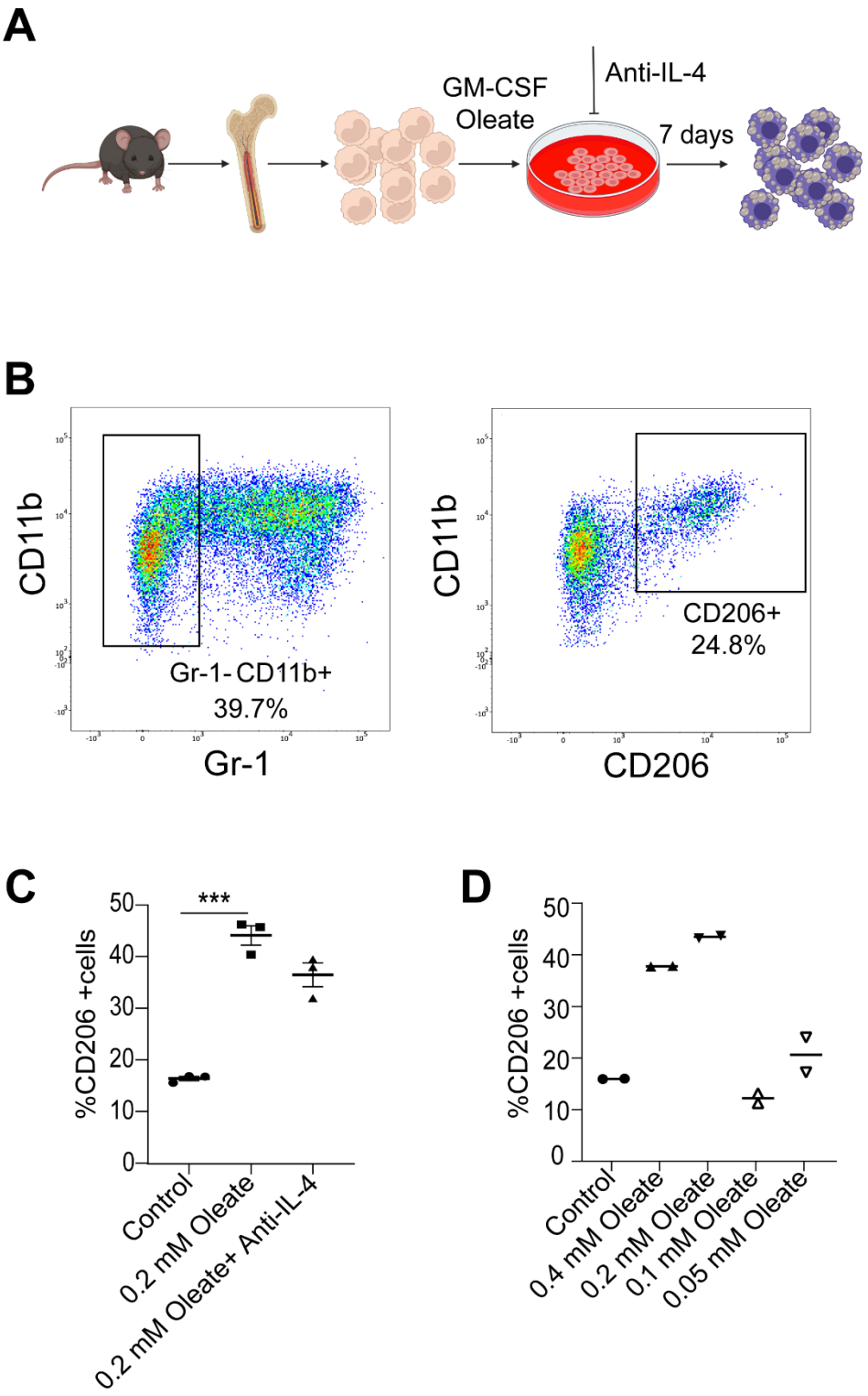

Figure 17: Immunosuppressive murine TAM polarization is independent of IL-4 signaling. *(**A**) Schematic presentation of experiment setup. (**B**) Schematic presentation of flow cytometry-based gating strategy used for analyzing the expression of CD11b⁺ Gr1⁻ CD206⁺ TAMs. (**C**) Percentage of CD11b⁺ Gr1⁻ CD206⁺ TAMs in presence of anti-IL-4 antibodies and 0.2 mM oleate (**D**) Percentage of CD11b⁺ Gr1⁻ CD206⁺ TAMs in response to varying oleate doses. **** P < 0.0001 *** P < 0.001. Error bars representative of standard error mean (SEM).*

4.2.2 CPT-1a-dependent fatty acid oxidation regulates the murine oleate-dependent immunosuppressive macrophage phenotype

The overall goal was to target oleate-dependent immunosuppressive TAMs with therapeutics and reduce the $CD206^+$ immunosuppressive macrophages. Towards this goal, we recently published that targeting various enzymes within the lipid and fatty acid metabolism pathway as shown in **(Figure 18A)** reverses immunosuppressive TAM phenotype[84]. However, another publication by Divakaruni *et al.* provided evidence indicating that when IL-4 polarized CD206 expressing immunosuppressive macrophages were treated with etomoxir, an inhibitor of the CPT-1a enzyme, it reversed the immunosuppressive macrophage phenotype. However, this reduction in CD206 expression was only observed upon treatment with higher doses of etomoxir (>3 µM up to 100 µM). These excessive molecules of etomoxir then bind to the intracellular coenzyme A (CoA), deplete the CoA stores and convert into etomoxiryl CoA. This etomoxiryl CoA further binds to enzyme complexes in the electron transport chain (ETC) and hamper the mitochondrial respiration. This is potentially the reason for the reduced CD206 expression in IL-4-dependent immunosuppressive macrophages **(Figure 18B)**. Herein, the same was tested in oleate-dependent immunosuppressive macrophages, which are independent of IL-4-dependent CD206 expression. Towards this goal, bone marrow-derived macrophages were polarized, as shown in **Figure 17A** and treated with increasing concentrations, 3 µM, 10 µM (low doses) and 40 µM (dose used in our publication). We observed that significant reduction in $CD206^+$macrophage cell number only resulted upon treatment with 40 µM etomoxir dose as compared to the lower doses shown in **Figure 18C.** Furthermore, SeahorseXF analyzer-based analysis was performed to study the mitochondrial respiratory changes based on oxygen consumption rate measurement (OCR) and as seen in **Figure 18D**. No changes were observed in the mitochondrial respiratory profile of oleate-dependent macrophages upon treatment with 40 µM dose of etomoxir. The possible reason for this could be that the constant oleate supplementation resulted in increased intracellular fatty acid oxidation and subsequently increased mitochondrial respiration. Simultaneously, the intracellular CoA is constantly utilized for the fatty acid oxidation which prevents the non-specific binding of excessive etomoxir to the available CoA.

Additionally, another experiment performed to evaluate if the 40 µM etomoxir treatment disrupts the intracellular CoA homeostasis and subsequently reduces the $CD206^+$ macrophage expression. Towards this aim, the BMDM were supplemented with 500 µM coenzyme A to restore or cope with intracellular CoA depletion potentially caused due to 40 µM etomoxir treatment which results in the formation of etomoxiryl CoA. The aim was to observe if this supplementation results in rescuing the reduced CD206 expression of macrophages. As seen in **Figure 18E**, CoA supplementation in macrophages that were treated with 40 µM etomoxir, did not result in a significant increase in the frequency of $CD206^+$ macrophages. These results suggest that oleate-dependent polarization of murine BMDM immunosuppressive phenotype is distinct from the IL-4-dependent immunosuppressive macrophages and is driven by increased fatty acid metabolism. Therefore, inhibition of CPT-1a with 40 µM of etomoxir reduces the CD206 expression independent of intracellular CoA homeostasis.

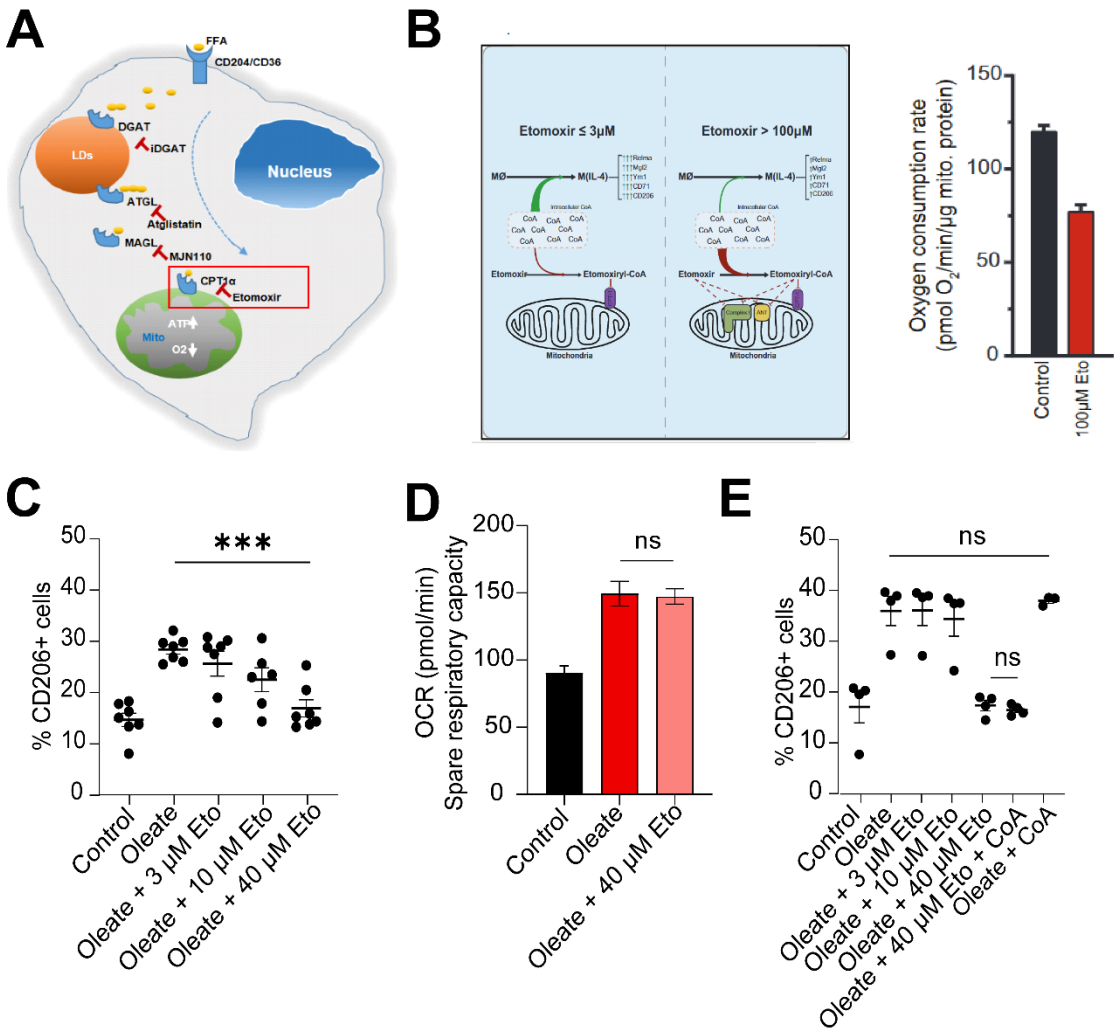

Figure 18: Treatment with 40 μM dose of etomoxir reduces CD206 expression of macrophages without altering intracellular coenzyme A stores. *(**A**) Previously published schematic presentation demonstrating the enzymes as targets to reverse oleate polarized immunosuppressive macrophages. (**B**) Graphical presentation adapted from Divakaruni et al demonstrating the effect of higher doses of etomoxir treatment on IL-4 polarized macrophages[60]. (**C**) The percentage of CD11b⁺ Gr1⁻ CD206⁺ TAMs in response to increasing concentrations of etomoxir during polarization. (**D**) Mitochondrial spare respiration capacity as measured by oxygen consumption rate (OCR) levels in response to 0.2 mM oleate and 40 μM etomoxir treatment. (**E**) The percentage of CD11b⁺ Gr1⁻ CD206⁺ TAMs in response to 500 μM coenzyme A supplementation. **** P < 0.0001 *** P < 0.001. Error bars representative of standard error mean (SEM).*

4.3 Aim 3

4.3.1 Generation of a mouse model to investigate the role of DGAT1 and DGAT2 enzyme in myeloid cell phenotype

To investigate the role of the enzymes DGAT1 and DGAT2 in mediating the formation of immunosuppressive macrophage phenotype, two separate mouse lines were generated. The mouse lines harbored targeted deletion of the *Dgat1* and *Dgat2* gene specifically in the myeloid compartment, generated by crossing *Dgat1*$^{fl/fl}$ or *Dgat2* $^{fl/fl}$ with transgenic mice with nuclear-localized Cre recombinase under the lysozyme 2 (*Lyz2*) promoter region. Therefore, *Dgat1*$^{fl/fl}$*-LysMcre* and *Dgat2*$^{fl/fl}$*-LysMcre* mice harbor deletion of the respective gene in the myeloid cell lineage. The gene deletion for the same was assessed using PCR based genotyping. **Figure 19** depicts the expression of LysMcre, *Dgat1*$^{fl/fl}$*,* and *Dgat2*$^{fl/fl}$ *in myeloid cells*.

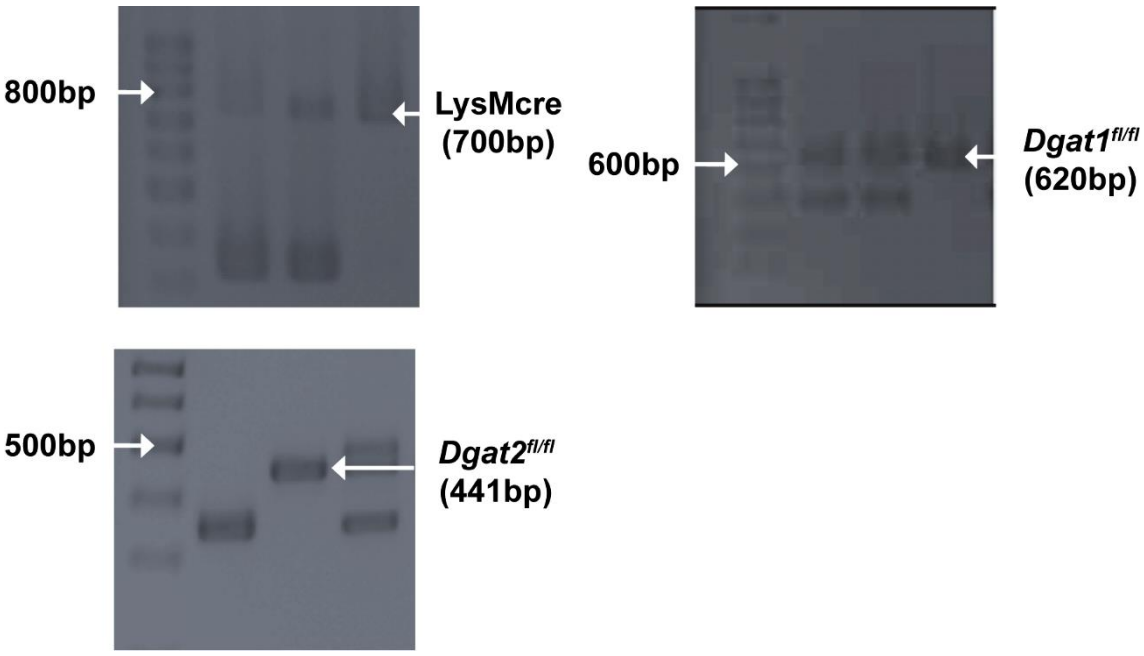

Figure 19: PCR-based confirmation of Dgat1$^{fl/fl}$-LysMcre and Dgat2$^{fl/fl}$-LysMcre knockout mice in myeloid cells.

4.3.2 DGAT1 identified as key player in oleate-dependent lipid accumulation in murine bone marrow-derived macrophages

The enzymes DGAT1 & 2 together play a role in synthesizing triacylglycerol (TAGs) dependent lipid droplets (LDs). However, various reports discuss the importance of independent enzymes in mediating cellular LD-dependent phenotype. Based on this

information, the role of each enzyme in synthesizing LDs was evaluated using an oleate-dependent bone marrow derived myeloid cells (BMDM) polarization strategy for the single gene knockout mice. For this, BMDM cells were polarized into macrophages in presence of 0.2 mM oleate and GM-CSF as growth factor. As observed in **Figure 20**, BMDMs from *Dgat1$^{fl/fl}$-LysMcre store significantly less lipid droplets compared to macrophages from wild type mice. On the other hand, Dgat2$^{fl/fl}$-LysMcre did not show a reduction in LD accumulation compared to wild type control. This observation emphasizes the importance of further evaluating the Dgat1$^{fl/fl}$-LysMcre single gene knockout myeloid compartment.*

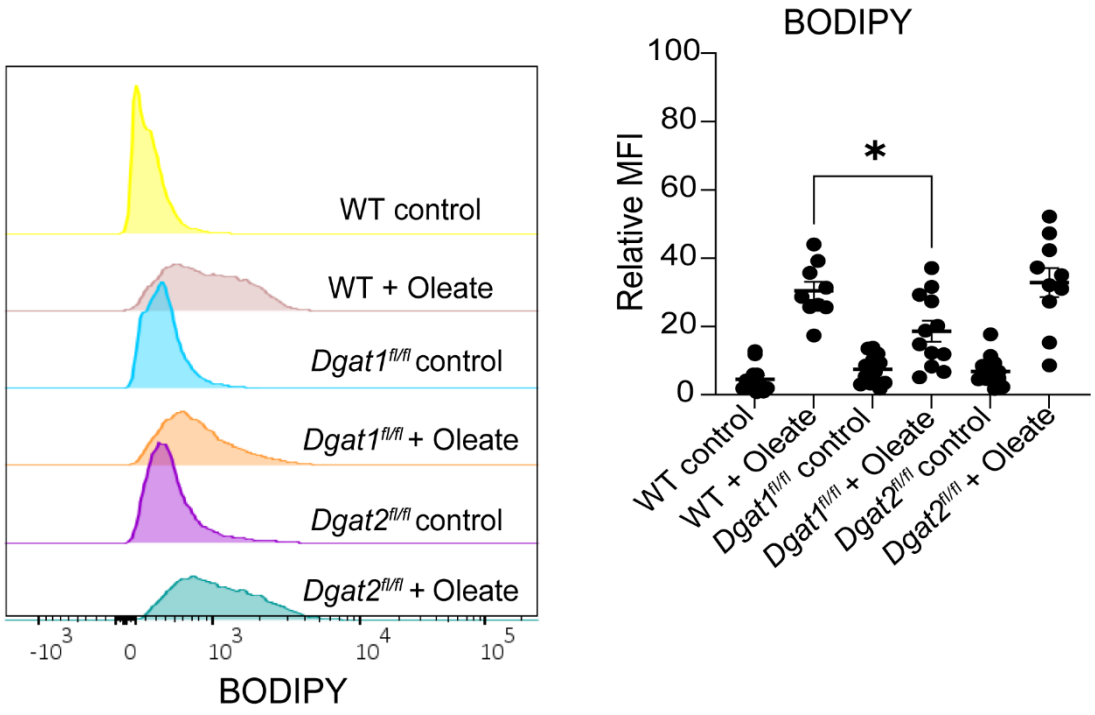

***Figure 20: Analysis of lipid droplet accumulation in bone marrow-derived macrophages from DGAT1$^{fl/fl}$-LysMcre and DGAT2$^{fl/fl}$-LysMcre mice in response to 0.2 mM oleate-dependent in vitro polarization**. Flow cytometry-based histogram plots show relative lipid droplets in cells using BODIPY staining (left). BODIPY staining based relative mean fluorescence intensity calculated and shown as scatter plots generated using graphpad prism (right). * P < 0.05 ns P > 0.05. Error bars representative of standard error mean (SEM).*

4.3.3 Deletion of Dgat1 or 2 does not alter the surface marker profile of oleate-dependent polarized macrophages

As seen above, *Dgat1$^{fl/fl}$-LysMcre* macrophages store significantly less LD compared to wild type macrophages. The next step was to identify if this reduced lipid droplet

accumulation results in significant phenotypic changes associated with CD206 expression and other macrophage surface markers compared to wild type macrophages. As seen in **Figure 21A**, CD206, F4/80, and MHC II expression did not alter in the macrophages from the knockout mice compared to the wild type control.

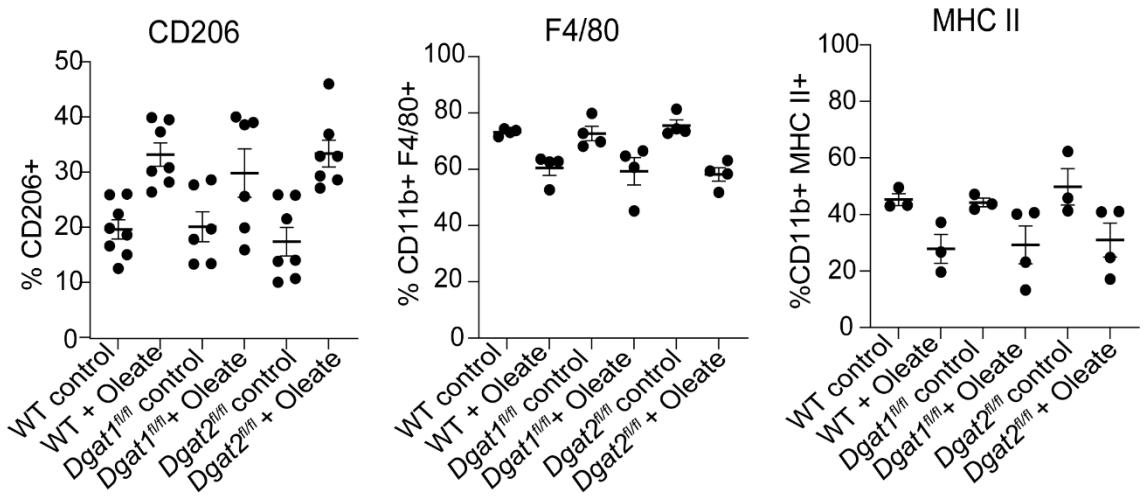

Figure 21: Surface marker expression profile of BMDM from Dgat1$^{fl/fl}$-LysMcre and Dgat2$^{fl/fl}$-LysMcre mice in response to 0.2mM oleate-dependent in vitro polarization*. Flow cytometry based CD206 (left), F4/80 (center), MHC class II (right), expression analysis shown as scatter plots generated using graphpad prism.*

4.3.4 Deletion of Dgat1 or 2 does not alter the β-oxidation of fatty acid in oleate-dependent polarized macrophages

Our previous publications demonstrate that DGAT1 & 2 enzyme dependent lipid droplet formation and subsequent fatty acid oxidation plays a role in regulating the immunosuppressive macrophage phenotype. For further evaluating the involvement of the β-oxidation pathway in immunosuppressive macrophage phenotype, an assay based on the Seahorse XF analyzer was introduced, which analyzes the real-time dependence of the cells on fatty acid oxidation. Herein, the polarized macrophages are seeded in appropriate assay medium and dependency on fatty acid oxidation was analyzed as described in section 3.2.16. As seen in **Figure 22A**, etomoxir injection resulted in significant reduction of oxygen consumption rate (OCR value) of oleate-dependent wild type as well as the knockout macrophages. Next, the dependency on β-oxidation was evaluated using Agilent Seahorse Wave 2.6.0 software. As demonstrated in **Figure 22B**, no significant changes in dependency on fatty acid oxidation were observed in knockout macrophages compared to the wild type.

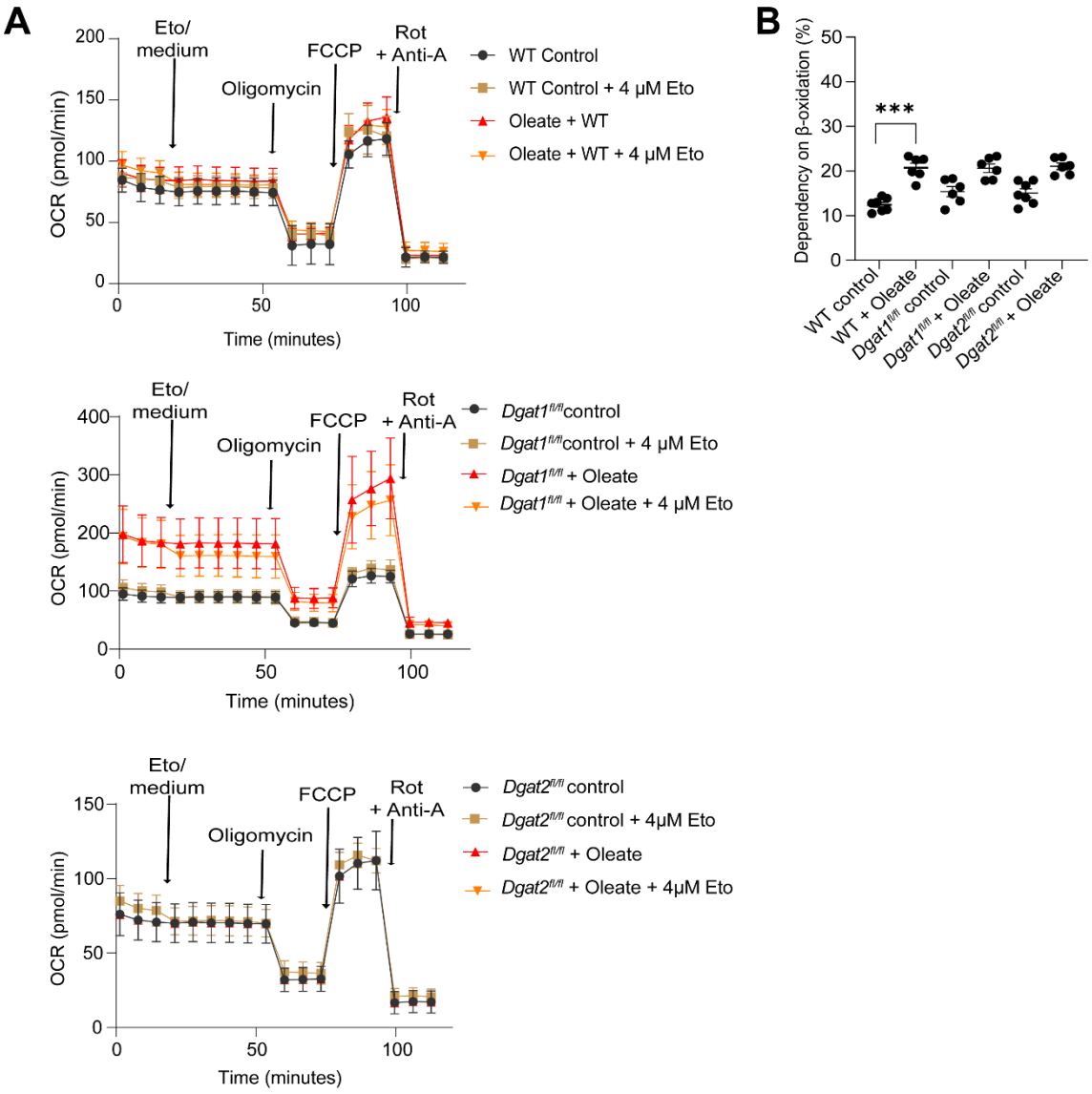

Figure 22: β-oxidation analysis in wild type and Dgat1$^{fl/fl}$-LysMcre and Dgat2$^{fl/fl}$-LysMcre bone marrow-derived macrophages. *(**A**) β-oxidation analysis based on oxygen consumption rate (OCR) measured by seahorse XF analyzer in response to 4 µM etomoxir (inhibitor), 2 µM oligomycin, 1 µM FCCP and 0.5 µM rotenone/antimycin A (Rot + Anti-A) injection. (n=3 biologically independent samples). (**B**) Scatter plots showing dependency of polarized macrophages on β-oxidation, calculated using seahorse XF analyzer software. *** P < 0.001, ns P > 0.05. Error bars representative of standard error mean (SEM).*

4.3.5 Deletion of Dgat1 or 2 does not alter bone marrow resident myeloid progenitor population in steady state

As discussed in section 1.3.3, lipid storage and metabolism play an essential role in myelopoiesis. Based on available literature to identify myeloid progenitor cell percentage in response to genetic interventions, a flow cytometry-based panel was applied **(Figure 23A)** to evaluate changes in the myeloid progenitor cell percentage in

response to *Dgat1* & *2* gene deletion. Herein, the cell populations which are negative for all lineage (lin) markers including B220, CD3, CD4, CD8, CD11b, CD11c, Gr-1, and Ter-119, and cKIT^{+} (myeloid progenitor marker) are defined as lineage^{-}cKIT^{+} (LK cells), myeloid progenitor population. Further, based on expression of CD34 (hematopoietic stem cell marker) and CD16/32, the progenitor population was divided into Lin^{-} cKIT^{+} CD16/32$^{int/-}$ CD34^{+} expressing common myeloid progenitor (CMP), the Lin^{-} cKIT^{+} CD16/32^{+} CD34^{+} expressing granulocytic myeloid progenitor (GMP), and the Lin^{-} cKIT^{+} CD16/32^{-} CD34^{-} megakaryocyte-erythroid progenitor (MEP)[143]. However, as observed in **Figure 23B**, no differences were detected in the percentage of CMP, GMP, and MEP in bone marrow resident myeloid progenitors. Thus, indicating that single gene knock out does not alter myelopoiesis in steady-state mice bone marrow compared to wild type controls.

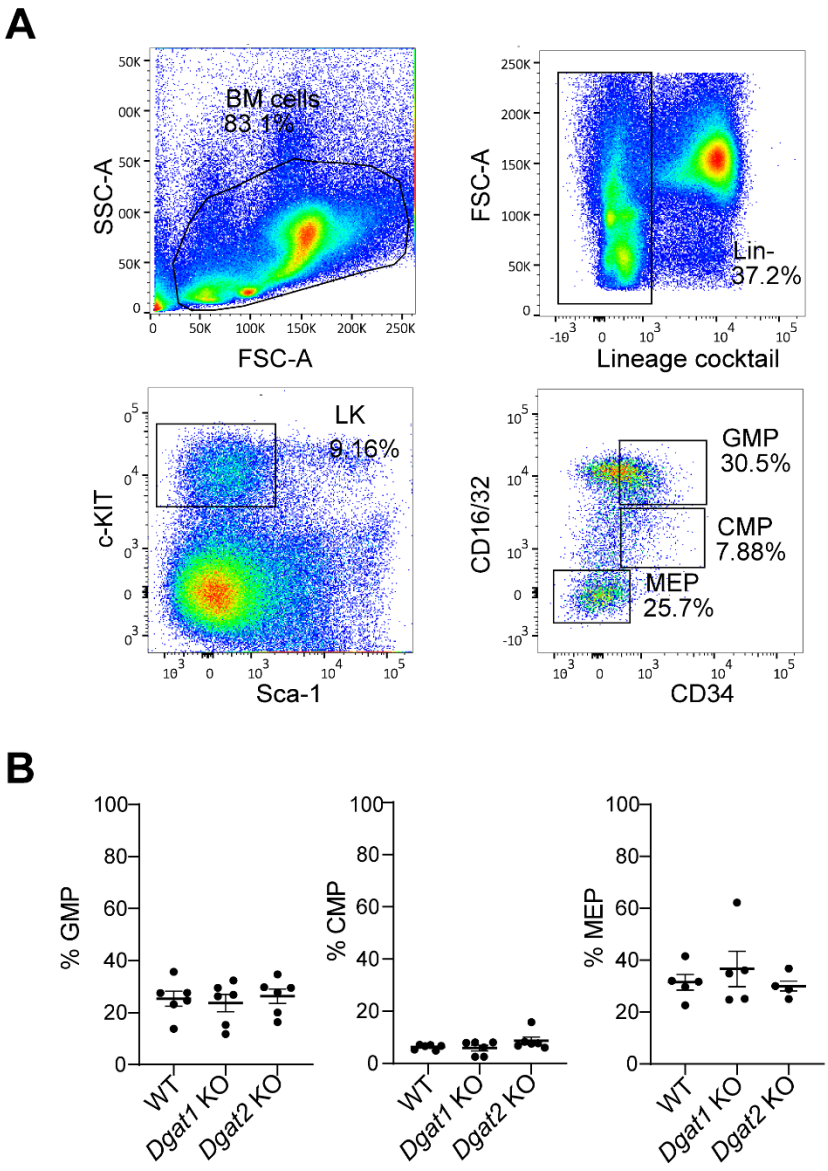

Figure 23: Analyzing myeloid progenitor cell population in the bone marrow of Dgat1 & 2 knockout mice. *(**A**) Schematic representation of the gating strategy used to identify GMP (Lin$^-$ cKIT$^+$ Sca-1$^-$ CD16/32$^+$ CD34$^+$), CMP (Lin$^-$ cKIT Sca-1$^-$ CD16/32$^{int/-}$ CD34$^+$), and MEP (Lin$^-$ cKIT, Sca- 1$^-$ CD16/32$^-$ CD34$^-$), (**B**) Percentages of GMP, CMP, and MEP cells from wild type v/s Dgat1$^{fl/fl}$-LysMcre and Dgat2$^{fl/fl}$-LysMcre mice. Only viable cells based on zombie aqua live dead staining were considered (not shown in figure). Each value denotes an individual data point ± SEM; n = 6 mice/ group. LK = Lineage marker $^-$ cKIT $^+$, CMP = common myeloid progenitor, MEP = megakaryocyte-erythroid progenitor, GMP = granulocytic myeloid progenitor.*

5 Discussion

Macrophages are an essential component of the innate immune system and are capable of polarizing into various subtypes depending on their environmental cues. The two extreme ends of these subtypes are considered as M1 inflammatory phenotype and M2 anti-inflammatory phenotype and are associated with pro-inflammatory or wound-healing associated outcome, respectively. However, recent discoveries emphasize the overlapping involvement of both inflammatory and anti-inflammatory subtypes in development of diseases. Atherosclerosis and cancer development are two well-studied pathological diseases responsible for causing deaths all over the world. Atherosclerosis is widely defined as an obesity associated metabolic disease and emerging evidence largely suggests that cancer is rather also a metabolically driven disease than just a genetically altered state. All the available facts provide an understanding that disease progression in both atherosclerosis and cancer are multifactorial processes depending on genetic and metabolic alterations within the tissue and immune compartment. These alterations include increased oxidative stress, chronic inflammation, altered lipid/fatty acid accumulation and metabolism, and altered immune response. Macrophages constitute a major immune infiltrate residing in adipose tissue, atherosclerotic plaques as well as within solid tumors. Detailed macrophage phenotypes in cancer and atherosclerosis are described in the section 1.2.1 and 1.2.2 respectively. In brief, fatty acid- and lipid-induced phenotypic switching of macrophages are reported in obesity-associated diseases such as diabetes, atherosclerosis and cancer[45, 48, 64, 97]. Herein, we showed that fatty acid (oleate) dependent polarization of murine bone marrow-derived myeloid cells results immunosuppressive macrophages characterized by CD206 expression, which is independent of IL-4 signaling. The effect of oleate-dependent lipid droplet formation in human monocyte-derived macrophages was further analyzed. Herein, we observed that oleate-based lipid droplet accumulation during monocyte polarization into macrophages resulted in downregulation of immunosuppressive phenotype associated surface scavenger receptors including CD200R1 and CD163. Furthermore, it also resulted in upregulation of ER stress response characterized by XBP-1 expression, which has been associated with immunosuppressive myeloid cells. Oleate-dependent polarization of human monocyte-derived macrophages also resulted in upregulation of GATA3 transcription factor, which has been associated with immunosuppressive

macrophage phenotype. Additionally, these macrophages also expressed high levels of the fatty acid transporter protein, FABP4 and the scavenger receptor, CD36 associated with an uptake of fatty acids and subsequent phenotypic modification. Overall, our data reveals the importance of evaluating lipid accumulation and metabolism in identifying new targets, which can be identified as single therapeutic drug against various metabolic diseases.

5.1 Aim 1: The role of oleate-mediated lipid droplet formation in human CD14^{+} monocyte-derived macrophages

5.1.1 Lipid metabolism in diseased states

Metabolic alterations in cancer cells, as discussed by Menendez and Lupu, encompass increased expression of the enzyme fatty acid synthase (FASN) with increasing stages of cancer[144]. This expression pattern of FASN was observed in almost every solid tumor type, and it is constitutively overexpressed in the metastatic stages, thus, confirming increased overall fatty acid synthesis in cancer cells[144]. Another report demonstrated that breast cancer cells isolated from patient-derived biopsies secret higher amounts of fatty acids into the culture medium. This experimental analysis was performed in comparison to normal breast tissue cells. Gas chromatography-based analysis further confirmed that oleic acid constituted 30 to 40% of the total fatty acids secreted by cancer cells, followed by palmitate and stearate[145]. These reports emphasize the importance of understanding the process and effects of increased fatty acid synthesis and secretion by cancer cells, namely, increased oleic acid in response to cancer growth. Along with the ongoing internal fatty acid dependent metabolic changes of cancer cells, their uncontrolled proliferation also plays a role in limiting nutrients and oxygen availability of the TME. This results in an acidic, hypoxic, and glucose depleted environment. As a result, the lipids and fatty acids synthesized and secreted by the cancer cells, constitute a major source of energy metabolism for infiltrating immune cells. Myeloid cells including macrophages and immature activated MDSCs are major infiltrating immune cells within tumor.

Additionally, obesity-associated diseases are characterized by abnormal lipid metabolic state which results in elevated levels of triglycerides, VLDL and cholesterol circulating in the serum. Another attribute of obesity is measured in terms of increased

lipid accumulation in adipose tissues (AT). This increased lipid accumulation in AT is associated with increased inflammation. Moreover, a constant low-grade systemic inflammation is a well-recognized contributing factor for atherosclerotic plaque formation[101]. Weisberg *et al.* also demonstrated that adipose tissue macrophages (ATM) increase in number with an increase in obesity and are responsible for the subsequent pro-inflammatory pathological symptoms observed in obese individuals[146]. Additionally, the advancement of atherosclerosis is characterized by the increased accumulation of cholesterol rich lipids and subsequent fatty streak formation. Monocytes derived foam cell populations within these plaques resulting from increased accumulation of cholesterol have been associated with initiation and progression of atherosclerosis[101].

Overall, several reports confirm the influence of tissue metabolic imbalance on molecular changes in macrophage phenotype and influence formation of various macrophage phenotypic subtypes across the two diseased states and are summarized in **Figure 2** and **Figure 4**. Metabolic imbalance in macrophages driven by increased fatty acid import has been associated with the upregulation of fatty acid transporting scavenger receptor CD36. Macrophages expressing CD36 are reported in cancer as well as atherosclerosis and have been associated with poor disease prognosis[16, 17]. Another fatty acid transporter chaperone protein widely associated with lipid accumulating macrophage subtypes is FABP4 and its expression has been associated with pro-inflammatory outcome in atherosclerosis, whereas FABP4 expressing macrophages have been identified in human breast cancer patients and have been associated with poor survival[82, 106]. Other publications discuss the importance of CPT-1a driven FAO, DGAT1 and DGAT2 driven fatty acid storage into lipid droplets as well as lysosomal acid lipase (LAL) driven lipolysis in immunosuppressive macrophages and MDSCs **(Figure 1)**[57, 63, 84, 89]. We recently reported in murine bone marrow-derived macrophages that inhibition of lipid droplet storage using chemical inhibitors for DGAT1 & 2 enzymes results in reduced CD206 expressing immunosuppressive macrophages[84]. These reports overall highlight the importance of further evaluating the role of FAO and lipid droplet accumulation in immunosuppressive macrophages.

Herein, we established an *in vitro* model system to study the effect of oleate on human monocyte-derived macrophage (human MoDM) polarization within an isolated

system. This system was generated to get a better understanding of the role of fatty acid uptake and storage during human MoDM polarization. Our experimental setup revealed significant lipid accumulation upon oleate-dependent polarization of human monocytes which was confirmed using BODIPY staining as an indicator of increased neutral lipid synthesis. This was the first criterion applied for validating that the overall macrophage phenotype resulting from oleate-dependent polarization was dependent on LD formation.

Additionally, the effect of DGAT1 & 2 enzyme inhibition in the polarized macrophages was investigated. We previously used 5.0 µM of the inhibitor combination for treating murine BMDM. While working with the same inhibitor concentration in human MoDM, an increased apoptosis was observed during polarization process. Therefore, a suitable concentration of the inhibitor combination was evaluated that would effectively reduce lipid accumulation and not cause cell death. Treatment with a ten-fold lower concentration 0.5 µM iDGAT did not result in apoptotic response and inhibited lipid droplet formation. Therefore, this concentration was selected for further experimentation with human MoDM. Moreover, the reliability of the chosen oleate concentration was explored. Thus, three doses of oleate including 0.2 mM (which was also used for murine BMDM experimentation), 0.1 mM and 0.05 mM were tested. Treatment with all three oleate concentrations resulted in a downregulation of CD14, 200R1 and CD163. Lower concentrations of oleate (0.05 mM and 0.1 mM) induced a downregulation of these markers, but no significant differences compared to control groups. Nevertheless, 0.2 mM of oleate resulted in a significant downregulation of all surface markers, indicating a dose-dependent effect of oleate in downregulating these markers. Hence, 0.2 mM oleate was selected as a reliable dose for *in vitro* experimentation.

5.1.2 Characterization of human immunosuppressive macrophages

CD206 is a C-lectin type mannose receptor associated with immunosuppressive macrophages. It is widely applied as a prognostic tool to evaluate the aggressiveness of tumors[22, 23]. We recently confirmed the role of oleate-dependent lipid droplet formation in polarizing murine BMDM into $CD206^+$ immunosuppressive phenotype, and we also demonstrated that pharmacological inhibition of lipid droplet synthesizing enzymes DGAT1 & 2 results in reduced $CD206^+$ macrophages[61]. In continuation with

this research, our aim was to further evaluate upregulation of CD206 expression in oleate-dependent human MoDM. For this, human MoDM were polarized in the presence of oleate and M-CSF and showed an upregulated expression of CD206. However, no significant differences were observed in comparison to the control group since M-CSF-primed macrophages (control group) also expressed high levels of CD206. Available literature discusses the influence of M-CSF or GM-CSF priming on upregulating the expression of CD206[147]. Therefore, indicating that CD206 was not a suitable marker for analyzing *in vitro* polarized human immunosuppressive macrophages. Thereafter, CD163 and CD200R1 were introduced as new markers that could be used to study immunosuppressive phenotype in oleate-dependent macrophages[15, 26]. Herein, macrophages were polarized in the presence of GM-CSF or M-CSF growth factor along with oleate or oleate and DGAT1 & 2 inhibitor. This experiment was performed to verify if the combined effect of oleate with either of the growth factors (GM-CSF or M-CSF) changes the surface marker expression profile. GM-CSF-dependent activation of myeloid cells results in upregulation of CD200R1 expression and subsequent immunosuppressive MDSC formation[148 149]. On the other hand, polarization of human monocytes in the presence of M-CSF results in an immunosuppressive phenotype[150]. Therefore, the expression of immunosuppressive markers in presence of both M-CSF and GM-CSF along with oleate treatment was evaluated. However, the expression of markers under investigation was higher in M-CSF-primed macrophages compared to GM-CSF-primed macrophages. Therefore, concluding that M-CSF polarized macrophages served as a better control group to study the immunosuppressive macrophages. Additionally, the comparative effect of oleate-dependent polarization on immunosuppressive surface markers was more significant in M-CSF-primed macrophages compared to GM-CSF-primed macrophages. According to available literature, CD14 expression is downregulated in immunosuppressive macrophages[25]. We observed that oleate-dependent macrophages in the presence of M-CSF showed significant downregulation of CD14 expression. Therefore, indicating that oleate treatment in M-CSF-primed macrophages results in phenotypic similarities when compared to immunosuppressive macrophages. Remarkably, oleate-dependent polarization of M-CSF-primed human MoDM resulted in significant downregulation of CD163 and CD200R1. These overall results confirmed that lipid droplet accumulation in response to oleate-dependent polariza-

tion modulates macrophage phenotype by downregulating immunosuppressive surface markers with more prominent downregulation occurring due to the combined effect of M-CSF and oleate as compared to GM-CSF and oleate.

We previously demonstrated the immunosuppressive capacity of murine BMDM by co-culturing with $CD4^+$ T cells, which resulted in reduced proliferation of $CD4^+$ T cells as indicated by CFSE based proliferation assay[84]. Herein, the immune modulating capacity of human MoDM polarized with GM-CSF and oleate or M-CSF and oleate was investigated. This experiment was performed to evaluate if oleate-dependent polarization in the presence of either growth factor would result in an immunosuppressive macrophage. However, co-culturing of GM-CSF-primed or M-CSF-primed, oleate-dependent human MoDM with $CD4^+$ T cells did not induce significant changes in the $CD4^+$ T cell proliferation capacity. Since oleate-dependent macrophage polarization resulted in significant downregulation of immunosuppressive scavenger receptors, we expected this phenotype to be associated with an overall increased pro-inflammatory capacity which is known to increase T cell proliferative response. However, as observed in this experiment, GM-CSF-primed or M-CSF-primed, oleate-dependent human MoDM did not result in any changes in T-cell proliferation. This indicates that oleate-dependent polarization of human macrophages results in an anergic macrophage phenotype with no immune-modulating capacity.

5.1.3 Lipid droplet formation, ER stress response and myeloid cell phenotype

As discussed above in section 1.3.2, the ER stress response maintains ER homeostasis through UPR activation. It acts by promoting the activation of molecular chaperones and other enzyme targets, which are responsible for maintaining ER-dependent degradation of cellular organelles to prevent cell death. Overstimulation of IRE-1α in response to prolonged exposure to stress inducing stimuli and subsequent spliced XBP-1 (sXBP-1) expression analysis is widely associated with ER stress response mediated apoptosis[151, 152, 153]. Furthermore, increased uptake of fatty acids and cholesterol via scavenger receptor A and subsequent accumulation of these free fatty acids and unesterified cholesterol within the ER membrane accounts for dysregulation of ER homeostasis and causes increased cells death[154]. Cholesterol esterification is mediated via the ACAT enzyme, and increased accumulation of unesterified

free cholesterol in response to ACAT enzyme inhibition results in excessive cellular cholesterol accumulation, ER stress response via the CCAAT/Enhancer binding protein homologous protein (CHOP) transcription factor regulated-CHOP pathway and subsequent apoptosis in macrophages[155, 156]. This highlights the importance of managing intracellular free fatty acid and cholesterol load to maintain cellular lipogenesis, associated ER homeostasis, and apoptosis.

The overload of UPR activation pathways results is an adaptive response that is also associated with cell phenotype and activation status. Various reports associate the activation of these UPR responses with the myeloid cell phenotype. For example, increased lipid peroxidation by-products such as ROS-generated 4-Hydroxy-trans-2-nonenal (4-HNE) results in the activation of XBP-1 mRNA (spliced) in tumor-associated dendritic cells (tDCs). This is further associated with increased lipid accumulation due to the activation of triglyceride biosynthesis pathways and subsequent immunosuppressive tDCs generation[157]. Additionally, toll-like receptors (TLR 2 and TLR 4) facilitated pathogen sensing in macrophages results in a pathogen-induced ER stress response, which is mediated via sXBP-1 and leads to concomitant cytokine production, which fights pathogen invasion[158]. Metabolic dysregulation-induced ER stress in obesity primarily promotes inflammation and disease progression. Under steady physiological conditions, ATM possess M2 phenotype. However, ER stress thereafter enhances activation of adipose tissue macrophage (ATM) and switching towards M1 phenotype in an sXBP-1-dependent manner in high fat diet-induced obesity and metabolic imbalance[159]. As discussed earlier in section 1.2.2, macrophages play an essential role in atherosclerotic plaque formation. Their polarization into the M1 or M2 phenotype is crucial in regulating disease progression. IL-10- and LPS-mediated alternate activation of macrophages from diabetes patient followed by oxidized LDL supplementation results in induction of CD36 and SR-A1 scavenger receptors and subsequent upregulation of ER stress response resulting in foam cell formation. This foam cell phenotype was mediated by the induction of CD36 and SR-A1 scavenger receptors [160]. Similarly, ER stress response is also linked to immunosuppressive MDSCs. For example, LDL receptor LOX-1-mediated lipid uptake and ER stress response results in immunosuppressive PMN-MDSCs formation **(Figure 3)**[90]. These reports overall discuss the importance of sXBP-1 mediated ER stress response in regulating myeloid cell phenotype.

Herein, we assessed if oleate treatment activates the expression of spliced XBP-1 as an indicator of immunosuppressive transcription factor. Additionally, although the iDGAT concentration was standardized (0.5 µM) for treating human MoDM, some donor samples when treated with oleate and 0.5 µM of the DGAT inhibitor still resulted in increased cell death. Therefore, we assessed if iDGAT based inhibition of TAG synthesis resulted in prolonged ER stress response due to increased accumulation of free fatty acids. This could potentially result in ER stress associated cell death and is indicated by spliced XBP-1 expression analysis. Oleate-dependent polarization of human MoDM resulted in low-grade sXBP-1 expression associated with potential immunosuppressive phenotype. This finding is consistent with the available literature and indicates that uptake of free fatty acids (FFAs) activates UPR signaling and drives expression of sXBP-1 transcription factor in oleate-dependent macrophages **Figure 5**, prompting towards immunosuppressive phenotype.

Moreover, co-treatment with oleate and the DGAT inhibitor resulted in increased accumulation of FFAs in the ER membrane due to decreased conversion of FFAs into TAGs. Possibly leading to prolonged ER stress and associated cellular apoptosis. Additionally, treatment with the DGAT inhibitor did not result in any significant alleviation of the oleate-induced effect, but rather amplified the downregulation of surface markers and further increased ER stress resulting in apoptosis. Therefore, indicating that iDGAT inhibitor was not suitable for studying the effect of oleate on human MoDM in our experimental setup.

So far, we observed that oleate-dependent human MoDM downregulated immunosuppressive surface markers and did not show a direct immune modulating characteristic upon co-culturing with $CD4^+$ T cells. Additionally, these oleate-dependent MoDM also showed sXBP-1 transcription factor activation, which has been associated with an immunosuppressive phenotype. Furthermore, we investigated the global gene expression changes resulting from oleate treatment in human MoDM using bulk RNA sequencing. The RNA sequencing results performed with the donor samples from each treatment group showed unexpectedly high intra-individual variability. The possible reason for this could be due to anonymity of donors from buffy coat samples with respect to age, gender, and lifestyle. Recent reports discuss the impact of genetic and environmental predispositions in altering circulating blood

monocyte population[161]. Additionally, the dietary fatty acid intake alters the monocyte-derived dendritic cell maturation and activation thereby causing increased systemic inflammation and alters the circulating monocyte population [162]. Similar report by Jordan *et al.* shows that fasting in healthy humans results in monocyte egression back into the bone marrow and alters the circulating inflammatory monocyte population[163]. These reports highlight the influence of diet, genetic and environmental factors in regulating the activation of circulating monocytes and support our findings that *in vitro* oleate-dependent polarization of human $CD14^{+}$monocytes, isolated from anonymous donors can show differing response to the oleate treatment due to dietary, genetic, and environmental biasing factors that cause altered response of monocytes to oleate treatment. However, despite the high intra-individual differences, heatmap analysis demonstrated a clear difference between the oleate-treated and control groups, highlighting that oleate treatment does result in differential gene expression. Further analysis of the data showed low differentially expressed genes.However, we identified genes that are metabolically (FABP4) and immunologically (GATA3) relevant to macrophage phenotypic characterization. Further screening of the dataset helped to identify additional genes that could be associated with macrophage fatty acid and lipid metabolism (CPT-1a and CD36) as well as immunosuppressive (CD204, CD206, CCR7, IL-6) phenotype. Real-time PCR-based experiments were performed to confirm differential expression of these genes. While performing these confirmation experiments, the samples from age and gender matched healthy donors were polarized together to reduce donor variability. Although, age and gender matched healthy donor samples were used, high intra-individual variability was still observed between the donors. However, the expression profile of FABP4, CPT-1a and CD36 showed a tendency towards higher expression in oleate polarized samples. Therefore, the experiments were repeated by increasing sample size with a mixed donor population by including samples from anonymous donors (buffy coats). This resulted in significant differences between control and oleate-treated groups. Hence, indicating that oleate treatment of human MoDM results in an overall significant effect on the donor population irrespective of sample source and genetic, dietary, and environmental factors do not influence the effect of oleate on human MoDM.

Based on these real-time PCR validation experiments, we confirmed an increased expression of fatty acid uptake genes CD36 and FABP4 as well as upregulation of fatty acid metabolism gene, CPT-1a. This experimental evidence indicates that oleate-dependent human MoDM show a metabolic dependence on fatty acid uptake and metabolism. According to the available literature discussed in section 1.2.1, expression of these genes points towards a phenotypic similarity with immunosuppressive lipid accumulating TAM phenotype. Additionally, expression of the transcription factor GATA3 was significantly upregulated in the oleate-treated group. As discussed in section 1.1.5, IL-33-mediated GATA3 activation regulates metabolic rewiring which has been associated with an alternative immunosuppressive macrophage activation[35]. However, no further significant differences were observed in the other markers including CD204, CD206, CCR7 and IL-6. This indicated an overall phenotypic tendency of oleate-dependent human MoDM towards an immunosuppressive phenotype. However, the downregulation of immunosuppressive surface markers and the lack of significant difference in expression of IL-6 and other immunologic markers directs the phenotype towards being rather functionally anergic albeit immunosuppressive. Elia *et al.* reported a similar but rather pro-inflammatory anergic macrophage phenotype, where factors secreted by a pancreatic tumor cell line resulted in downregulation pro-inflammatory markers as well as no significant activation of immunosuppressive genes[164].

5.1.4 Oleate-dependent foam cell formation

Additionally, as discussed in section 1.2.2, treatment with various lipids and metabolites results in monocyte polarization into FABP4 expressing foam cells, which have been reported in obesity-induced carcinogenesis and in atherosclerosis progression[83, 106, 165]. Herein, experiments were performed to evaluate if the oleate treatment would result in a FABP4 and CD36 expressing immunosuppressive foam cell phenotypes. Experimental evidence provided by Mei *et al.* and Zhao *et al.* demonstrates that oxLDL based cholesterol ester accumulation in macrophages results in increased CD36 expressing foam cell formation and this phenotype can be reversed upon treatment with SB203580 (pharmacological inhibitor for p38 MAPK downstream activity). They reported that SB203580 treatment instigates lipophagy, reduces intracellularly stored lipids and further downregulates CD36 expression. These

processes play an important role in regulating the foam cell phenotype in a p38-dependent manner[107, 108]. Herein, we assessed if SB203580 treatment would result in a similar lipophagic response, which could reverse the oleate-dependent immunosuppressive phenotype of macrophages. **Figure 15** indicates an increased lipophagy indicated by an increased ratio of LC-3BII to LC-3BI, upon treatment with oleate and SB203580. Further analysis indicates a decreased expression of FABP4 and CD36 along with decreased lipid accumulation but no subsequent changes in the expression of CD14, CD200R1, and CD163. This underlines that treatment with oleate results in an effect on human macrophage that regulates surface marker profile via pathways other than p38 kinase dependent LD formation. These data indicate that since cellular metabolites and macrophage polarization are mutually linked, increased oleate uptake *via* CD36 and FABP4, and lipid storage results in increased expression of sXBP-1 and GATA3, which are transcription factors associated with immunosuppressive phenotype.

Our previously published work demonstrated that *in vitro* oleate-dependent polarization of murine bone marrow-derived macrophages results in a CD206 expressing immunosuppressive macrophage type which can be reversed upon treatment with pharmacological inhibitors for DGAT1 & 2 enzymes[84]. In contrast to this work, oleate-dependent polarization of human monocyte-derived macrophages results in down-regulation of immunosuppressive scavenger receptors albeit retain avid expression of transcriptional markers associated with immunosuppressive phenotype, thus, displaying an overall immunosuppressive anergic phenotype. Additionally, DGAT inhibitor treatment proved to be incompatible for this immunosuppressive human MoDM phenotype.

5.2 Aim 2: Oleate-dependent polarization into CD206^{+} tumor-associated macrophage phenotype is independent of IL-4 signaling

As discussed in section 1.1.3 and 1.1.7, IL-4 stimulation plays an important role in alternative immunosuppressive macrophage activation. This results in subsequent metabolic switching to fatty acid-dependent OXPHOS[47, 166]. On the contrary, we re-

cently published that oleate-dependent polarization of BMDM results in immunosuppressive macrophages. We also showed that these macrophages synthesize and store lipids which are further utilized via the mitochondrial OXPHOS pathway in a CPT-1a enzyme-dependent manner, and play a role in regulating the immunosuppressive phenotype[84]. Herein, we performed oleate-dependent polarization of macrophages in the presence of anti-IL-4 antibodies and demonstrated for the first time that this oleate-dependent lipid accumulating immunosuppressive TAM phenotype is independent of IL-4 signaling and is characterized by high CD206 expression **(Figure 17)**. Additional reports show that IL-4 stimulated CD206 expressing immunosuppressive macrophages can be reversed by treatment with the CPT-1a inhibitor etomoxir. However, treatment with low concentrations of etomoxir (<3 µM) did not reduce the expression of CD206 whereas, concentrations above 3 µM reduced CD206 expressing macrophages due to off-target effects of etomoxir. The excessive etomoxir molecules link with the intracellular coenzyme A and result in formation of etomoxiryl CoA. This etomoxiryl CoA formation depletes the intracellular coenzyme A stores and targets electron transport chain (ETC) complexes. Thus, overall reducing the mitochondrial respiratory capacity. These reports highlight the importance of evaluating dose-dependent effect of etomoxir in immunosuppressive macrophages[60]. Herein, we evaluated the dose of etomoxir that effectively reduced CD206 expressing macrophages and observed that only 40 µM of etomoxir successfully reduced the oleate-dependent CD206 expressing immunosuppressive macrophages. This could possibly be due to the increased dependency of these macrophages on lipid and fatty acid metabolism and subsequently increased dependency on CPT-1a enzyme-mediated fatty acid oxidation. Therefore, increased concentrations of etomoxir inhibitor are required for reversing CD206 expressing macrophages. Additionally, treatment with 40 µM etomoxir, did not alter the mitochondrial respiratory capacity possibly because of constantly replenished fatty acid oxidation sourced from the stored lipids.

Moreover, we also evaluated whether coenzyme A plays a role in regulating the CD206 expression in oleate-dependent macrophages. For this, we supplemented the oleate-dependent BMDM during polarization with coenzyme A. However, coenzyme A supplementation did not alter CD206 expression in 40 µM etomoxir-treated

macrophages. Therefore, indicating that CD206 expression in oleate-dependent immunosuppressive macrophage phenotype is regulated and reversed independent of coenzyme A homeostasis.

5.3 Aim 3: The role of the enzymes DGAT1 & 2 in regulating myeloid compartment and macrophage phenotype

Recent reports highlight the role of LD formation in regulating foamy inflammatory macrophage phenotype as well as in immunosuppressive phenotype[63, 84, 100]. Despite all this availability of contrasting datasets arguing about macrophage lipid metabolism in immunosuppressive or pro-inflammatory disease conditions. The importance of lipogenesis and lipid storage enzymes in the myeloid cell compartment is not researched to its full potential. Especially, the role of individual DGAT1 & 2 enzymes in regulating macrophage phenotype is yet to be fully understood.

Towards this aim, we used a simple genetic strategy to generate transgenic knockout mice. For this, we crossed mice with loxP-flanked alleles encoding DGAT1 (*Dgat1*$^{fl/fl}$) or DGAT2 (*Dgat2*$^{fl/fl}$) with transgenic mice harboring nuclear-localized Cre recombinase under the lysozyme 2 (*Lyz2*) promoter region. Thus, generating two separate mouse lines with myeloid lineage–specific deletion of genes encoding DGAT1 & 2 enzymes. This provides a powerful tool for studying the role of each enzyme in lipid droplet formation within the myeloid cell lineage including monocytes, mature macrophages and granulocytes as well as in regulating the innate immune response. Much of the current experimental evidence indicating that lipid droplet formation is required for M2 macrophage polarization has relied on pharmacological approaches, particularly the use of the chemical inhibitors or antisense oligonucleotides targeting these enzymes[63, 84, 167]. Therefore, generation of the genetic mouse models provides a stable tool for detailed analysis of the role of these enzymes under various disease states. The first *in vitro* oleate-dependent polarization of BMDM from the knockout mice indicated that *Dgat1*$^{fl/fl}$*-LysMcre* knockout macrophages synthesize significantly less lipid droplets compared to wild type BMDMs and *Dgat2*$^{fl/fl}$*-LysMcre* mice derived macrophages. This novel finding emphasizes that DGAT1 enzyme plays a crucial role in regulating lipid droplet formation. The results also indicate that DGAT2 knock-

out macrophages with a functional DGAT1 enzyme activity are still capable of synthesizing lipids in DGAT1 enzyme dependent manner. Next step was to evaluate whether this reduced lipid accumulation in *Dgat1* gene knockout macrophages results in significant reduction in CD206 expression. However, this reduced lipid accumulation did not correlate with significant downregulation of CD206 expression in *in vitro* oleate treated macrophages or changes in other phenotypic markers (F4/80, MHC-II) compared to wild type BMDM. This indicated that the regulation of surface marker expression profile is a more complex process and can be downregulated in response to complete inhibition of lipid synthesis rather than just reduced lipid synthesis. Additionally, evaluation of fatty acid oxidation in these polarized macrophages did not highlight any significant changes compared to wild type. Even though macrophages from Dgat1 gene knockout mice synthesized and stored lesser lipid droplets, these macrophages still continue to utilize the available free fatty acids as well as the stored lipids and balanced the process of fatty acid oxidation. Therefore being a possible reason for no alterations in fatty acid oxidation profile. Overall, the single enzyme knockout mouse lines indicate that to see a significant change in lipid metabolism-dependent immunosuppressive phenotype, complete inhibition of lipid droplet synthesis is required for which double enzyme knockouts are required. Towards this, we are currently generating *Dgat1*$^{fl/fl}$*-Dgat2*$^{fl/fl}$*-LysMcre* double knockouts for future experimental work. Since the effect observed *in vitro* is only due to the accumulation of oleate-dependent lipid formation, we conclude that overall *in vitro* oleate-dependent culture condition provides a limited criteria for complete evaluation of these enzymes. However, *in vivo* settings can possibly allow an in-depth assessment of DGAT1 & 2 in the regulating myeloid cell phenotype in response to high-fat diet supplemented with various fatty acids. Likewise, the involvement of DGAT1 & 2 enzymes in regulating macrophage phenotype in obesity-linked diseases such as atherosclerosis progression will also be evaluated using the high-fat diet mouse models.

This will help to understand the role of DGAT1 & 2 enzymes in regulating myeloid lineage in response to dietary alterations. Additionally, to assess the role of these enzymes in regulating myeloid lineage-mediated response to disease progression, we are also working towards generating tumor injection models with the knockout mice.

As discussed in section1.3.3, lipid storage and metabolism play a role in regulating myeloid progenitor population. Therefore, we evaluated if the deletion of DGAT1 & 2 enzymes respectively alters the myeloid progenitor population. However, we did not observe any significant differences in the bone marrow myeloid progenitor population in DGAT1 & 2 knockout mice compared to wild type mice. This possibly indicates that under steady state conditions, the lipid synthesizing enzymes do not influence myelopoiesis. Additionally, to further confirm the association of DGAT1 & 2 enzymes in regulating myelopoiesis, we aim at performing the analysis in double gene knock-out mice. In addition, these results also indicate that since the enzymes play a role in lipid synthesis and storage, alternate high fat diet supplementation and altered lipid metabolism is potentially required for complete investigation of DGAT1 and 2 in regulating myelopoiesis in diseased or metabolically challenged state.

5.4 Conclusion

Overall, the project focused on understanding the role of lipid accumulation in regulating the overall immunological phenotype of macrophage, with emphasis on human monocyte-derived macrophages under various pathological conditions such as in tumor microenvironment or atherosclerosis. We successfully established an *in vitro* model for polarizing human $CD14^+$ monocytes in the presence of oleate. This resulted in a phenotype characterized by significant fatty acid metabolism as seen by upregulation of genes associated with fatty acid uptake and metabolism including CD36, FABP4 and CPT-1a- as well as with increased lipid droplet synthesis. Furthermore, we aimed at analyzing immunosuppressive characteristics, if any, of the oleate-dependent macrophages. Herein, we identified that oleate-dependent human MoDMs successfully upregulated the expression of transcription factors, GATA3 and spliced XBP-1, which have been associated with an immunosuppressive phenotype and subsequently rewire the macrophage metabolism orienting it towards fatty acid and lipid metabolizing immunosuppressive macrophages. Largely, we identified that these oleate-dependent human MoDMs also significantly downregulate immunosuppressive surface markers CD200R1 and CD163 with no associated characteristic functional changes as seen by the T cell suppression assay. Additionally, lipid and fatty acid accumulating macrophages are reported in physiological conditions such as atherosclerosis as well as certain types of solid tumors and are called foam cells.

They have associated with poor disease prognosis. In our research, we provide evidence that *in vitro* oleate-dependent polarization of human MoDM results in a novel macrophage phenotype which downregulated immunosuppressive scavenger receptors and expresses no direct effect on T-cell proliferating capacity albeit harbors an active transcriptional character of immunosuppressive macrophages similar to foam cells.

Additionally, we successfully generated novel mouse models for evaluating the role of DGAT1 & 2 enzymes in regulating the myeloid cell phenotype. In line with the current research, we demonstrate herein for the first time, that DGAT1 enzyme deletion effectively results in lower lipid droplet accumulation in macrophages. These mouse model provide a novel genetic tool for further evaluation of the role of DGAT1 & 2 enzymes in regulating the myeloid cell phenotype.

6 Appendix

6.1 Abbreviations

ACAT1 & 2	Acyl CoA acetyltransferase1 & 2
APC Cy7	Allophycocyanin-Cy7
APC	Allophycocyanin
ATF6α	Activating transcription factor 6α
ATP	Adenosine triphosphate
AT	Adipose tissue
ATM	Adipose tissue macrophages
BM	bone marrow
BMDM	Bone marrow derived macrophages
BSA	Bovine serum albumin
BV	Brilliant violet
CD	Cluster of differentiation
CE	Cholesterol esters
CFSE	carboxyfluorescein diacetate succinimidyl ester
CHOP	CCAAT/Enhancer binding protein homologous protein
CoA	Coenzyme A
CMP	Common myeloid progenitor
CPT-1α	Carnitine palmitoyl transferase 1α
CPT-2	Carnitine palmitoyl transferase 2
DGAT1 & 2	Diglycerol acyl transferase1 & 2

DMEM	Dulbecco’s Modified Eagle Medium
ECL	Enhanced chemiluminescence reagent
EDTA	Ethylenediaminetetraacetic acid
ER	Endoplasmic reticulum
ETC	Electron transport chain
FABP	Fatty acid binding protein
FAO	Fatty acid oxidation pathway
FASN	Fatty acid synthase
FAT	fatty acid translocase
FCCP	Carbonyl cyanide 4-(trifluoromethoxy) phenylhydrazone
FCS-PBS	Fetal calf serum- phosphate buffered saline
FFA	Free fatty acids
FIT1 & 2	Fat storage inducing transmembrane protein-1 & 2
FITC	Fluorescein isothiocyanate
GM-CSF	Granulocyte macrophage colony stimulating factor
GMP	Granulocytic myeloid progenitor
GPI	Glycosylphosphatidylinositol
HIF-1α	Hypoxia inducible factor-1α
MoDM	Monocyte-derived macrophages
iDGAT	pharmacological inhibitor combination for DGAT1 & 2 enzymes
IFN	Interferon
IL	Interleukin
iNOS	inducible Nitric oxide synthase
IRE-1α	Inositol requiring enzyme-1 α

LC-3B	Microtubule associated protein light chain 3B
LD	Lipid droplet
LDAF-1	Lipid droplet assembly factor 1
LDL	Low-density lipoproteins
LPS	Lipopolysaccharide
Lyz2	Lysozyme 2 promoter
MACS	Magnetic–activated cell sorting buffer
MARCO	Macrophage receptor with collagenous structure
M-CSF	Macrophage colony stimulating factor
MDSC	Myeloid-derived suppressor cells
MEP	Megakaryocyte-erythroid progenitor
MoDM	Monocyte-derived macrophages
MPS	Mononuclear phagocytic System
MSR	Macrophage scavenger receptor
Nrf2	Nuclear factor erythroid 2-related factor 2
OCR	Oxygen consumption rate
PBMC	Peripheral blood mononuclear cells
PCA	Principle component analysis
PE Cy7	Phycoerythrin Cyanine 7
PE	Phycoerythrin
PerCP	Peridinin chlorophyll protein
PERK	Protein kinase R-like endoplasmic reticulum kinase
PGC-1β	PPARγ coactivator-1β
PGE2	Prostaglandin E2

PI	Propidium Iodide
PPAR	Peroxisome proliferator-activated receptor
PPP	Pentose phosphate pathway
PVDF	Polyvinylidene difluoride
RIN	RNA integrity number
RIPA	Radioimmunoprecipitation assay buffer
Sca-1	Stem cell antigen-1
SDS-PAGE	Sodium dodecyl sulfate-Polyacrylamide gel electrophoresis
SE	Sterol esters
SR	Scavenger receptor
SREBP	Sterol regulatory-element binding protein
TAGs	Triacylglycerols
TAM	Tumor-associated macrophages
TBST	Tris-buffered saline with 0.1% Tween 20 detergent
tDCs	Tumor dendritic cells
TGF	Tumor growth factor
TLR	Toll like receptor
TME	Tumor microenvironment
TNF	Tumor necrosis factor
UPR	Unfolded protein response
VLDL	Very low-density lipoproteins
XBP-1	X-box binding protein

6.2 Figures

6.3 Tables

6.4 References

1. Tauber, A.I. Metchnikoff and the phagocytosis theory. *Nature Reviews Molecular Cell Biology* **4**, 897-901 (2003).

2. Ginhoux, F. & Guilliams, M. Tissue-Resident Macrophage Ontogeny and Homeostasis. *Immunity* **44**, 439-449 (2016).

3. R. Van Furth, Z.A.C., J. G. HIRSCH, J. H. HUMPHREY, W. G. SPECTOR, & H. L. LANGEVOORT. The mononuclear phagocyte system: a new classification of macrophages, monocytes, and their precursor cells. (1972).

4. Frederic Geissmann, M.G.M., Steffen Jung, Michael H. Sieweke, Miriam Merad, Klaus Ley. Development of Monocytes,

Macrophages, and Dendritic Cells. (2010).

5. Ginhoux, F., Lim, S., Hoeffel, G., Low, D. & Huber, T. Origin and differentiation of microglia. *Front Cell Neurosci* **7**, 45 (2013).

6. Pollard, J.W. Trophic macrophages in development and disease. *Nature Reviews Immunology* **9**, 259-270 (2009).

7. Biswas, S.K. & Mantovani, A. Macrophage plasticity and interaction with lymphocyte subsets: cancer as a paradigm. *Nature Immunology* **11**, 889-896 (2010).

8. Peter *et al.* Macrophage Activation and Polarization: Nomenclature and Experimental Guidelines. *Immunity* **41**, 14-20 (2014).

9. Chambers, M. *et al.* Macrophage Plasticity in Reproduction and Environmental Influences on Their Function. *Front Immunol* **11**, 607328 (2020).

10. Martinez, F.O., Gordon, S., Locati, M. & Mantovani, A. Transcriptional profiling of the human monocyte-to-macrophage differentiation and polarization: new molecules and patterns of gene expression. *J Immunol* **177**, 7303-7311 (2006).

11. Taylor, P.R. *et al.* MACROPHAGE RECEPTORS AND IMMUNE RECOGNITION. *Annual Review of Immunology* **23**, 901-944 (2005).

12. Fu, Y.L. & Harrison, R.E. Microbial Phagocytic Receptors and Their Potential Involvement in Cytokine Induction in Macrophages. *Front Immunol* **12**, 662063 (2021).

13. Yu, X., Guo, C., Fisher, P.B., Subjeck, J.R. & Wang, X.-Y. Scavenger Receptors. Elsevier, 2015, pp 309-364.

14. Gudgeon, J., Marin-Rubio, J.L. & Trost, M. The role of macrophage scavenger receptor 1 (MSR1) in inflammatory disorders and cancer. *Front Immunol* **13**, 1012002 (2022).

15. Shi, B. *et al.* The Scavenger Receptor MARCO Expressed by Tumor-Associated Macrophages Are Highly Associated With Poor Pancreatic Cancer Prognosis. *Front Oncol* **11**, 771488 (2021).

16. Collot-Teixeira, S., Martin, J., McDermott-Roe, C., Poston, R. & McGregor, J.L. CD36 and macrophages in atherosclerosis. *Cardiovasc Res* **75**, 468-477 (2007).

17. Wang, J. & Li, Y. CD36 tango in cancer: signaling pathways and functions. *Theranostics* **9**, 4893-4908 (2019).

18. Marelli, G. *et al.* Lipid-loaded macrophages as new therapeutic target in cancer. *J Immunother Cancer* **10** (2022).

19. Chistiakov, D.A., Killingsworth, M.C., Myasoedova, V.A., Orekhov, A.N. & Bobryshev, Y.V. CD68/macrosialin: not just a histochemical marker. *Laboratory Investigation* **97**, 4-13 (2017).

20. Hirsch, H.A. *et al.* A Transcriptional Signature and Common Gene Networks Link Cancer with Lipid Metabolism and Diverse Human Diseases. *Cancer Cell* **17**, 348-361 (2010).

21. Khaidakov, M. *et al.* Oxidized LDL Receptor 1 (OLR1) as a Possible Link between Obesity, Dyslipidemia and Cancer. *PLoS ONE* **6**, e20277 (2011).

22. Xu, Z.-J. *et al.* The M2 macrophage marker CD206: a novel prognostic indicator for acute myeloid leukemia. *OncoImmunology* **9**, 1683347 (2020).

23. Haque, A.S.M.R. *et al.* CD206+ tumor-associated macrophages promote proliferation and invasion in oral squamous cell carcinoma via EGF production. *Scientific Reports* **9** (2019).

24. Naeim, F., Nagesh Rao, P., Song, S.X. & Phan, R.T. Principles of Immunophenotyping. *Atlas of Hematopathology*, 2018, pp 29-56.

25. Landmann, R., Ludwig, C., Obrist, R. & Obrecht, J.P. Effect of cytokines and lipopolysaccharide on CD14 antigen expression in human monocytes and macrophages. *Journal of Cellular Biochemistry* **47**, 317-329 (1991).

26. Koning, N. *et al.* Expression of the Inhibitory CD200 Receptor Is Associated with Alternative Macrophage Activation. *Journal of Innate Immunity* **2**, 195-200 (2010).

27. Furuhashi, M. & Hotamisligil, G.S. Fatty acid-binding proteins: role in metabolic diseases and potential as drug targets. *Nature Reviews Drug Discovery* **7**, 489-503 (2008).

28. Hotamisligil, L.M.a.G.S. Fatty Acid Binding Proteins—The Evolutionary Crossroads of Inflammatory and Metabolic Responses. *Journal of Nutrition* (2004).

29. Ross, R. Atherosclerosis — An Inflammatory Disease. *New England Journal of Medicine* **340**, 115-126 (1999).

30. Krausgruber, T. *et al.* IRF5 promotes inflammatory macrophage polarization and TH1-TH17 responses. *Nature Immunology* **12**, 231-238 (2011).

31. Lawrence, T. & Natoli, G. Transcriptional regulation of macrophage polarization: enabling diversity with identity. *Nature Reviews Immunology* **11**, 750-761 (2011).

32. Litvak, V. *et al.* Function of C/EBPδ in a regulatory circuit that discriminates between transient and persistent TLR4-induced signals. *Nature Immunology* **10**, 437-443 (2009).

33. Zhong, Y. & Yi, C. MicroRNA-720 suppresses M2 macrophage polarization by targeting GATA3. *Biosci Rep* **36** (2016).

34. Chinetti, G., Fruchart, J.C. & Staels, B. Peroxisome proliferator-activated receptors (PPARs): Nuclear receptors at the crossroads between lipid metabolism and inflammation. *Inflammation Research* **49**, 497-505 (2000).

35. Faas, M. *et al.* IL-33-induced metabolic reprogramming controls the differentiation of alternatively activated macrophages and the resolution of inflammation. *Immunity* **54**, 2531-2546 e2535 (2021).

36. Chavez-Galan, L., Olleros, M.L., Vesin, D. & Garcia, I. Much More than M1 and M2 Macrophages, There are also CD169(+) and TCR(+) Macrophages. *Front Immunol* **6**, 263 (2015).

37. Park, S.H. Regulation of Macrophage Activation and Differentiation in Atherosclerosis. *Journal of Lipid and Atherosclerosis* **10**, 251 (2021).

38. Hard, G.C. Some biochemical aspects of the immune macrophages. *British Journal of Experimental Pathology*, 97-105 (1970).

39. Newsholme, P., Gordon, S. & Newsholme, E.A. Rates of utilization and fates of glucose, glutamine, pyruvate, fatty acids and ketone bodies by mouse macrophages. *Biochemical Journal* **242**, 631-636 (1987).

40. Freemerman, A.J. *et al.* Metabolic Reprogramming of Macrophages. *Journal of Biological Chemistry* **289**, 7884-7896 (2014).

41. Semenza, G.L. *et al.* Hypoxia Response Elements in the Aldolase A, Enolase 1, and Lactate Dehydrogenase A Gene Promoters Contain Essential Binding Sites for Hypoxia-inducible Factor 1. *Journal of Biological Chemistry* **271**, 32529-32537 (1996).

42. Tannahill, G.M. *et al.* Succinate is an inflammatory signal that induces IL-1β through HIF-1α. *Nature* **496**, 238-242 (2013).

43. Wang, T. *et al.* HIF-1α-Induced Glycolysis Metabolism Is Essential to the Activation of Inflammatory Macrophages. *Mediators of Inflammation* **2017**, 1-10 (2017).

44. Meiser, J. *et al.* Pro-inflammatory Macrophages Sustain Pyruvate Oxidation through Pyruvate Dehydrogenase for the Synthesis of Itaconate and to Enable Cytokine Expression. *Journal of Biological Chemistry* **291**, 3932-3946 (2016).

45. Baardman, J. *et al.* A Defective Pentose Phosphate Pathway Reduces Inflammatory Macrophage Responses during Hypercholesterolemia. *Cell Reports* **25**, 2044-2052.e2045 (2018).

46. Tan, Z. *et al.* Pyruvate Dehydrogenase Kinase 1 Participates in Macrophage Polarization via Regulating Glucose Metabolism. *The Journal of Immunology* **194**, 6082-6089 (2015).

47. Wang, F. *et al.* Glycolytic Stimulation Is Not a Requirement for M2 Macrophage Differentiation. *Cell Metabolism* **28**, 463-475.e464 (2018).

48. Nomura, M. *et al.* Fatty acid oxidation in macrophage polarization. *Nature Immunology* **17**, 216-217 (2016).

49. Ren, W. *et al.* Glutamine Metabolism in Macrophages: A Novel Target for Obesity/Type 2 Diabetes. *Adv Nutr* **10**, 321-330 (2019).

50. Abhishek *et al.* Network Integration of Parallel Metabolic and Transcriptional Data Reveals Metabolic Modules that Regulate Macrophage Polarization. *Immunity* **42**, 419-430 (2015).

51. Infantino, V., Iacobazzi, V., Menga, A., Avantaggiati, M.L. & Palmieri, F. A key role of the mitochondrial citrate carrier (SLC25A1) in TNFα- and IFNγ-triggered inflammation. *Biochimica et Biophysica Acta (BBA) - Gene Regulatory Mechanisms* **1839**, 1217-1225 (2014).

52. Infantino, V., Iacobazzi, V., Palmieri, F. & Menga, A. ATP-citrate lyase is essential for macrophage inflammatory response. *Biochemical and Biophysical Research Communications* **440**, 105-111 (2013).

53. Li, Y. *et al.* Immune Responsive Gene 1 (IRG1) Promotes Endotoxin Tolerance by Increasing A20 Expression in Macrophages through Reactive Oxygen Species. *Journal of Biological Chemistry* **288**, 16225-16234 (2013).

54. Lampropoulou, V. *et al.* Itaconate Links Inhibition of Succinate Dehydrogenase with Macrophage Metabolic Remodeling and Regulation of Inflammation. *Cell Metabolism* **24**, 158-166 (2016).

55. Mills, E.L. *et al.* Itaconate is an anti-inflammatory metabolite that activates Nrf2 via alkylation of KEAP1. *Nature* **556**, 113-117 (2018).

56. Kobayashi, E.H. *et al.* Nrf2 suppresses macrophage inflammatory response by blocking proinflammatory cytokine transcription. *Nature Communications* **7**, 11624 (2016).

57. Huang, S.C.-C. *et al.* Cell-intrinsic lysosomal lipolysis is essential for alternative activation of macrophages. *Nature Immunology* **15**, 846-855 (2014).

58. Vats, D. *et al.* Oxidative metabolism and PGC-1β attenuate macrophage-mediated inflammation. *Cell Metabolism* **4**, 13-24 (2006).

59. Namgaladze, D. & Brune, B. Fatty acid oxidation is dispensable for human macrophage IL-4-induced polarization. *Biochim Biophys Acta* **1841**, 1329-1335 (2014).

60. Divakaruni, A.S. *et al.* Etomoxir Inhibits Macrophage Polarization by Disrupting CoA Homeostasis. *Cell Metab* **28**, 490-503 e497 (2018).

61. Wu, H. *et al.* Lipid droplet-dependent fatty acid metabolism controls the immune suppressive phenotype of tumor-associated macrophages. *EMBO Molecular Medicine*; 2019. pp. 1-17.

62. Wu, H. *et al.* Oleate but not stearate induces the regulatory phenotype of myeloid suppressor cells. *Sci Rep* **7**, 7498 (2017).

63. Castoldi, A. *et al.* Triacylglycerol synthesis enhances macrophage inflammatory function. *Nature Communications* **11** (2020).

64. Camell, C. & Smith, C.W. Dietary Oleic Acid Increases M2 Macrophages in the Mesenteric Adipose Tissue. *PLoS ONE* **8**, e75147 (2013).

65. Im, S.-S. *et al.* Linking Lipid Metabolism to the Innate Immune Response in Macrophages through Sterol Regulatory Element Binding Protein-1a. *Cell Metabolism* **13**, 540-549 (2011).

66. J L. Funk, K.R.F., A H. Moser and C Grunfeld. Lipopolysaccharide stimulation of RAW 264.7 macrophages induces lipid accumulation and foam cell formation. *Atherosclerosis* **98** (1993).

67. Feingold, K.R. *et al.* Mechanisms of triglyceride accumulation in activated macrophages. *J Leukoc Biol* **92**, 829-839 (2012).

68. Sun, J.X., Xu, X.H. & Jin, L. Effects of Metabolism on Macrophage Polarization Under Different Disease Backgrounds. *Front Immunol* **13**, 880286 (2022).

69. Martinez, F.O. Macrophage activation and polarization. *Frontiers in Bioscience* **13**, 453 (2008).

70. Warburg, O. On the Origin of Cancer Cells. *Science* (1956).

71. Hanahan, D. & Weinberg, R.A. Hallmarks of cancer: The next generation. *Cell*: Elsevier Inc.; 2011. pp. 646-674.

72. Pombo Antunes, A.R. *et al.* Single-cell profiling of myeloid cells in glioblastoma across species and disease stage reveals macrophage competition and specialization. *Nature Neuroscience* **24**, 595-610 (2021).

73. Casanova-Acebes, M. *et al.* Tissue-resident macrophages provide a pro-tumorigenic niche to early NSCLC cells. *Nature* **595**, 578-584 (2021).

74. Che, L.-H. *et al.* A single-cell atlas of liver metastases of colorectal cancer reveals reprogramming of the tumor microenvironment in response to preoperative chemotherapy. *Cell Discovery* **7** (2021).

75. Su, P. *et al.* Enhanced Lipid Accumulation and Metabolism Are Required for the Differentiation and Activation of Tumor-Associated Macrophages. *Cancer Res* **80**, 1438-1450 (2020).

76. Di Conza, G. *et al.* Tumor-induced reshuffling of lipid composition on the endoplasmic reticulum membrane sustains macrophage survival and pro-tumorigenic activity. *Nature Immunology* **22**, 1403-1415 (2021).

77. Mulder, K. *et al.* Cross-tissue single-cell landscape of human monocytes and macrophages in health and disease. *Immunity* **54**, 1883-1900.e1885 (2021).

78. Hanahan, D. & Robert. Hallmarks of Cancer: The Next Generation. *Cell* **144**, 646-674 (2011).

79. Cheng, S. *et al.* A pan-cancer single-cell transcriptional atlas of tumor infiltrating myeloid cells. *Cell* **184**, 792-809.e723 (2021).

80. Zhang, L. *et al.* Single-Cell Analyses Inform Mechanisms of Myeloid-Targeted Therapies in Colon Cancer. *Cell* **181**, 442-459.e429 (2020).

81. Talks, K.L. *et al.* The Expression and Distribution of the Hypoxia-Inducible Factors HIF-1α and HIF-2α in Normal Human Tissues, Cancers, and Tumor-Associated Macrophages. *The American Journal of Pathology* **157**, 411-421 (2000).

82. Hao, J. *et al.* Expression of Adipocyte/Macrophage Fatty Acid-Binding Protein in Tumor-Associated Macrophages Promotes Breast Cancer Progression. *Cancer Res* **78**, 2343-2355 (2018).

83. Liu, S. *et al.* FABP4 in obesity-associated carcinogenesis: Novel insights into mechanisms and therapeutic implications. *Front Mol Biosci* **9**, 973955 (2022).

84. Wu, H. *et al.* Lipid droplet-dependent fatty acid metabolism controls the immune suppressive phenotype of tumor-associated macrophages. *EMBO Molecular Medicine* **11**, 1-17 (2019).

85. Al-Khami, A.A. *et al.* Exogenous lipid uptake induces metabolic and functional reprogramming of tumor-associated myeloid-derived suppressor cells. *OncoImmunology* **6**, e1344804 (2017).

86. Bronte, V. *et al.* Recommendations for myeloid-derived suppressor cell nomenclature and characterization standards. *Nature Communications* **7**, 12150 (2016).

87. Veglia, F., Sanseviero, E. & Gabrilovich, D.I. Myeloid-derived suppressor cells in the era of increasing myeloid cell diversity. *Nature Reviews Immunology* **21**, 485-498 (2021).

88. Gabrilovich, D.I. Myeloid-Derived Suppressor Cells. *Cancer Immunology Research* **5**, 3-8 (2017).

89. Hossain, F. *et al.* Inhibition of Fatty Acid Oxidation Modulates Immunosuppressive Functions of Myeloid-Derived Suppressor Cells and Enhances Cancer Therapies. *Cancer Immunol Res* **3**, 1236-1247 (2015).

90. Condamine, T. *et al.* Lectin-type oxidized LDL receptor-1 distinguishes population of human polymorphonuclear myeloid-derived suppressor cells in cancer patients. *Science Immunology* **1**, aaf8943-aaf8943 (2016).

91. Adeshakin, A.O. *et al.* Regulation of ROS in myeloid-derived suppressor cells through targeting fatty acid transport protein 2 enhanced anti-PD-L1 tumor immunotherapy. *Cell Immunol* **362**, 104286 (2021).

92. Liu, G. *et al.* SIRT1 limits the function and fate of myeloid-derived suppressor cells in tumors by orchestrating HIF-1alpha-dependent glycolysis. *Cancer Res* **74**, 727-737 (2014).

93. Gabrilovich, D.I. *et al.* The Terminology Issue for Myeloid-Derived Suppressor Cells. *Cancer Research* **67**, 425-425 (2007).

94. Corzo, C.A. *et al.* HIF-1α regulates function and differentiation of myeloid-derived suppressor cells in the tumor microenvironment. *Journal of Experimental Medicine* **207**, 2439-2453 (2010).

95. Hamad Alshetaiwi, N.P., Laura Lynn McIntyre, Dennis Ma, Quy Nguyen, Jan Akara Rath, Kevin Nee, Grace Hernandez, Katrina Evans, Leona Torosian, Anushka Silva, Craig Walsh, Kai Kessenbrock*. Defining the emergence of myeloid-derived suppressor cells in breast cancer using single-cell transcriptomics. *Science Immunology* (2020).

96. Yan, D. *et al.* Polyunsaturated fatty acids promote the expansion of myeloid-derived suppressor cells by activating the JAK/STAT3 pathway. *European Journal of Immunology* **43**, 2943-2955 (2013).

97. Lumeng, C.N., Bodzin, J.L. & Saltiel, A.R. Obesity induces a phenotypic switch in adipose tissue macrophage polarization. *Journal of Clinical Investigation* **117**, 175-184 (2007).

98. Morgan, P.K. *et al.* Macrophage polarization state affects lipid composition and the channeling of exogenous fatty acids into endogenous lipid pools. *Journal of Biological Chemistry* **297**, 101341 (2021).

99. Wilfling, F., Haas, J.T., Walther, T.C. & Jr, R.V.F. Lipid droplet biogenesis. *Current Opinion in Cell Biology* **29**, 39-45 (2014).

100. Koliwad, S.K. *et al.* DGAT1-dependent triacylglycerol storage by macrophages protects mice from diet-induced insulin resistance and inflammation. *Journal of Clinical Investigation* **120**, 756-767 (2010).

101. Gómez-Hernández, A., Beneit, N., Díaz-Castroverde, S. & Escribano, Ó. Differential Role of Adipose Tissues in Obesity and Related Metabolic and Vascular Complications. *International Journal of Endocrinology* **2016**, 1-15 (2016).

102. Boyle, J.J. *et al.* Coronary Intraplaque Hemorrhage Evokes a Novel Atheroprotective Macrophage Phenotype. *The American Journal of Pathology* **174**, 1097-1108 (2009).

103. Kadl, A., Galkina, E. & Leitinger, N. Induction of CCR2-dependent macrophage accumulation by oxidized phospholipids in the air-pouch model of inflammation. *Arthritis & Rheumatism* **60**, 1362-1371 (2009).

104. Kadl, A. *et al.* Identification of a Novel Macrophage Phenotype That Develops in Response to Atherogenic Phospholipids via Nrf2. *Circulation Research* **107**, 737-746 (2010).

105. Makowski, L. *et al.* Lack of macrophage fatty-acid–binding protein aP2 protects mice deficient in apolipoprotein E against atherosclerosis. *Nature Medicine* **7**, 699-705 (2001).

106. Hayden, J.M. *et al.* Induction of monocyte differentiation and foam cell formation in vitro by 7-ketocholesterol. *Journal of Lipid Research* **43**, 26-35 (2002).

107. Mei, S. *et al.* p38 Mitogen-activated Protein Kinase (MAPK) Promotes Cholesterol Ester Accumulation in Macrophages through Inhibition of Macroautophagy. *Journal of Biological Chemistry* **287**, 11761-11768 (2012).

108. Zhao, M. *et al.* Activation of the p38 MAP kinase pathway is required for foam cell formation from macrophages exposed to oxidized LDL. *APMIS* **110**, 458-468 (2002).

109. Shapiro, H. *et al.* Adipose tissue foam cells are present in human obesity. *J Clin Endocrinol Metab* **98**, 1173-1181 (2013).

110. Gleissner, C.A., Shaked, I., Little, K.M. & Ley, K. CXC chemokine ligand 4 induces a unique transcriptome in monocyte-derived macrophages. *J Immunol* **184**, 4810-4818 (2010).

111. Jaitin, D.A. *et al.* Lipid-Associated Macrophages Control Metabolic Homeostasis in a Trem2-Dependent Manner. *Cell* **178**, 686-698.e614 (2019).

112. Guerrini, V. & Gennaro, M.L. Foam Cells: One Size Doesn't Fit All. *Trends Immunol* **40**, 1163-1179 (2019).

113. Cohen, S. Lipid Droplets as Organelles. Elsevier, 2018, pp 83-110.

114. Olzmann, J.A. & Carvalho, P. Dynamics and functions of lipid droplets. *Nature Reviews Molecular Cell Biology* **20**, 137-155 (2019).

115. Engin, A.B.E.A. Obesity and lipotoxicity. *Advances in Experimental Medicine and Biology* **960** (2017).

116. Zhang, X. & Zhang, K. Endoplasmic Reticulum Stress-Associated Lipid Droplet Formation and Type II Diabetes. *Biochem Res Int* **2012**, 247275 (2012).

117. Jarc, E. & Petan, T. Lipid droplets and the management of cellular stress. *Yale J. Biol. Med.* **92**, 435–452 (2019).

118. Knight, M., Braverman, J., Asfaha, K., Gronert, K. & Stanley, S. Lipid droplet formation in Mycobacterium tuberculosis infected macrophages requires IFN-γ/HIF-1α signaling and supports host defense. *PLOS Pathogens* **14**, e1006874 (2018).

119. Li, L.O., Klett, E.L. & Coleman, R.A. Acyl-CoA synthesis, lipid metabolism and lipotoxicity. *Biochimica et Biophysica Acta (BBA) - Molecular and Cell Biology of Lipids* **1801**, 246-251 (2010).

120. Buhman, K.K., Chen, H.C. & Farese, R.V. The Enzymes of Neutral Lipid Synthesis. *Journal of Biological Chemistry* **276**, 40369-40372 (2001).

121. Walther, T.C. & Farese, R.V. Lipid Droplets and Cellular Lipid Metabolism. *Annual Review of Biochemistry* **81**, 687-714 (2012).

122. Yen, C.-L.E., Stone, S.J., Koliwad, S., Harris, C. & Farese, R.V. Thematic Review Series: Glycerolipids. DGAT enzymes and triacylglycerol biosynthesis. *Journal of Lipid Research* **49**, 2283-2301 (2008).

123. Chung, J. *et al.* LDAF1 and Seipin Form a Lipid Droplet Assembly Complex. *Developmental Cell* **51**, 551-563.e557 (2019).

124. Gross, D.A., Zhan, C. & Silver, D.L. Direct binding of triglyceride to fat storage-inducing transmembrane proteins 1 and 2 is important for lipid droplet formation. *Proceedings of the National Academy of Sciences* **108**, 19581-19586 (2011).

125. Skinner, J.R. *et al.* Diacylglycerol Enrichment of Endoplasmic Reticulum or Lipid Droplets Recruits Perilipin 3/TIP47 during Lipid Storage and Mobilization. *Journal of Biological Chemistry* **284**, 30941-30948 (2009).

126. Hotamisligil, L.M.a.G.S. Fatty Acid Binding Proteins—The Evolutionary Crossroads of Inflammatory and Metabolic Responses1. *Journal of Nutrition* (2004).

127. Han, J. & Kaufman, R.J. The role of ER stress in lipid metabolism and lipotoxicity. *Journal of Lipid Research* **57**, 1329-1338 (2016).

128. Baiceanu, A., Mesdom, P., Lagouge, M. & Foufelle, F. Endoplasmic reticulum proteostasis in hepatic steatosis. *Nature Reviews Endocrinology* **12**, 710-722 (2016).

129. Hetz, C., Chevet, E. & Harding, H.P. Targeting the unfolded protein response in disease. *Nature Reviews Drug Discovery* **12**, 703-719 (2013).

130. Cui, W. *et al.* Free Fatty Acid Induces Endoplasmic Reticulum Stress and Apoptosis of β-cells by Ca2+/Calpain-2 Pathways. *PLoS ONE* **8**, e59921 (2013).

131. Sharmin, M.M. *et al.* Effects of fatty acids on inducing endoplasmic reticulum stress in bovine mammary epithelial cells. *Journal of Dairy Science* **103**, 8643-8654 (2020).

132. Yoshida, H., Matsui, T., Yamamoto, A., Okada, T. & Mori, K. XBP1 mRNA Is Induced by ATF6 and Spliced by IRE1 in Response to ER Stress to Produce a Highly Active Transcription Factor. *Cell* **107**, 881-891 (2001).

133. Lee, A.-H., Scapa, E.F., Cohen, D.E. & Glimcher, L.H. Regulation of Hepatic Lipogenesis by the Transcription Factor XBP1. *Science* **320**, 1492-1496 (2008).

134. Mizushima, N. Autophagy: process and function. *Genes & Development* **21**, 2861-2873 (2007).

135. Singh, R. *et al.* Autophagy regulates lipid metabolism. *Nature* **458**, 1131-1135 (2009).

136. Pon, L.A. Lipid droplet autophagy during energy mobilization lipid homeostasis and protein quality control. *Frontiers in Bioscience* **23**, 1552-1563 (2018).

137. Jiang, L. *et al.* Oleic acid induces apoptosis and autophagy in the treatment of Tongue Squamous cell carcinomas. *Scientific Reports* **7** (2017).

138. William *et al.* Bone Marrow Adipose Tissue Is an Endocrine Organ that Contributes to Increased Circulating Adiponectin during Caloric Restriction. *Cell Metabolism* **20**, 368-375 (2014).

139. Wang, H., Leng, Y. & Gong, Y. Bone Marrow Fat and Hematopoiesis. *Front Endocrinol (Lausanne)* **9**, 694 (2018).

140. Pernes, G., Flynn, M.C., Lancaster, G.I. & Murphy, A.J. Fat for fuel: lipid metabolism in haematopoiesis. *Clinical & Translational Immunology* **8** (2019).

141. Dragoljevic, D., Westerterp, M., Veiga, C.B., Nagareddy, P. & Murphy, A.J. Disordered haematopoiesis and cardiovascular disease: a focus on myelopoiesis. *Clin Sci (Lond)* **132**, 1889-1899 (2018).

142. Liu, C. *et al.* Lipoprotein lipase regulates hematopoietic stem progenitor cell maintenance through DHA supply. *Nature Communications* **9** (2018).

143. Lemus-Conejo, A. *et al.* MUFAs in High-Fat Diets Protect against Obesity-Induced Bias of Hematopoietic Cell Lineages. *Molecular Nutrition & Food Research* **65**, 2001203 (2021).

144. Menendez, J.A. & Lupu, R. Fatty acid synthase and the lipogenic phenotype in cancer pathogenesis. *Nature Reviews Cancer* **7**, 763-777 (2007).

145. Kleinfeld, A.M. & Okada, C. Free fatty acid release from human breast cancer tissue inhibits cytotoxic T-lymphocyte-mediated killing. *Journal of Lipid Research* **46**, 1983-1990 (2005).

146. Weisberg, S.P. *et al.* Obesity is associated with macrophage accumulation in adipose tissue. *Journal of Clinical Investigation* **112**, 1796-1808 (2003).

147. Lescoat, A. *et al.* Distinct Properties of Human M-CSF and GM-CSF Monocyte-Derived Macrophages to Simulate Pathological Lung Conditions In Vitro: Application to Systemic

and Inflammatory Disorders with Pulmonary Involvement. *International Journal of Molecular Sciences* **19**, 894 (2018).

148. Ruffolo, L.I. *et al.* GM-CSF drives myelopoiesis, recruitment and polarisation of tumour-associated macrophages in cholangiocarcinoma and systemic blockade facilitates antitumour immunity. *Gut* **71**, 1386-1398 (2022).

149. Kotwica-Mojzych, K., Jodłowska-Jędrych, B. & Mojzych, M. CD200:CD200R Interactions and Their Importance in Immunoregulation. *International Journal of Molecular Sciences* **22**, 1602 (2021).

150. Hamilton, J.A. Colony-stimulating factors in inflammation and autoimmunity. *Nature Reviews Immunology* **8**, 533-544 (2008).

151. Ogata, M. *et al.* Autophagy Is Activated for Cell Survival after Endoplasmic ReticulumStress. *Molecular and Cellular Biology* **26**, 9220-9231 (2006).

152. Tabas, I. & Ron, D. Integrating the mechanisms of apoptosis induced by endoplasmic reticulum stress. *Nature Cell Biology* **13**, 184-190 (2011).

153. Lindner, P., Christensen, S.B., Nissen, P., Møller, J.V. & Engedal, N. Cell death induced by the ER stressor thapsigargin involves death receptor 5, a non-autophagic function of MAP1LC3B, and distinct contributions from unfolded protein response components. *Cell Communication and Signaling* **18** (2020).

154. Devries-Seimon, T. *et al.* Cholesterol-induced macrophage apoptosis requires ER stress pathways and engagement of the type A scavenger receptor. *Journal of Cell Biology* **171**, 61-73 (2005).

155. Stoudt, G., Bamberger, M., Warner, G.J., Johnson, W.J. & Rothblat, G.H. Cell Toxicity Induced by Inhibition of Acyl Coenzyme A:Cholesterol Acyltransferase and Accumulation of Unesterified Cholesterol. *Journal of Biological Chemistry* **270**, 5772-5778 (1995).

156. Feng, B. *et al.* The endoplasmic reticulum is the site of cholesterol-induced cytotoxicity in macrophages. *Nature Cell Biology* **5**, 781-792 (2003).

157. Cubillos-Ruiz, J.R. *et al.* ER Stress Sensor XBP1 Controls Anti-tumor Immunity by Disrupting Dendritic Cell Homeostasis. *Cell* **161**, 1527-1538 (2015).

158. Martinon, F., Chen, X., Lee, A.-H. & Glimcher, L.H. TLR activation of the transcription factor XBP1 regulates innate immune responses in macrophages. *Nature Immunology* **11**, 411-418 (2010).

159. Shan, B. *et al.* The metabolic ER stress sensor IRE1α suppresses alternative activation of macrophages and impairs energy expenditure in obesity. *Nature Immunology* **18**, 519-529 (2017).

160. Oh, J. *et al.* Endoplasmic Reticulum Stress Controls M2 Macrophage Differentiation and Foam Cell Formation. *Journal of Biological Chemistry* **287**, 11629-11641 (2012).

161. Patel, A.A. & Yona, S. Inherited and Environmental Factors Influence Human Monocyte Heterogeneity. *Front Immunol* **10**, 2581 (2019).

162. Vazquez-Madrigal, C. *et al.* Dietary Fatty Acids in Postprandial Triglyceride-Rich Lipoproteins Modulate Human Monocyte-Derived Dendritic Cell Maturation and Activation. *Nutrients* **12**, 3139 (2020).

163. Jordan, S. *et al.* Dietary Intake Regulates the Circulating Inflammatory Monocyte Pool. *Cell* **178**, 1102-1114.e1117 (2019).

164. Elia, A. *et al.* A role for immunotherapy: preventing macrophage anergy in the tumour environment. *Journal for ImmunoTherapy of Cancer* **1**, P185 (2013).

165. Xu, W. *et al.* Global Metabolomics Reveals the Metabolic Dysfunction in Ox-LDL Induced Macrophage-Derived Foam Cells. *Front Pharmacol* **8**, 586 (2017).

166. Wang, H.W. & Joyce, J.A. Alternative activation of tumor-associated macrophages by IL-4: priming for protumoral functions. *Cell Cycle* **9**, 4824-4835 (2010).

167. Choi, C.S. *et al.* Suppression of Diacylglycerol Acyltransferase-2 (DGAT2), but Not DGAT1, with Antisense Oligonucleotides Reverses Diet-induced Hepatic Steatosis and Insulin Resistance. *Journal of Biological Chemistry* **282**, 22678-22688 (2007).

168 Figure 1 to 5 created with BioRender.com

6.5 Acknowledgement

This Ph.D. was one of the most challenging journeys I could have ever asked for. Starting as a naïve young research enthusiast, I could never anticipate the resilience I would develop by enduring this journey. The pandemic outbreak and lockdowns only added to the difficulties of this process. However, this endeavor would not be possible without the help of all the people around me whose support inspired me to keep going, grow my knowledge and to be a successful researcher.

Firstly, I would like to thank my supervisor Prof. Dr. Britta Siegmund for allowing me to work on this exciting project, and for providing me insights and constant support throughout my Ph.D. journey. I would also like to thank Prof. Dr. Sigmar Stricker for being the reviewer of my thesis.

I am deeply thankful to Dr. Rainer Glauben for all the scientific discussions and arguments, which helped grow my scientific knowledge and worked positively towards bringing this project to completion. I am also grateful for all the fun conversations and interactive events he planned that helped me settle in and feel integrated with the group.

I would like to especially thank Inka Freise who was one of the most important person in my lab journey and always helped me immensely with her scientific and technical support.

I would like to express my deepest gratitude to all the past and present members of AG Siegmund for all their support. Special thanks to Cansu Yerinde for teaching me all about the seahorse instrument and T cell suppression assays. Thanks to Laura Golusda for being a constant supporting and understanding friend in all the difficult times. This Ph.D. would be unimaginably difficult without you both. I would like to extend my gratitude to Lorenz Gerbeth, Hsiang-Jung Hsaio, Nadra Alzain, Diana Bösel, and Doga Bingol for all the comforting talks. I would also like to thank Stefanie Althoff, Lisa, Gora, and other members of Charité. I am also deeply grateful to the BSIO Ph.D. selection committee for giving me a chance and access to an international research environment.

A special thanks to Nikita, Manoj, & Ashifa for always listening to my lab stories. Especially a big thanks to Tannu, Rishabh, and Sandhya for always being supportive

of having scientific discussions about my projects even during social gatherings. A big thanks to all my dance gurus Hannah, Francesca and Christina for always making me believe in myself and my abilities. I would also like to thank my friends Kathie and Donnah for making every class fun and for always being supportive.

Thank you Max for coming into my life when everything looked impossible. I owe you big time for helping me bring back my sanity. This journey would not be complete without you. Thank you ji for also sharing your MS Office expertise with me.

I dedicate this work to my beloved father Tahir Siddiqui whose presence in a certain way has always kept me going especially on days when I did not find the courage to continue.

Finally, a big thank you to my mother Shahnaz Siddiqui. It has been an unspoken dream of hers to have me achieve more in life. I owe all this success to her. Thank you Mom for always making sure I was educated despite all the difficult situations and I hope my degree brings to you the joy that life tried to steal from you many times. Thank you for all that you did all along from running to school with our lunch boxes to working round the clock to make sure we always had enough. Thank you for being patient with me when I was struggling to find a science-related job and for always supporting my curiosity about science. None of this success would be possible without your resilient support.

6.6 Selbständigkeitserklärung

Hiermit erkläre ich, dass ich diese Arbeit selbständig verfasst habe und keine anderen als die angegebenen Quellen und Hilfsmittel in Anspruch genommen habe. Ich versichere, dass diese Arbeit in dieser oder anderer Form keiner anderen Prüfungsbehörde vorgelegt wurde.

Berlin, May, 2023 Siddiqui, Sophiya Tabassum Tahir

6.7 Publications:

6.7.1 Additional publications during the period of this thesis

1) Wu, H., Han, Y., Rodriguez Sillke, Y., Deng, H., **Siddiqui, S**., Treese, C., Schmidt, F., Friedrich, M., Keye, J., Wan, J., Qin, Y., Kühl, A. A., Qin, Z., Siegmund, B., & Glauben, R. (2019). Lipid droplet-dependent fatty acid metabolism controls the immune suppressive phenotype of tumor-associated macrophages. *EMBO molecular medicine*, *11*(11), e10698. https://doi.org/10.15252/emmm.201910698
2) Wu, H., Reimann, S, **Siddiqui, S**., Haag, R., Siegmund, B., Dernedde, J., Glauben, R., dPGS Regulates the Phenotype of Macrophages via Metabolic Switching. *Macromolecular Bioscience* 2019, 19, 1900184. https://doi.org/10.1002/mabi.201900184

6.7.2 Review article published related to the thesis topic

1) **Siddiqui, S.**, & Glauben, R. (2022). Fatty Acid Metabolism in Myeloid-Derived Suppressor Cells and Tumor-Associated Macrophages: Key Factor in Cancer Immune Evasion. *Cancers*, *14*(1), 250. https://doi.org/10.3390/cancers14010250